Evaluation of post-CHOPS (Cold Heavy Oil Production with Sands)

Enhanced Oil Recovery Methods

by

Alireza RANGRIZSHOKRI

A thesis submitted in partial fulfillment of the requirements for the degree of

Doctor of Philosophy

in

Petroleum Engineering

Department of Civil and Environmental Engineering

University of Alberta

Abstract

Due to its lower cost, the cold heavy oil production with sands (CHOPS) method is a common primary production recovery technique, not only in Canada where it originated, but also in many other countries including Venezuela, Kuwait, Russia, and China. However, this method has several practical limitations. It continuously changes the geomechanical and petro-physical properties of the reservoir due to the sand produced, resulting in high permeability channels known as wormholes. In addition, this method has a low oil recovery factor (5-15 %) and this entails further recovery techniques.

Thermal methods after CHOPS are not usually favourable due to heterogeneity and reservoir instability. In addition, CHOPS wells are not completed for thermal (steam) operations. The CHOPS method is typically applied in thin formations in which heating by injected steam is characteristically inefficient. Solvent injection possesses similar problems caused by heterogeneity and cost. An option could be the hybrid application of steam/solvent. Assessment of this technique first requires a realistic modeling of the CHOPS process. Due to dynamic changes in reservoir properties, no valid model was available to accurately simulate field-scale CHOPS production.

Therefore, a part of this thesis presents a quick workflow for CHOPS modeling to investigate efficient EOR/IOR (Enhanced/Improved Oil Recovery) methods after CHOPS. To achieve this, we first propose a partial-dual porosity approach coupled with algorithms for wormhole generation to create realistic static reservoir models. After generating fractal wormhole patterns of different kinds using a diffusion limited aggregation (DLA) algorithm, they were introduced into a reservoir model. Based on fractal analysis, novel upgridding procedures for wormhole network in partial-dual porosity models were introduced. After validation of the models using data obtained from a field in Alberta, several preliminary post-CHOPS scenarios including thermal, solvent, and thermal/solvent hybrid applications were simulated. In addition, a

3D geomechanical model was used to calculate the stress distribution in the history matched field. The hydro-geomechanical model was then used for field development planning, reservoir management and assessment of near wellbore regions during cyclic injection and production. The field-wide deformation and stress changes were analyzed in deep overburden, cap rock, and reservoir to show the influence of local stress orientations in soft and stiff layers.

Next, an experimental set-up consisting of a sand-pack with different configurations of complexity of wormhole patterns was designed. The experiment was aimed to mimic cyclic solvent stimulation at reservoir conditions. The sand-pack experiments were numerically simulated and effective diffusion coefficients were obtained. To generate accurate predictions in field-scale simulation, an up-scaling procedure from laboratory results of the cyclic solvent injection process was suggested. The overall findings suggest that an improved heavy oil recovery could be achieved using combined light and heavy solvents in CHOPS reservoirs. Steam (or hot-water) was found to play a positive role in solvent retrieval. Finally, an uncertainty screening procedure was performed to assess the feasibility of cyclic solvent stimulation as a post-CHOPS method. An economics model was developed and after-tax NPV (Net Present Value) of the field at the end of cyclic solvent stimulation process was calculated. Such calculations have the priority to oil recovery factor or cumulative oil production as it could incorporate costs and sales simultaneously by performing continuous discounting and allow the asset holder to maximize NPVs and select the best development strategy.

Acknowledgements

First of all, I would like to express sincere appreciations to my research supervisor, Dr. Tayfun Babadagli, for providing me with an opportunity to work on a good PhD title in addition to his time and efforts during my stay at the University of Alberta.

I am thankful to Dr. Lijun Deng, Dr. Ergun Kuru, Dr. Andy Li, Dr. Ryosuke Okuno, Dr. Fanhua Zeng, my examining committee members, and Dr. Vivek Bindiganavile, my candidacy committee member, for their time and suggestions.

My thanks are extended to Faculty of Graduate Studies and Research (FGSR) and Graduate Students' Association (GSA) - University of Alberta for their partial financial support and travel grants. In addition, I am grateful for the support of EOGRRC members (students and staff), colleagues, and friends.

This research was conducted under Dr. Babadagli's NSERC Industrial Research Chair in Unconventional Oil Recovery (industrial partners are CNRL, SUNCOR, Petrobank (Touchstone Exploration), Sherritt Oil, APEX Engineering, PEMEX, Saudi Aramco, and Husky Energy). I gratefully acknowledge these supports. I also thank Schlumberger for providing the ECLIPSE/PETREL/VISAGE software packages for research purposes.

Last, but most importantly, thanks go to my family who supported me during each step I took around the world.

Table of Contents

Chapter 1: Introduction **1**

Introduction 2

Statement of the Problem 4

Objectives and Philosophy of the Research 5

Outline 7

Chapter 2: Modelling of Cold Heavy-Oil Production with Sand for Subsequent Thermal/Solvent Injection Applications **10**

Abstract 11

Introduction 12

Literature Review 14

Physics of the CHOPS Process 15

Significant Recovery Mechanisms 15

Current CHOPS Models 16

Typical Signature of a CHOPS Well 18

Desirable Engineering Data. 18

The Practice of CHOPS Modelling 19

Fundamental Limitations and Assumptions. 19

Numerical Simulation Workflow. 21

Introduction of a Growing Wormhole Network. 21

Integrated Fractal Wormhole Model for Sand Production 22

Foamy-Oil Flow and Alternative Modelling Approaches 24

Effective Properties of a Partial Dual-Porosity Model. 25

Step-By-Step Simulation Technique. 26

Initialization of a Post-CHOPS Study. 27

Results and Discussion 28

Sensitivity Study 29

Model Verification Through History Matching. 29

Wormhole Network Patterns. 31

Gridblock Size Sensitivity. 35

Predicting the CHOPS Well Performance. 37

Post-CHOPS Applications 38

Model Options and Inherent Difficulties 38

Post-CHOPS EOR. 39
Conclusions 45
References 45
Chapter 3: Field Scale Modeling of CHOPS and Solvent/Thermal Based post CHOPS EOR Applications Considering Non-Equilibrium Foamy Oil Behavior and Realistic Representation of Wormholes 52
Abstract 53
Introduction 54
CHOPS Flow Behaviour 56
CHOPS Modeling Workflow 57
Challenges in CHOPS Modeling. 57
Methodology Followed for Simulation 58
Assigning Reservoir Properties to Flow Model 60
Capturing the Foamy Oil Flow Behavior 63
Application of Integrated Fractal-Wormhole Model 64
Post-CHOPS Modeling 65
Results and Discussions 66
Implementation of Methodology for Field-Scale Study 66
Upgridding of Fractal Patterns in Partial Dual Porosity Model 67
Upscaling Properties and Generating/Testing Multiple Realizations 70
Field-Scale History Matching 71
Post-CHOPS Applications 74
Economic Analysis 78
Conclusions 79
References 80
Chapter 4: Field-Scale Deformation Analysis of Cyclic Solvent Stimulation in Thin Unconsolidated Heavy Oil Reservoirs with Developed Wormhole Network 82
Abstract 83
Introduction 84
Description of Reservoir Fluid Flow Model 86
Field overview. 86
Wormhole network growth. 87
Foamy oil behavior. 88
Fluid characterization. 89

3D geomechanical model construction. 89
Geometric description of MEM and coupling schemes. 90
Material properties and failure criterion model. 91
Boundary conditions and stress initialization 91
Results and Discussions 92
Full field history matching. 92
Field-wide deformations and stress changes. 92
Geomechanical analysis in reservoir segment and wormhole network. 93
Geomechanical analysis in deep overburden and cap rock segment. 96
Geomechanical response from cyclic loading and unloading due to solvent injection. 98
Impact of fluid injection stream 99
Porosity and permeability update in coupled cyclic solvent stimulation. 101
Conclusions 104
References 105
Chapter 5: Laboratory Measurements and Numerical Simulation of Thermally-Aided Cyclic Solvent Stimulation in the Presence of Wormholes after CHOPS 109
Abstract 110
Introduction 111
Fluid Characterization and Modeling 113
Post-CHOPS CSI: Experiments and Simulation 119
Sand-Pack Experiments 119
Simulated Sand-Pack Characteristics 122
Results and Discussions 124
Experiment 1: Low pressure injection of C7 in a linear wormhole. 124
Experiment 2: Low pressure injection of diluents in a linear wormhole. 127
Experiment 3: Low pressure injection of C7 in a branched wormhole. 128
Experiment 4: High pressure injection of C7 in a linear wormhole. 128
Experiment 5: High pressure injection of CO2 in a linear wormhole. 129
Ultimate Oil and Solvent Recoveries 129
Simulation Results 131
Up-scaling Diffusion Process 137
Conclusions and Remarks 138
References 140

Chapter 6: A Sensitivity and Uncertainty Analysis of Cyclic Solvent Stimulation for Post-CHOPS EOR: Application on an Actual Field Case 142
Abstract 143
Introduction 143
Model Description 144
Reservoir Grid Properties 145
PVT and Fluid Modeling 146
Economic Assumptions 148
Results and Discussions 149
Base Model Description 149
Selection of Injection Pattern 150
Selection of Injection Rate 152
Selection of Injection/Soaking Time 153
Solvent Dissolution/Exsolution 154
Impact of Wormhole Vertical Location 156
Economic Analysis 158
Conclusions and Remarks 160
References 161
Chapter 7: Summary, Conclusions, Remarks and Contributions 163
Summary, Conclusions and Remarks 164
Specific Contributions 167
Numerical Work 167
Experimental Work 168
Bibliography 169

List of Tables

Table 2- 1: Reservoir Properties used in the Reservoir Simulation. 26
Table 2- 2: Specification of the Upgridded Wormhole Models. 37

Table 3- 1: Reservoir Properties used in the Field-Scale Simulation. 61
Table 3- 2: Fluid Properties for Foamy Oil Flow and Solvent Injection. 62
Table 3- 3: Thermal Properties for Heat Loss Calculations. 63
Table 3- 4: Base Prices used in Economic Analysis. 78
Table 3- 5: Total injection and production volumes and estimated money recovered after 6 cycles of solvent/steam stimulation. 79

Table 4- 1: Reservoir Properties used in Fluid Flow Simulation Models 87
Table 4- 2: Fluid Properties for Foamy Oil Flow and Solvent Injection. 89
Table 4- 3: Description of Material Properties and Failure Criteria Models. 91

Table 5- 1: Fluid Properties of Original Dead Oil. 114
Table 5- 2: Full Description of EOS Parameters. 115
Table 5- 3: Fluid Compositions of Original Oil and Solvents. 115
Table 5- 4: Binary Interaction Coefficients (BICs). 116
Table 5- 5: Overall Sand-Pack Properties used in CSI Experiments. 120
Table 5- 6: Grid Block Properties of Simulated Sand-pack Experiments. 123

Table 6- 1: Reservoir Properties used in Fluid Flow Simulation Models 146
Table 6- 2: Fluid Properties of Original Dead Oil. 147
Table 6- 3: Fluid Properties for Foamy Oil Flow Models and Solvent Injection. 147
Table 6- 4: Economic Assumptions 148

List of Figures

Figure 1- 1: Representation of possible wormhole network based on field experience (a) CHOPS well on production, (b) Developed dilated region, (c) Based on dilated region theory, "well A" should see the altered zone, but not "well B". (d) Field experience shows "well A" does not see the altered zone, but "well B" does, supporting the existence of wormholes. 3
Figure 1- 2: Schematic of research philosophy....7

Figure 2- 1: Representation of possible wormhole network based on field experience (a) CHOPS well on production, (b) Developed dilated region, (c) Based on dilated region theory, "well A" should see the altered zone, but not "well B". (d) Field experience shows "well A" does not see the altered zone, but "well B" does, supporting the existence of wormholes. 13
Figure 2- 2: Typical signature of a CHOPS well. WOPR (Well Oil Production Rate); WWPR (Well Water Production Rate); WSPR (Well Sand Production Rate); WGPR (Well Gas Production rate). 18
Figure 2- 3: A typical fractal pattern used for wormhole model. 24
Figure 2- 4: Step-by-step simulation technique to match oil and sand production based on a growing wormhole pattern (black circles: oil rate history; red squares: sand rate history; lines: simulation rates). Note the growing nature of wormhole based on sand production shown in each step. 27
Figure 2- 5: Production profile of well 1 (a) Field oil production rate and matched simulation data for well 1 (dotted black line: well history; solid black line: step-by-step simulation results; dotted black line: CHOPS with no wormhole), (b) Fractal wormhole pattern, (c) Oil saturation profile. 30
Figure 2- 6: Production profile of well 2 (a)Field oil production rate and matched simulation data for well 2 (dotted black line: well history; solid black lines: step-by-step simulation results), (b) Fractal wormhole pattern, (c) Oil saturation profile. 30
Figure 2- 7: Production profile of well 3 (a)Field oil production rate and matched simulation data for well 3 (dotted black line: well history; solid black lines: step-by-step simulation results), (b) Fractal wormhole pattern, (c) Oil saturation profile. 30
Figure 2- 8: Fractal pattern 01 for wormhole domain. 32
Figure 2- 9: Large-Conduit pattern for wormhole domain. 32
Figure 2- 10: Distant-Sand-Sourcing pattern for wormhole domain....32
Figure 2- 11: Field Oil Production Rate (dotted black line: well history; solid red line: fractal pattern 01; solid blue line: large-conduit pattern; solid green line: distant-sand-sourcing pattern; solid brown line: extended fractal pattern 01). 33
Figure 2- 12: Fractal pattern 01 and its resulted oil saturation profile. 34
Figure 2- 13: Fractal pattern 02 and its resulted oil saturation profile. 34
Figure 2- 14: Fractal pattern 03 and its resulted oil saturation profile. 34
Figure 2- 15: Fractal pattern 04 and its resulted oil saturation profile. 34

Figure 2- 16: Fractal pattern 05 and its resulted oil saturation profile.....35
Figure 2- 17: Fractal pattern 06 and its resulted oil saturation profile.....35
Figure 2- 18: Field oil production rate for several fractal patterns shown in Figures 2-12 through 2-17 (dotted black line: well history; solid green line: fractal pattern 01; solid dark blue line: fractal pattern 02; solid light blue line: fractal pattern 03; solid purple line: fractal pattern 04; solid yellow line: fractal pattern 05; solid red line: fractal pattern 06).....35
Figure 2- 19: A single fractal pattern for wormholes with different box dimensions.....36
Figure 2- 20: Field oil production rate and matched simulation data for well 1 with different grid block sizes (See Table 2-3).....37
Figure 2- 21: Predicting oil production rate based on a tuned wormhole growth pattern (black dots: simulated oil rate, grey dots: oil rate history).....38
Figure 2- 22: Well#1 - Field oil production rate due to injection of (a) steam (hot water) (grey-line), (b) solvent (miscible gas) (thick-black), and (c) steam-over-solvent (thin-black).....42
Figure 2- 23: Oil saturation profile from top view at the end of first cycle of (a) steam (hot water) injection, (b) solvent (miscible gas) injection and (c) steam-over-solvent injection over the wormhole plane.....42
Figure 2- 24: Oil saturation profile from top view at the end of first cycle of (a) steam (hot water) injection, (b) solvent (miscible gas) injection and (c) steam-over-solvent injection in the wormhole plane.....42
Figure 2- 25: Well#1 - Field reservoir pressure at the start of injection of steam (hot water) grey-line, solvent (miscible gas) thick-black and steam-over-solvent thin-black.....44
Figure 2- 26: Effect of soaking period and the injection fluid on oil recovery factor.....45
Figure 2- 27: Relative incremental oil recovery at the end of first cycle in a single well.....45

Figure 3- 1: CHOPS well signature: WOPR (Well Oil Production Rate); WWPR (Well Water Production Rate); WSPR (Well Sand Production Rate); WGPR (Well Gas Production rate) of a typical CHOPS well.....56
Figure 3- 2: Step-by-step simulation technique to match oil and sand production based on a growing wormhole-fractal pattern (black circles: oil rate history; red squares: sand rate history; lines: simulation rates). Note the growing nature of wormhole based on sand production history indicated at each step.....60
Figure 3- 3: Inclusion of heat loss to adjacent layers (a) Top view of the CHOPS field and well locations (b) Thin CHOPS layer (2-5 m) and thermal boundaries for heat loss.....62
Figure 3- 4: Comparison of different approaches to capture foamy oil effect in a single well study (1) using kinetic reactions (circles - dotted black line) (2) no kinetic reaction, but an increase in critical gas saturation (red line) (3) no kinetic reactions and no increase in critical gas saturation (blue line).....64
Figure 3- 5: Field-scale application of fractal-wormhole model.....65
Figure 3- 6: Field scale wormhole-growth model at time t_1 to t_4 in a wormhole network plane.....67
Figure 3- 7: Field-scale wormhole upgridding.....69
Figure 3- 8: Different levels of upgridding for Huff'n'Puff in a quarter of a single CHOPS well.....69
Figure 3- 9: Justification of upgridding procedure during huff 'n' puff process in a quarter of a single CHOPS well. Note the significant decrease in CPU time. The difference in CPU time of 2X to 5X upscaled models is negligible that could not be recognized in this figure.....70
Figure 3- 10: An example of multiple realization and resulted permeability distribution in the upscaled model.....71
Figure 3- 11: History matched field oil production rate.....72
Figure 3- 12: History matched oil and gas production rate on a well basis.....73

Figure 3- 13: Effect of upgridding on oil saturation of non-wormhole domain in a layer close to wormhole network (top view).....74
Figure 3- 14: Solvent injection in wormhole network as post-CHOPS option (a) converting some production wells into injectors (b) soaking period (c) production phase.....76
Figure 3- 15: Field oil production rate, history matched model followed by aggressive pressure depletion and solvent stimulation.....76
Figure 3- 16: Field total oil production at the end of primary production followed by (a) cold solvent stimulation and (b) thermally-aided solvent stimulation.....77

Figure 4- 1: Mechanical Earth Model Construction (a) embedded grid contains full field flow model (b) Full field model for fluid simulation (c) upscaled wormhole network within full field flow model (d) refined sector model around a single well.....90
Figure 4- 2: History matched field production data, simulated oil data (blue line), historic oil data (blue circles), simulated gas data (red line), historic gas data (red circles).....92
Figure 4- 3: Vertical displacement profile after primary production (a) top view of Mechanical Earth Model and location of reservoir section for further analysis (b) downward movement of upper reservoir layer shown with cold colors (c) no significant displacement in wormhole layer (d) upward movement of lower reservoir layer shown in warm colors.....94
Figure 4- 4: Reservoir compaction, overburden subsidence and underburden rebound in the sector model...95
Figure 4- 5: Principal effective stress tensor (a) before and (b) after primary production. Note the increase in the vertical effective stress compared to changes in horizontal components.....96
Figure 4- 6: Maps of effective stress change around a production well (a) before and (b) after primary production. Note the re-orientation of the stress components due to aggressive pressure depletion around well.....96
Figure 4- 7: Analysis of displacement with the presence of a wormhole network. (a) Upscaled wormhole network in field-scale simulation model (b) vertical displacement of the interface of reservoir layer and cap rock. Note the compaction features are well separated for large well spacing (well 15 and well 11).....97
Figure 4- 8: Geomechanical response of cyclic solvent stimulation near wellbore region.....99
Figure 4- 9: Reservoir performance during two cycles of solvent stimulation.....101
Figure 4- 10: Comparison of coupled and uncoupled schemes during two cycles of solvent stimulation.....104

Figure 5- 1: Gas chromatography characterization of diluents and original dead oil.....117
Figure 5- 2: Density and viscosity variations of heavy oil with solvent content and temperature.....119
Figure 5- 3: Experimental set-up to study thermally aided cyclic solvent stimulation in the presence of wormholes.....120
Figure 5- 4: Schematic of thermally aided cyclic solvent stimulation in the presence of wormholes.....121
Figure 5- 5: Chemical and heat resistant rubber used at the inlet/outlet to ascertain that fluid injection/production is only through wormhole (a) rubber, (b) rubber inserted at the inlet/outlet, (c) rubber removed at the end of experiment.....122
Figure 5- 6: (a) simulated sand-pack in Cartesian grid, (b) inactivating the redundant cells to get cylindrical shape, (c) linear wormhole shown in vertical cross-section of the sand-pack, (d) branched wormhole shown in horizontal cross-section of the sand-pack.....123

Figure 5- 7: Relative permeability curves used in non-wormhole (saturation region 1) and wormhole (saturation region 2) domains. 123
Figure 5- 8: Liquid volumes recovered during experiment 1 (low pressure injection of C7 in a linear wormhole)....125
Figure 5- 9: Residual oil and solvent after the whole experiment of low pressure C7 injection (solvent phase and hot water injection phase) was conducted. (a) Cross-section of sand-pack at natural light, (b) enhanced version of (a) with corrected white balance and exposure. 126
Figure 5- 10: Asphaltene precipitation observed after collecting oil and solvent (C7) mixture in graduated cylinder....127
Figure 5- 11: Liquid volumes recovered during experiment (low pressure injection of diluents in a linear wormhole)....127
Figure 5- 12: Liquid volumes recovered during experiment 3 (low pressure injection of C7 in a branched wormhole)....128
Figure 5- 13: Liquid volumes recovered during experiment 4 (high pressure injection of C7 in a linear wormhole)....129
Figure 5- 14: Solvent recovery factor after solvent phase and whole experiment (solvent and hot-water phase). 130
Figure 5- 15: Oil recovery factor after solvent phase and whole experiment (solvent and hot-water phase)..131
Figure 5- 16: (a) simulated and (b) linear wormhole shown in vertical cross-section of the sand-pack, (c) branched wormhole and (d) corresponding simulated model shown in horizontal cross-section of the sand-pack. 131
Figure 5- 17: Simulated and experimental liquid volumes recovered during CSI experiments. 132
Figure 5- 18: (a) Top view of a horizontal cross section at the middle of sand-pack with branched wormhole. The blue and red colors are reserved for non-wormhole and wormhole domains, respectively. (b) Mixing zone of injected solvent with original oil after several cycles. 133
Figure 5- 19: Field-scale application of fractal-wormhole model to develop wormhole network based on sand production data (Rangriz Shokri and Babadagli 2012). 134
Figure 5- 20: Simulated and experimental liquid volumes recovered during low pressure injection of diluents in a linear wormhole. 134
Figure 5- 21: Simulated and experimental liquid volumes recovered during high pressure injection of C7 in a linear wormhole. 135
Figure 5- 22: Simulated CO_2 invasion during CSI process....136
Figure 5- 23: Simulated and experimental liquid volumes recovered during CO_2 injection in a linear wormhole....136
Figure 5- 24: Simulated and experimental gas volumes recovered during CO_2 injection in a linear wormhole. 137

Figure 6- 1: Field scale wormhole-growth model at time t_1 to t_4 in a wormhole network plane. 145
Figure 6- 2: Field oil production rate: history matched model followed by pressure depletion and cyclic solvent stimulation. 149
Figure 6- 3: Possible cyclic solvent injection patterns in CHOPS reservoirs....150
Figure 6- 4: Performance of cyclic solvent stimulation in different injection patterns. 151
Figure 6- 5: Performance of cyclic solvent stimulation with different injection rates....153
Figure 6- 6: Performance of cyclic solvent stimulation with different injection times. 154

Figure 6- 7: Performance of cyclic solvent stimulation for C1 and CO2 with delayed gas dissolution/exsolution. 156
Figure 6- 8: Possible sand grain distribution in CHOPS reservoirs 157
Figure 6- 9: Simulated wormhole network developed at (a) formation bottom and (b) formation top. 157
Figure 6- 10: Performance of cyclic solvent stimulation for different wormhole locations. 158
Figure 6- 11: Technical tornado plot shows relative incremental oil production. 160
Figure 6- 12: Economical tornado plot shows project's net present value. 160

Chapter 1: Introduction

Introduction

CHOPS (Cold Heavy Oil Production with Sand) is accounted as one of the emerging primary production techniques in unconsolidated sand reservoirs, mostly applied in Alberta, Canada. The aggressive co-production of sand and heavy oil using PCPs (progressive cavity pump) enhances the oil production rate at economic conditions. Hence, CHOPS is a low cost but a practical production technology. However, non-stopping changes in petro-physical and geomechanical properties are inevitable due to the withdrawal of sands from the reservoir. It creates high-permeability channels, i.e. wormholes, in the reservoir, and consequently may turn into a network serving as a natural multi-branched system among the wells. The so-called foamy oil is another issue to be considered in this recovery process.

Despite its low primary recovery factor, CHOPS has received a great deal of attention due to its lower cost compared to surface mining and other EOR methods. Field experience supports the idea of generation of a high-permeability channel-like medium during production by CHOPS. Continuous sand production causes the wormholes to grow more, leading to a wormhole network, which connects the wells to each other. 4D seismic imaging of some CHOPS reservoirs indicates tens of meters of linear channels away from the wellbore (Loughead et al. 1992). Another justification for produced sand is the dilation theory. This theory assumes that sand production would lead to an altered region around the well, rather than generating a wormhole network. Based on the amount of sand production, the moving dilation theory suggests that the damaged region should be extended up to ~50 meters away from the well after a certain time. But, field experience has shown that a well drilled just 300 meters away encounters mud loss due to hitting a wormhole channel (**Figure 1-1**).

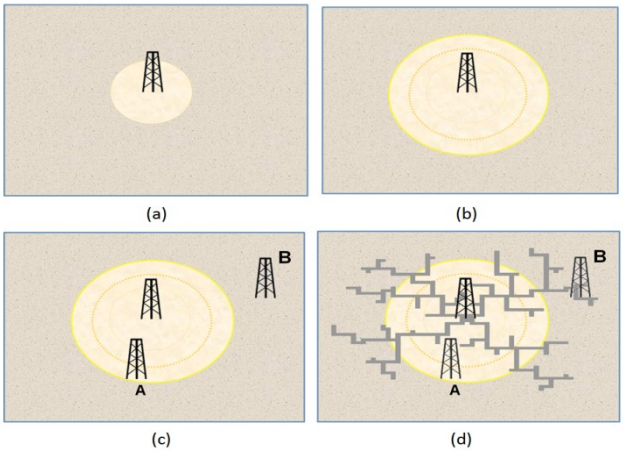

Figure 1- 1: Representation of possible wormhole network based on field experience (a) CHOPS well on production, (b) Developed dilated region, (c) Based on dilated region theory, "well A" should see the altered zone, but not "well B". (d) Field experience shows "well A" does not see the altered zone, but "well B" does, supporting the existence of wormholes.

The growing nature of a wormhole changes the stress conditions and reservoir properties, including permeability, porosity and formation compressibility in a dynamic fashion. Such an alteration needs to be treated with a dynamic geological model, which is mostly referred to as static reservoir model in conventional approach. In addition, when the reservoir pressure goes below the bubble point pressure and the dissolved gas comes out of solution, the gas bubbles are not willing to coalesce to form a single gas phase; rather, they prefer to remain as dispersed bubbles in the oil until they reach a critical saturation. In other words, the heavy oil tends to behave like foam.

This research begins with a critical review of CHOPS, mainly focusing on the practical outcomes of CHOPS modeling. Many of our efforts have been devoted to the demonstration of how the governing mechanisms can be modeled through convenient yet available engineering tools without much compromise. One of the key objectives is to show the connections found useful among CHOPS, fractured reservoirs, and fractal analysis. Having defined a practical workflow for the history matching of CHOPS wells, we end up with a full field model that is ready for any EOR studies and feasible optimization revisions.

Statement of the Problem

As stated earlier, in CHOPS technology, sand is allowed to be produced along with oil. This co-production of oil and sand increases the oil production rate in a dramatic fashion. Literature review revealed the successful applications of this technique at the field scale. Two issues, however, are to be addressed: (1) very low ultimate recovery of CHOPS that definitely requires challenging further EOR applications, and (2) understanding the physics of the wormhole growth process and representing it accurately in the simulation model for further EOR assessment applications.

The production of sand, leading to a complex wormhole network, is absolute evidence of all the changes that occur in the reservoir. The most probable explanation is that the sand production leads to the generation of a network of wormholes that continues to grow and develop in the vicinity of the wellbore or far beyond it. This means that as long as the sand production takes place, the fundamental geological parameters such as permeability, porosity, and formation compressibility are altered. Therefore, any model that utilizes a time-independent static model for its flow simulation shall not be considered a suitable one. Foamy oil behaviour should also be considered during heavy oil and sand production. Foamy oil is the reluctance of small gas bubbles to coalesce to create a continuous phase. Thus, the small bubbles preferentially remain as dispersed in the oil rather than being a free phase. This phenomenon causes the oil to swell, which provides more drive energy and, as long as the free-gas saturation is still zero, the dispersed gas moves with the same velocity as the oil phase; i.e. there is no free gas movement. One may compare this fact with conventional oil in which the emergence of free-gas saturation decreases the oil mobility due to a higher gas relative permeability and lower viscosity.

One of the main challenges in CHOPS reservoirs is the application of EOR methods once the CHOPS stage is completed. This is referred to as post-CHOPS. In addition to nominating feasible EOR candidates, one of the challenges is to model these possible EOR options accurately. This requires realistic description of high-permeability wormhole networks and foamy oil behaviour. For instance, the rapid communication among some wells through wormhole network would reject any continuous injection. Apart from fluid interactions,

such unconsolidated reservoirs also suffer from mechanical changes in their strength properties. Abrupt pressure depletion due to sand production eventually leads to the development of a softer material in reservoir layers, which can carry less of the overburden stress. Then the question arises whether the altered formation is still able to support the overburden load during post-CHOPS applications. In the next section, we define our objectives based on the above mentioned problems.

Objectives and Philosophy of the Research

As highlighted above, the key question is very low recovery factor of CHOPS and one of our main objectives in this research is to investigate possible ways to recover this remaining oil using efficient, but not necessarily exotic, EOR methods. To do so, there is a need to understand CHOPS and to illustrate the changes in the reservoir caused by this technology. No unique solution has been reported to model CHOPS in practice; hence, there is no "CHOPS" option in any commercial simulator software. Assessment of such a process through numerical simulation, as the cheapest yet most powerful tool, necessitates a comprehensive modeling approach to capture its dynamic physical nature. Only through such a realistic model can one obtain reasonably reliable reservoir characteristics after CHOPS that are critically important to assess post-CHOPS applications. Therefore, a part of this proposal defines new workflow for quick CHOPS modeling considering its significant recovery mechanisms, including wormhole growth and foamy oil behaviour.

The next part of the research addresses the possible EOR options in CHOPS reservoirs. The principal difficulties with CHOPS reservoirs are the ultra-high oil viscosity in the reservoir conditions, the possible sand production, and the inherent reservoir heterogeneity. The cliché of EOR lies in increasing oil mobility with thermal and solvent injection, increasing reservoir drive energy (especially in shallow reservoirs), and decreasing the pressure draw-down in order to avoid mobilizing more sands. The established wormhole network is the key factor to nominate the post-CHOPS applications. At first sight, it rejects any continuous steam or solvent injection, but with a smart production/injection pattern, such injection may be implemented in the form of so-called huff 'n' puff processes. A reduction in oil viscosity due to thermal effects and much lighter heavy oil due to solvent injection are the chief active mechanisms in post-CHOPS. In this practice,

steam/hot water (or no steam/no water) can be injected into the wormhole network, followed by solvent injection and a soaking period while the wells are shut down. Reservoir drive energy would be provided through these injections. The well is then allowed to produce in a blow-down period. These cycles would be potentially repeated.

During post-CHOPS applications, geomechanics may play its role to provide insight into the subsurface stress state. With the help of a finite element simulator, a 3D Mechanical Earth Model (MEM) can be constructed to capture the complex interplay of pore pressure depletion, re-pressurization and loading process, reservoir geometry, and material properties. Although it is difficult to obtain data to calibrate the 3D hydro-geomechanical model, it allows for reliable investigation of reservoir performance and gives deeper insight than using flow simulation alone. The assessment of the potential of geomechanics can ascertain whether a more detailed modeling is necessary.

Experimentation is an inevitable part of any study in heavy oil. To complete the work, the interactions of wormhole and non-wormhole domains are considered in post-CHOPS conditions. Cyclic solvent stimulation in a long core (sand pack) with pre-generated wormholes was selected for experimental part of this research using liquid and gas solvents. The objective was to test the impact of solvent type and soaking time on oil recovery considering scaling ratio of wormhole and non-wormhole domains obtained from our earlier simulation models. In addition to experimental work, the last section was reserved for optimization of the potential post-CHOPS options in field scale. Using the history matched model and obtained data from experimental work, an uncertainty screening procedure was performed to assess the feasibility of cyclic solvent stimulation as a post-CHOPS method. An economics model was developed and after-tax NPV of the field at the end of cyclic solvent stimulation process was calculated as a profitability index of the process. In short, the philosophy of this research, depicted in **Figure 1-2**, is to create value from CHOPS reservoirs.

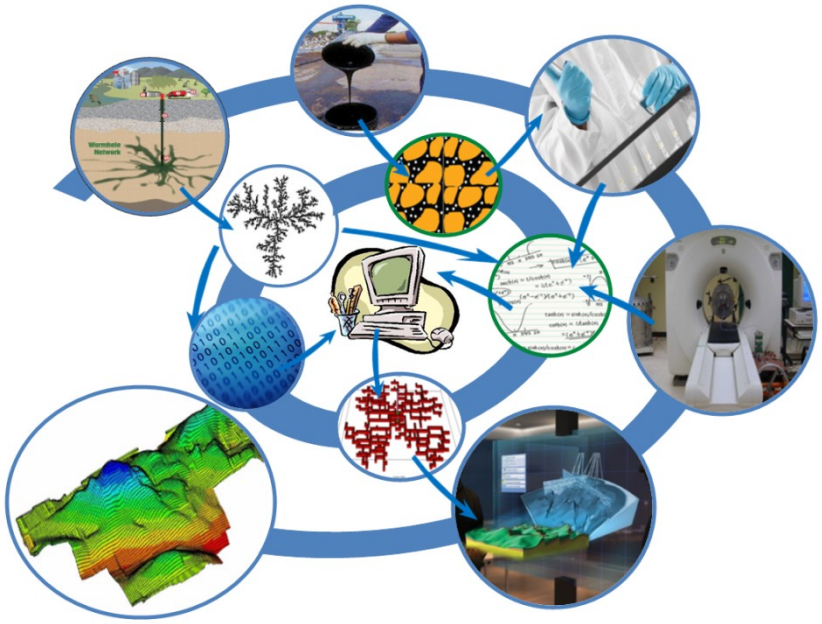

Figure 1- 2: Schematic of research philosophy.

Outline

This is a paper-based thesis. Five papers presented at different conferences and/or published in (or submitted to) different journal publications comprise the five chapters of the thesis. Each chapter has its own introduction, literature survey, conclusions, and references. Therefore, the thesis does not contain any specific chapter covering these for the whole work, except a short introduction chapter with a few references. At the end, a short chapter covering the contributions of this research is provided.

In chapter 2, a practical workflow for CHOPS modelling based on a step-by-step simulation technique and a fractal pattern for wormhole network was defined. A DLA pattern was presented and implemented in a reservoir simulator with a partial dual-porosity approach. An integrated fractal wormhole model was introduced to help with the growing nature of wormholes based on reservoir properties and sand-production data. Moreover, foamy-oil flow was modelled with sufficient accuracy through a modified gas relative permeability. History matching was achieved in three single CHOPS wells. The compatibility of our approach with thermal and compositional processes was studied through a simple huff 'n' puff process with cyclic

injection of steam, solvent, or steam or solvent together. Such a process might be considered as a technical possibility to increase the ultimate oil recovery from the CHOPS reservoir.

In chapter 3, the workflow was extended to field scale with 15 wells. In this workflow, an integrated fractal-wormhole model incorporated sand production history and wormhole network in the numerical simulations. In addition to a modified version of gas relative permeability curve, it was shown that foamy oil flow can be modeled in practice using first-order kinetic reactions to replace the in-situ flash process. Regular and special upgridding procedures in partial dual porosity were also defined and implemented. Multiple realizations of upscaled models were used to check the quality of history matching process. After history matching of the CHOPS performance in the selected field, several post-CHOPS scenarios as modified versions of Steam-Over-Solvent in Fractured Reservoirs (SOS-FR) technique were studied at field scale. It was observed that in an iso-thermal process, additional oil can be produced from wormhole network. The use of hot fluids as well as solvent-aided process would be effective in increasing oil recovery from non-wormhole domain.

In chapter 4, a 3D Mechanical Earth Model was constructed to understand the contribution of production schedule on stress changes on CHOPS reservoir. The hydro-geomechanical model was used for assessment of near wellbore regions during cyclic injection and production. The field-wide deformation and stress changes were analyzed in deep overburden, cap rock, and reservoir region to show the influence of local stress orientations in soft and stiff layers. It was shown how stress arching re-distribute the cyclic injection-production induced stresses to flow around soft inclusions in the suspected wormhole layer. The study was then focused on a sector model to assess EOR processes with different solvent streams. This chapter also addresses how a 3D hydro-geomechanical model with very limited data can be used for reliable investigation of reservoir performance to give deeper insight than using flow simulation alone. The assessment of the potential of geomechanics can then ascertain whether a more detailed modeling is necessary.

In chapter 5, with notion to the potential use of solvents in post-CHOPS, five experiments (liquid and gas solvents) were conducted to study the performance of thermally aided cyclic solvent stimulation. The interactions between wormhole and non-wormhole domains were inspected based on scaled wormhole/non-

wormhole volume ratios (i.e. wormhole coverage index, WCI) and configurations. A comprehensive EOS-based fluid modeling was presented and used to simulate the sand-pack experiments. Experimental and numerical results were analyzed and effective liquid diffusion coefficients for different solvents were obtained. These experiments suggested that an improved heavy oil recovery could be achieved using hybrid application of solvents and hot water in CHOPS reservoirs. Also, to generate accurate predictions in field-scale simulation, an up-scaling procedure from laboratory results of the CSI process was suggested so that field-scale diffusion coefficients can be calculated based on different field properties.

In chapter 6, the obtained results were used in the field-scale history matched model to develop an uncertainty screening workflow. Field-scale cyclic solvent stimulation was performed and the main contributing factors - uncertain parameters and operational input - were recognized. An economics model was developed and after-tax NPV of the field at the end of cyclic solvent stimulation process was calculated as a profitability index of the process.

The final chapter summarizes the main contributions to the literature and industry.

Chapter 2: Modelling of Cold Heavy-Oil Production with Sand for Subsequent Thermal/Solvent Injection Applications

A version of this chapter was accepted for presentation at the SPE 2012 Energy Conference and Exhibition, Port of Spain, Trinidad, 11–13 June 2012, and was also published in Journal of Canadian Petroleum Technology, March 2014 issue, volume 53, number 2, pages 95-108.

Abstract

Although proved beneficial and economic for thin reservoirs, the cold heavy-oil production with sand (CHOPS) method has several limitations. The sand produced during CHOPS changes the geomechanical and petrophysical properties continuously and results in open channels in the reservoir known as wormholes. Also, the CHOPS method results in a low oil recovery (8–10% original oil in place). This entails a follow-up enhanced-oil-recovery (EOR) process, which is always an option for further exploitation, referred to as post-CHOPS.

Assessment of such a process through numerical simulation, as the most inexpensive yet most powerful tool, necessitates a comprehensive modelling approach to capture its dynamic physical nature. Only through such a realistic model can one obtain reasonably reliable reservoir characteristics after CHOPS that are critically important to assess post-CHOPS applications. To this end, we implemented a fractal pattern of different kinds by use of a diffusion-limited aggregation (DLA) algorithm as wormhole domain with a partial dual-porosity approach and a step-by-step simulation technique, taking advantage of a simple mathematical model to integrate the sand-production data with fractal patterns. The wormhole network is assumed to grow with more sand production, respecting geological conditions and well perforation. Moreover, its effective properties and the contained fluid can be controlled along its length and pattern at different steps. Such an option is of great assistance in the history-matching process. The model was validated successfully with available Alberta field data. As a preliminary step to post-CHOPS, several thermal, solvent, and hybrid combinations of both scenarios were considered.

The proposed method for CHOPS modelling is a useful approach to initiate a quick post-CHOPS study in practice if sand-production history is provided. One may also take advantage of its compatibility with any black-oil, compositional, or thermal simulators.

Introduction

CHOPS is accounted as one of the emerging primary production techniques in unconsolidated-sand reservoirs, mostly applied in Alberta, Canada. The aggressive coproduction of sand and heavy oil using progressing cavity pumps enhances the oil-production rate at economic conditions. Hence, CHOPS is a low-cost but practical production technology. However, non-stopping changes in petrophysical and geomechanical properties are inevitable, because of the withdrawal of sands from the reservoir. That creates high-permeability channels (i.e., wormholes) in the reservoir, which consequently may turn into a network serving as a natural multi-branched system among the wells. The so-called foamy oil is another issue to be considered in this recovery process.

Despite its low primary recovery factor, CHOPS has received a great deal of attention because of its lower cost compared with surface mining and other EOR methods. Field experience supports the idea of generation of a high-permeability channel-like medium during production by CHOPS. Continuous sand-production causes the wormholes to grow more, leading to a wormhole network, which connects the wells to each other. 4D-seismic imaging of some CHOPS reservoirs indicates tens of metres of linear channels away from the wellbore (Loughead and Saltuklaroglu 1992). Another justification for produced sand is the dilation theory. This theory assumes that sand production would lead to an altered region around the well, rather than generating a wormhole network. On the basis of the amount of sand production, the moving dilation theory suggests that the damaged region should be extended up to approximately 50 m away from the well after a certain time. But, field experience has shown that a well drilled only 300 m away encountered mud loss caused by hitting a wormhole channel **(Figure 2-1).**

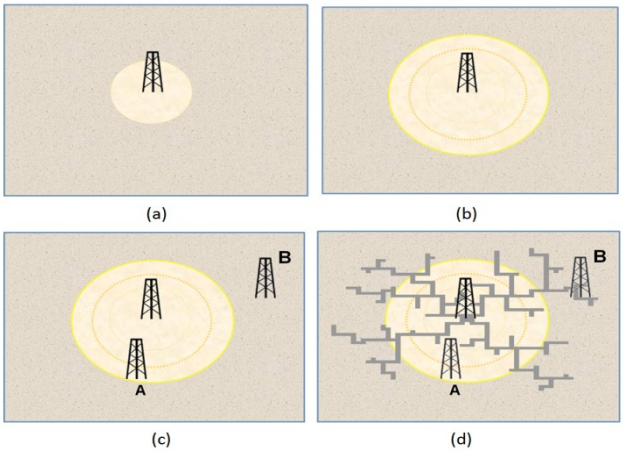

Figure 2- 1: Representation of possible wormhole network based on field experience (a) CHOPS well on production, (b) Developed dilated region, (c) Based on dilated region theory, "well A" should see the altered zone, but not "well B". (d) Field experience shows "well A" does not see the altered zone, but "well B" does, supporting the existence of wormholes.

The growing nature of a wormhole changes the stress conditions and reservoir properties, including permeability, porosity, and formation compressibility in a dynamic fashion. Such an alteration needs to be treated with a dynamic geological model, which is mostly referred to as static reservoir model in the conventional approach. In addition, when the reservoir pressure goes below the bubble point pressure and the dissolved gas is removed from the solution, the gas bubbles do not coalesce to form a single gas phase; rather, they remain as dispersed bubbles in the oil until they reach a critical saturation. In other words, the heavy oil tends to behave like foam.

In this paper, we begin with a critical review of CHOPS, focusing mainly on the practical outcomes of CHOPS modelling. Many of our efforts have been devoted to the demonstration of how the governing mechanisms can be modelled through convenient yet available engineering tools without significant compromise. One of the key objectives is to show the connections found useful among CHOPS, fractured reservoirs, and fractal analysis. Having defined a practical workflow for the history matching of CHOPS wells, we end up with a full-field model that is ready for any EOR studies and feasible optimization revisions.

Literature Review

We provided an extensive review of the efforts on CHOPS applications (modelling and field tests) in the conference version of the present paper (Rangriz Shokri and Babadagli 2012a). For brevity, we cover only the most remarkable findings that are supportive to our modelling methodology.

It can be argued that CHOPS is the most indebted procedure to Canadian companies who are the major contributors to heavy-oil production (Huang et al. 1998; Tremblay et al. 1996). Deliberate sand production along with viscous oil (500–15,000 cp) avoiding the use of sand-prevention techniques (slotted liners, gravel packs) results in higher oil-production rates and a high-permeability/porosity region or a wormhole network in the reservoir, confirmed by tracer tests, rapid interwell communications, linear-flow well signatures, seismic surveys, and laboratory observations (Coombe et al. 2001; Dusseault 1993; Lebel 1994; Meza 2001; Tremblay et al. 1996, 1997, 1999b; Squires 1993; Elkins et al. 1972; Yeung 1995; Smith 1986; Loughead and Saltuklaroglu 1992). These are typically thin (2–10 m) and shallow (350- to 600-m depth) reservoirs with high porosity (30–35%) and high permeability (1–5 darcie). Wells are mostly drilled vertically, rather than deviated, with large perforations (1 in.) and 20- to 40-acre well spacing (Sawatzky 2008-2009).

A limited number of experimental works published on cold production of oil and sand in vertical wells used sand-packs followed by X-ray scanning to obtain computed-tomography (CT) images of the examined samples (Mccaffrey and Bowman 1991; Squires 1993; Tremblay et al. 1996, 1997, 1998a, 1999a). The presence of a high-porosity/-permeability region, developed in line with perforations, was the first major observation. It was also observed that the development of a high-permeability channel needs a critical pressure gradient (Tremblay et al. 1997, 1998b). In another attempt, a recent experimental work was published using a triaxial cell to create sufficiently consistent stress conditions (Wong 2003).

EOR scenarios were also considered recently in relatively simpler models, both in ambient and non-ambient (close to reservoir pressure) conditions, providing ideas explaining post-CHOPS studies from waterflooding to thermal and solvent injections (Kantzas and Brook 2002). It should be noted that because of the nature of

CHOPS, post-CHOPS EOR experiments are difficult to conduct, but the overall findings are useful in understanding the processes.

To consider continuous sand production and foamy-oil flow, numerous analytical and numerical models have also been suggested. Some of the noteworthy work in CHOPS modelling are a 3D analytical model for transient flow (Wang and Chen 2002), a model to estimate sand transport in a partially filled wormhole (Yuan et al. 2002), a probabilistic active walker (Yuan et al. 1999), a fractal geostatistical model for wormhole growth (Liu and Zhao 2004), a transmissibility multiplier (Denbina et al. 2001) with a dual-porosity/dual-permeability approach (Tan et al. 2003), the use of negative skins around wells (Sanyal and Al-Sammak 2011), a dynamic well-radius module or a moving dilation region to improve well-productivity index (Istchenko and Gates 2011), and a coupled geomechanical and fluid-flow model (Liu and Zhao 2004). Most of these are used mainly to study the effect of wormhole patterns on oil production rather than for field history matching (Wang and Chen 2002). If there is no tool available to detect the wormhole network, using an equivalent damaged zone to model the wormhole-network extent would be a more-practical approach to follow (Rivero et al. 2010).

Physics of the CHOPS Process

Significant Recovery Mechanisms. There are two recovery mechanisms in CHOPS that may not be found in conventional reservoirs. The growth of a wormhole network as a consequence of sand production from the reservoir is the major reason for a higher oil-recovery rate. It increases reservoir access through the wormholes and, more importantly, improves both productivity and injectivity in heavy-oil reservoirs. The wormhole network may grow to distances up to hundreds of metres, tending to grow in preferred layers of clean sands with higher porosity (Sawatzky et al. 2002). Some CHOPS reports may not support a wormhole-network assumption. The absence of a wormhole in these fields can be explained with a lower oil viscosity and lack of strong directional geomechanical trend, resulting in sand settle down and sand pileup inside the well (Sanyal and Al-Sammak 2011). The wormhole branching in the field is reasonable because of the

inherent reservoir heterogeneity, but it would not be justified simply with pressure distribution along the wormhole length; more data are needed to explain the process.

The second recovery contributor is the foamy-oil behaviour of heavy oil. Foamy oil is simply the tendency of gas bubbles to not coalesce to create a continuous phase. Dispersed gas bubbles in oil (more compressible than the oil) move as slowly as the oil and cause the oil to swell, which provides drive energy through fluid expansion and reduces gas relative permeability as long as the free-gas saturation remains at zero (Maini and Sarma 1993; Maini 1999; Urgelli et al. 1999). Practical modelling of these two key recovery mechanisms shapes the proposed workflow for CHOPS modelling.

Current CHOPS Models. There are mainly two different approaches to model CHOPS. The first category focuses on efforts to predict the wormhole trail, on the basis of certain criteria for its growth; for instance, the pressure gradient at the tip of each individual wormhole. The wormhole would then grow if it exceeds a critical pressure gradient determined by rock properties. These models are difficult to use in practice because of difficulties in verification. These models require a true representation of a large (and accurate) body of input data from a field, which is quite impossible to achieve even for a single-well study.

An alternative is to use probabilistic methods to generate the wormhole network on the basis of a fundamental assumption that the wormhole network can represent a random behaviour. This is a satisfactory assumption only if there are no wormhole data available from other sources. The most practical approach is to adjust and update the wormhole network with seismic data or other resources, if available, as will be discussed in later sections.

With a model to represent the wormhole network, the second category would be able to deal with the fluid flow in the wormhole network. A negative skin or a changing wellbore radius to account for the wormhole is not compatible with the growing nature of the wormholes, but rather with the dilation theory. A single porosity also calls for fine grids and is thus not recommended. A coupled model of flow in wormhole/non-

wormhole domains could be a solution; however, making assumptions about the slurry flow properties in this model may be more reasonable than obtaining the actual data because they need detailed experimentation at reservoir conditions, and most often the experiments would fail to represent the true CHOPS behaviour.

Despite increasing central-processing-unit (CPU) time and convergence problems, the wormholes can be modelled using multi-segmentation of wells and updated on the basis of sand-production data. The flow inside the wells also can be controlled easily through well-performance calculations, resulting in a good production history of the whole field. However, they might not be used in the future for post-CHOPS studies because the wells are not expected to deform as a result of geomechanical changes. In addition, the post-CHOPS solvent injection calls for a diffusion process in which wells should not be treated as an option for a proper modelling procedure. These wells suffer from the basic problem of a large gridblock (often on the order of metres) to well size (on the order of centimetres) relationship and a high pressure drop, and because of this, near-wellbore modelling should always be considered as an additional step. Nevertheless, the connection factor among the well segments and the reservoir grid pose uncertainty during injection and production of hot or diluted fluids.

Considering the use of the CHOPS model later for the purpose of post-CHOPS applications, a more-practical approach could be the use of dual-porosity models. These models have been developed and employed extensively for fractured-reservoir modelling and simulation. They are compatible with compositional and thermal options, and they can handle the geomechanical effects on fluid flow through a change in volume of the grid cell, porosity, permeability, or formation compressibility. Because the wormholes are not expected to grow in all cells, the model should be treated as a partial dual medium. They benefit from a continuous connection of wormhole/non-wormhole domain and have the priority of being cost-effective compared with dual-permeability models. In this study, we preferred using this type of modelling and the proposed approach was observed to be flexible and modifiable to meet the engineering requirements of a field-development plan.

Typical Signature of a CHOPS Well. Figure 2-2 shows a single-well CHOPS recovery behaviour obtained from a well in a field in Alberta, Canada. As shown, oil production in a typical CHOPS well increases with an increase in sand production and reaches a peak value. Then, oil production gradually decreases with a decrease in sand production. It seems that the maximum oil recovery is dependent directly on the maximum sand production (Kobbe 1997). Sand production may be divided into two periods: a rapid expansion period (when wormholes grow faster and most unconsolidated sands are produced), and a slow expansion period (when growth of small wormholes and possible branches is more probable) (Yuan et al. 1999).

CHOPS reservoirs are usually above or at bubble point pressure. With a foamy behaviour for heavy oil, one may expect a constant gas/oil ratio. As a result, the gas rate would follow the same trend as the oil-production rate. However, the gas may not follow such behaviour if the reservoir is below bubble point and oil viscosity is not sufficiently high to exhibit foamy-oil behaviour. It is also important to note that CHOPS is commonly used in unconsolidated-sand reservoirs with no bottom water drive (Dusseault and El-Sayed 1999). The water trend would then be justified with possible perched and isolated water in different layers.

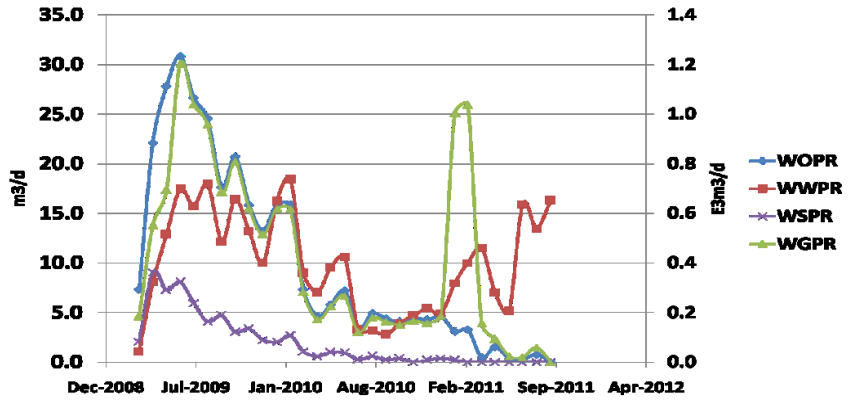

Figure 2- 2: Typical signature of a CHOPS well. WOPR (Well Oil Production Rate); WWPR (Well Water Production Rate); WSPR (Well Sand Production Rate); WGPR (Well Gas Production rate).

Desirable Engineering Data. For a continuous successful CHOPS practice, recording 4D-seismic data, running periodical well-log measurements, monitoring micro-seismic activities, and performing well tests are

needed. Updating the wormhole-network growth as a footprint of CHOPS is a challenging but essential step toward carrying out a field development. Such development could be interpreted from drilling infill wells to EOR implementations. Fluid analysis is another major issue. Obtaining accurate pressure/volume/temperature data to represent foamy-oil flow requires representative samples and detailed experimentation. Relative permeabilities, effective properties for slurry flow, and wormhole deformations should also be considered. Often, production rates are the only available data to build a model. In these cases, we should rely on valid correlations, models, and other tools in addition to our own engineering judgment. It is also important to work closely with other team members, from geologists to drilling engineers. The drilling report, especially sudden mud losses, geological maps, and interpreted seismic horizons are supportive in initiating the base model. All data from wells should be treated as a whole rather than as independently acting units. In short, the challenge would be to consider all (however limited) data from different origins in modelling the CHOPS process.

The Practice of CHOPS Modelling

Recalling previous attempts in modelling CHOPS, we prefer to follow the approaches of Tan et al. (2003) and Wang and Chen (2002), which include assuming that the wormhole network has a fractal pattern generated with a DLA algorithm extending from well/reservoir boundaries. However, we introduce two different porosity/permeability media to differentiate between wormhole/non-wormhole domain and what we refer to as partial dual porosity. The uncertainty is a yet-unknown kind of pattern type and its growth mechanism. Capturing the dynamic reservoir alterations, wormhole growth, and foamy-oil behaviour, and discovering the governing physics, are the main objectives of our research.

Fundamental Limitations and Assumptions. Considering the ultrahigh-permeability wormhole network, it is assumed that the reservoir is connected to the well through the wormhole domain. Wormholes are assumed to grow in clean sand layers because clean sands are expected to have a significantly weaker cohesive

strength. Because no detailed property map is available, a homogeneous and isotropic map is assumed for single-well studies. The DLA patterns then would develop in the selected layers to represent the wormhole network.

It is assumed that the slurry flow occurs only in the early life of the reservoir; therefore, it can be modelled through a change in fluid viscosity in wormhole domain. The pressure drop along the wormhole is the result of frictional, gravitational, and acceleration pressure gradient on the basis of the following equation (Liu and Zhao 2004):

$$\frac{\mathrm{d}P}{\mathrm{d}L} = -\tau_m \frac{\pi d}{A} - \rho_m g \sin\theta - \rho_m \frac{\mathrm{d}v^2}{\mathrm{d}L}. \quad \text{..... (2-1)}$$

As long as sand is present, and one is willing to consider a slurry flow in the wormholes, its viscosity may be introduced as μ_m, which represents mixture viscosity. Because of high oil viscosity, thin pays, and negligible vertical pressure drop, the vertical pressure gradient might be ignored. This leads eventually to the assumption of horizontal wormhole propagations rather than vertical ones because the wormhole has a tendency to grow in the direction of higher pressure gradient at its tip.

High oil viscosity, small wormhole diameter, and low velocity results in a Reynolds number sufficiently small to assume a laminar flow instead of a turbulent one. Gravity and kinetic components of pressure drop may be assumed to be negligible because of the almost-horizontal wormhole plane and low fluid velocity in the reservoir conditions. The remaining component, the friction term, can be summarized with fluid viscosity (preserving the wall frictional shear stress by itself). Therefore, modifying the Darcy equation through the viscosity and permeability terms seems sufficiently accurate to model a slurry flow in wormhole domain. One should notice that the wormhole-domain properties are totally different from non-wormhole domain, which is where the role of partial dual porosity comes into play. Needless to say, the pressure drop in the wormholes affects their fluid influx from non-wormhole domain.

For the post-CHOPS and late-life scenarios of CHOPS, we assume that wormholes have been practically emptied of sand; therefore, the fluid is no longer a slurry flow. This is an additional assumption to moderate the not-well-known slurry properties and should not be treated as a necessary condition.

Numerical Simulation Workflow. We propose an integrated approach combining the theory, fractured reservoir modelling, and an assisted history-matching process to model CHOPS. We have to find a compromise to meet some requirements, including integration between the geological and flow model in order to reproduce the dynamic response of a growing wormhole network, and to be flexible for subsequent updating. Moreover, we should be aware of the limited computation capabilities of commercial simulation software. To this end, a partial dual-porosity model is preferred to a single-porosity or a standard-dual-porosity model, or even a dual-porosity/dual-permeability approach. It is necessary to insist on the "partial" term in this approach, which means that all parts of the reservoir would be treated as a single-porosity medium; however, the wormhole network is taken into effect as a dual-porosity medium and would be attached to the single-porosity one, which was achievable using ECLIPSE and PETREL software (Schlumberger 2011). This approach reduces the CPU time significantly compared with other approaches and is more realistic for a conceptual flow model of the wormhole network. In our previous studies (Rangriz Shokri and Babadagli 2012a,b), we concluded that DLA or other fractal generating methods may be more reliable to represent the wormhole network. Public-domain Fractalyse 2.4 (L'Université de Franche-Comté 2014) was used for fractal analysis.

Introduction of a Growing Wormhole Network. A selected DLA pattern can be introduced to the geological model through a binarized form where unity represents the wormhole cells and zero represents the non-wormhole cells. The assigned cells with unity would be considered as dual-superposed grids—one for matrix and one for wormhole—and the assigned cells with zero would be treated as single-porosity grids. In the absence of data explaining porosity distribution or low-density regions, wormhole growth will be expected

to behave randomly, which might be the result of a random-nature distribution of petrophysical and geomechanical properties. It was also accepted that the pressure field in the wormhole network approximately obeys a Laplace equation, which is likely to be explained in terms of DLA (Liu and Zhao 2005a). A 2D-fractal pattern is assumed to extend along the reservoir layering, but the actual wormhole network would not be reserved only to one plane (Yuan et al. 1999). This may also be explained on the basis of overburden pressure acting as the central factor to impose the main stress; therefore, the lateral wormhole growth in a horizontal plane perpendicular to the main stress would be predictable. Nevertheless, the question pertaining to prediction of the wormhole growth remains unanswered.

These binarized fractal patterns are allowed to grow in the geological model at different time-steps on the basis of the cumulative sand production of each individual well. The role of additional active cells in the wormhole domain is enhanced with an increase in wormhole permeability. The added wormhole volume should be kept the same as the volume of sands produced. More sand production causes the wormhole to extend farther from the well toward the reservoir boundaries. One should consider that sand-production timing differs from well to well in a field study and makes the simulation unique to each case.

It may be argued that the model should reflect all the stress and pressure conditions to obtain accurate results. Literature contains different approaches for the characterization and representation of wormholes, but their use in practice may not quite be possible (Wang et al. 2001). For example, analytical and numerical failure models could not be used for field prediction in practice because they are not able to correctly predict the critical pressure gradient for sand production. At this step, what matters most is to capture the effect of the wormhole network on recovery rather than predicting the growth of each wormhole individually, which has never been verified to represent the underground structure (Tan et al. 2003).

Integrated Fractal Wormhole Model for Sand Production. The radius that a wormhole may develop around a well is critical in the history-matching process, especially in a field study, where different wells deliver different amounts of sand at different times. In the first sense, this radius as a function of time in a 2D

plane, $R(t)$ as depicted in **Figure 2-3**, would be a function of basic reservoir properties, mainly porosity and sand-production history as well as the overall stress conditions (Rangriz Shokri and Babadagli 2012b). If sand-production history is available for each well, then a simple volumetric calculation on sand data with selected fractal-pattern results in

$$V_s(t) = n\,[\pi\, R^2(t)\, f\, d\, \varphi_{add}\, NTG]\,, \quad \text{..... (2-2)}$$

and

$$V_s(t) = \Sigma Q_{sand} \Delta t_{sand}\,. \quad \text{..... (2-3)}$$

Here, V_s is the volume of sand produced as a function of time, Q_{sand} is the sand-production rate, Δt_{sand} is the sand-production time period, n is the number of assumed wormhole planes, f is the fractal pattern ratio, d is the wormhole diameter, Φ_{add} is the added porosity caused by sand produced, and NTG is net/gross ratio. Rearranging Eq. 2-3 gives

$$R(t) = m\sqrt{\frac{\Sigma(Q_{sand}\ \Delta t_{sand}\ )}{n\ \pi\ f d\, \varphi_{add}\ NTG}}\,. \quad \text{..... (2-4)}$$

The effect of overall stress conditions may be justified through a ratio m of two horizontal-stress components, σ_2 and σ_3. The fractal pattern ratio f can be obtained in a similar method, as in a box method, where

$$f = \frac{a}{\pi r^2}\,, \quad \text{..... (2-5)}$$

in which a is the surface area of the selected fractal pattern on an arbitrary circle (or oval), so that f becomes a unique function of each fractal pattern. Using the box method, we define

$$a = n_{cells} \times \Delta x_{cell} \times \Delta y_{cell}\,. \quad \text{..... (2-6)}$$

where n_{cells} denotes the number of wormhole cells in Circle r (or an oval, depending on the ratio of stress components), and Δx and Δy are cell dimensions in numerical model. A data set may be generated for each

selected fractal pattern. Higher values of f indicate that the fractal pattern spreads and takes more space in a 2D surface. Physically, this means the wormholes are more multi-branched. As wormholes develop, more fractal cells will be counted and f can be obtained appropriately. The integrated fractal pattern model may be used to specify the radius of the wormhole for each individual well in a field study, on the basis of different sand-time production.

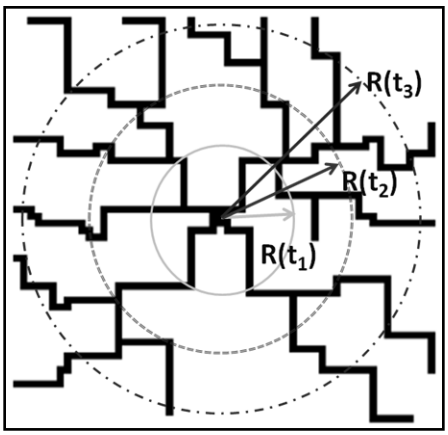

Figure 2- 3: A typical fractal pattern used for wormhole model.

Foamy-Oil Flow and Alternative Modelling Approaches. Heavy oil offers high critical gas saturation and slow gas nucleation process with a great tendency of the fluid to flow in a foamy-like pattern (Maini and Sarma 1993; Maini 1999; Urgelli et al. 1999). The gas relative permeability is small compared with oil relative permeability (Tang and Firoozabadi 2003). The foamy-oil compressibility is also significantly higher than the heavy-oil compressibility (Maini and Sarma 1993). It is also expected that foamy-oil stability increases with oil viscosity and higher dissolved-gas content and is more stable in porous media than in a bulk vessel (Sheng et al. 1997).

Two familiar models proposed by Total Fina Elf (TFE) and the Alberta Research Council (ARC) are available in literature (Bayon et al. 2002). The TFE model assumes gas could be described as solution gas (dissolved in the oil phase), dispersed gas (nonconnected bubbles moving slowly with oil phase), and free gas (connected gas phase moving faster than dispersed gas). The ARC model assumes four types of gases (including two dispersed gases). The gas relative permeability is a combination (or interpolation) of the dispersed- and free-

gas relative permeabilities. Implementing such models needs a broad range of laboratory and field data. It is also expected that a conventional two-phase model with appropriate parameters to heavy oil is more suitable for field application (Firoozabadi 2001). A higher critical gas saturation and depressed gas mobility are used in our study to capture the foamy-oil flow. In this method, the gas would not affect the oil-phase mobility adversely and would provide drive energy through gas expansion in each cell because of the higher critical gas saturation. This is consistent with what we know from foamy-oil flow. However, for an accurate representation of the relative permeability data, detailed experiments are needed.

Effective Properties of a Partial Dual-Porosity Model. For a single-well study, as a part of a full-field model, the geological grid was assumed to be homogeneous with respect to fundamental properties. For a field study, however, a uniform random distribution function is used to assign the porosity and permeability to each cell. The model is a fine grid so as to capture the ongoing physical mechanisms in our later applications and compositional studies. The absolute permeability and porosity of the matrix domain has an average value of 3,000 md and 0.35, respectively. The assigned value of the wormhole network is a function mainly of the assumed wormhole diameter. The permeability is assumed to be calculated as $k = 12.67\times10^6\, r^2$, based on laminar-flow theory (equality of Darcy and Poiseuille's equations). In this equation, k is permeability in darcices and r is pipe radius in cm, resulting in a permeability of 67,000 darcies, in our case. However, wormhole permeability might be used as a matching parameter. Wormhole porosity is approximately 65% in the reference case, which is sufficiently high for a realistic representation of the wormhole network. This porosity should be consistent with sand production and the integrated fractal wormhole model based on sand mass balance. The reservoir is as thin as 2.8–5 m, with a vertical anisotropy of 0.5, implying the inefficiency of gravity drainage. The wormhole matrix-transfer function is assumed to be similar to the conventional shape factor in a fractured reservoir, assigned as low as zero. **Table 2-1** summarizes the data used in the reservoir simulation.

Table 2- 1: Reservoir Properties used in the Reservoir Simulation

Reference model	Partial Dual Porosity
Grid dimension	60x60x20
Grid size	
X-direction	7.5 m
Y-direction	7.5 m
Z-direction	0.35 m
Initial reservoir pressure	2590 kPaa
Formation depth	425 mTVD
Average reservoir porosity	0.35
Average reservoir permeability	3,000 md
Dead oil viscosity	39,000 cP
Initial solution GOR	8-11 m3/m3
Average wormhole porosity	0.65
Average wormhole permeability	67,000,000 md

The oil viscosity was correlated using the Vasquez-Beggs and Beggs-Robinson correlations to take into account live heavy oil in reservoir temperature and pressure. The Wyllie and Gardner correlation in unconsolidated well-sorted sands was used to generate relative permeability curves in the matrix domain. Typical fracture relative permeability curves with no capillary pressure were used in wormhole domain. The oil viscosity in the wormhole domain may be adjusted with a slurry fluid, and foamy oil can be modelled with higher critical gas saturation and a depressed gas relative permeability.

Step-By-Step Simulation Technique. Because of the growing nature of the wormhole network, one needs to update the geological model. Sand-production data should be matched on the basis of the accuracy of the model. The common procedure is to divide the sand-production history into meaningful and practical periods, in orders of months. The simulation starts with a no-initial-wormhole assumption. The wormhole growth is predicted with the integrated fractal wormhole model for the first period, on the basis of the sand-production history and the selected fractal pattern. The simulation matches the fluid history in the first period and will provide a restart file to initialize the next step. The wormholes grow according to the fractal pattern until their extended volume equals the added sand production in the second period. Then, it will be followed with the fluid-flow simulation to match the production history in this step. This procedure is repeated until

the whole production history is matched. The history-matching process is illustrated in **Figure 2-4** for different stages of a single well. The choice of step size would depend mainly on the precision of the simulation results for sand production. Because a perfect match on sand data is not of high interest, a step size of 2–5 months is recommended, but it is possible to reduce the sand-calculation time-step to days without a significant change in final oil recovery. The authors would not recommend a small step size of sand calculations because it is time consuming and of no practical use.

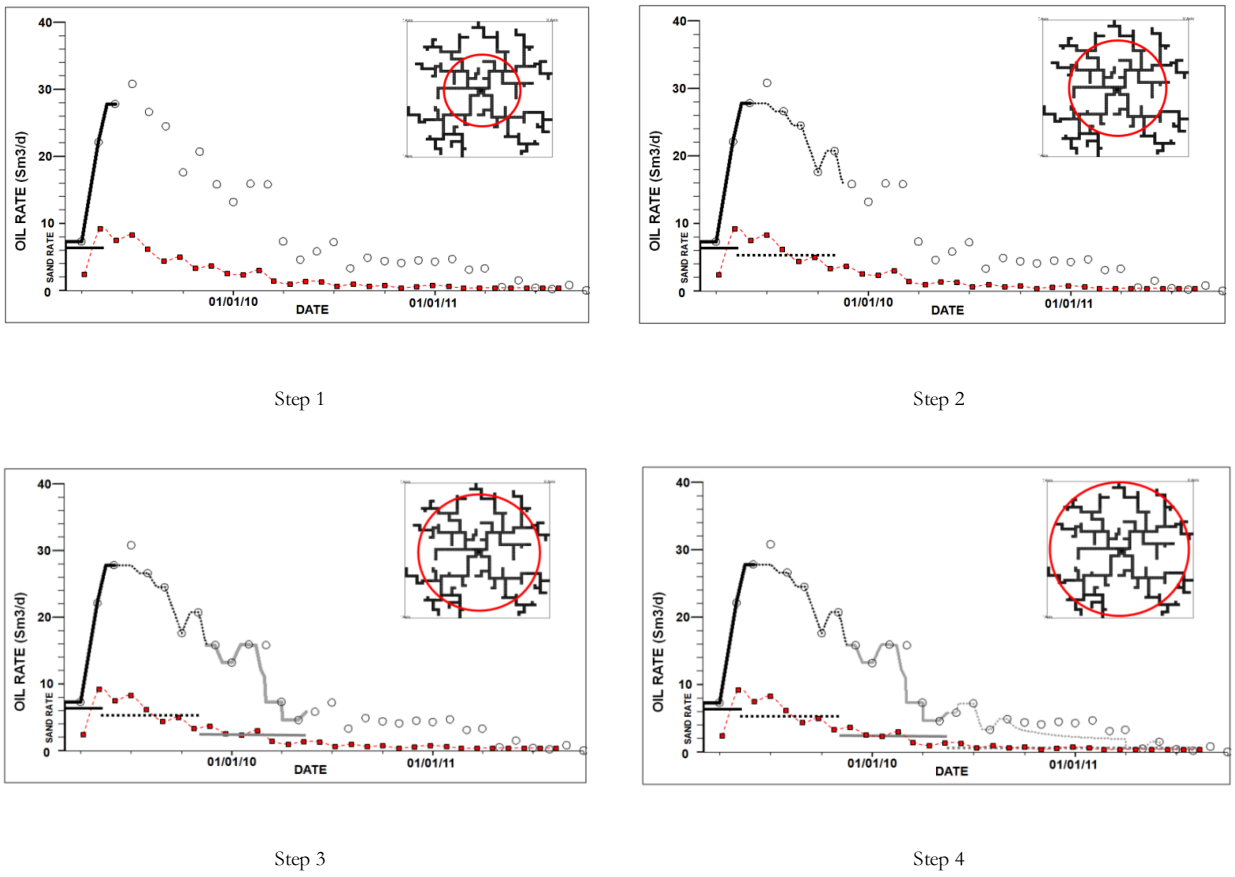

Figure 2- 4: Step-by-step simulation technique to match oil and sand production based on a growing wormhole pattern (black circles: oil rate history; red squares: sand rate history; lines: simulation rates). Note the growing nature of wormhole based on sand production shown in each step.

Initialization of a Post-CHOPS Study. Post-CHOPS simply refers to any EOR/improved-oil-recovery method used after CHOPS to increase the ultimate recovery factor. The history-matched model is now ready to be used to understand the effects of the wormhole network through compositional and coupled

geomechanical representation. As the trend of the sand-production curve suggests, the formation seems more stable after CHOPS has reached the end of its primary production, and there will not be a large amount of loose-sand production. This means the post-CHOPS scenarios may not even need to consider sand production in the modelling workflow if a nonaggressive recovery process is used. However, the model can be updated easily with new information obtained from 4D-seismic surveys and production data to investigate the broad category of EOR scenarios after CHOPS, and to optimize and predict the reservoir-fluid performance in such processes.

The principal difficulties with CHOPS reservoirs are the ultrahigh oil viscosity in the reservoir conditions, the possible sand production, and the inherent reservoir heterogeneity. The the common concern of EOR lies in increasing oil mobility with thermal and solvent injection, increasing reservoir drive energy (especially in shallow reservoirs), and decreasing the pressure drawdown in order to avoid mobilizing more sands.

The established wormhole network is the key factor to determine the post-CHOPS applications. At first look, it rejects any continuous steam and solvent injection, but with a smart production/injection pattern, such injection may be implemented in the form of so-called huff 'n' puff processes. A reduction in oil viscosity caused by thermal effects and significantly lighter heavy oil because of solvent injection are the chief active mechanisms in post-CHOPS. In this practice, the steam/hot water would be injected into the wormhole network, followed by a solvent/miscible-gas injection and a soaking period while the wells are shut in. Reservoir drive energy would be provided through these injections. The well is then allowed to produce in a blow-down period. These cycles would be potentially repeated.

Results and Discussion

First, we conducted a quick sensitivity analysis on uncertain parameters to accelerate the history-matching process. Then, we implemented our simulation workflow to match the production history of three wells from a field in Alberta. To check the compatibility of our model, some simple EOR scenarios were studied. Our main current effort is devoted to post-CHOPS applications in the whole field.

Sensitivity Study. A pre-generated fractal pattern was used to investigate how the reservoir would respond to a change in uncertain parameters. Initial reservoir pressure, rock compressibility, matrix and wormhole permeability, wormhole porosity, reservoir boundaries, oil viscosity, relative permeability, P_c curves, and skin of the production wells were the main data to be considered. The results were used as guidelines during the history-matching process.

Model Verification Through History Matching. Three wells were selected for the single-well history-match study, and each one was modelled individually with respect to the available data. Well 1 had a complete CHOPS signature, showing peak values in sand- and oil-production rates and a declining trend in both. A fractal pattern was selected, and the integrated fractal wormhole model was used along with a step-by-step simulation technique. At each time-step, the wormhole was allowed to grow on the basis of sand-production data and the permeability of the added wormhole cells was increased from matrix permeability to the calculated one, as described earlier, to obtain a history match as depicted in **Figure 2-5.** Note that the match on sand-production rate is not accurate, but we found it practically satisfying with respect to a better match on oil production and the time dedicated to the history-matching process (Figure 2-4).

Well 2 has not finished its primary production, as shown in **Figure 2-6,** and on the basis of sand-production data, the wormholes are not fully developed to reach the reservoir boundaries. Well 3 **(Figure 2-7)** exhibits the same behaviour as Well 1, given in Figure 2-5. It is interesting to see that the simulation results are suggesting primary production comes first from the vicinity of the wormhole network and the wormhole growth is dependent mainly on sand production, as is obvious in Well 2.

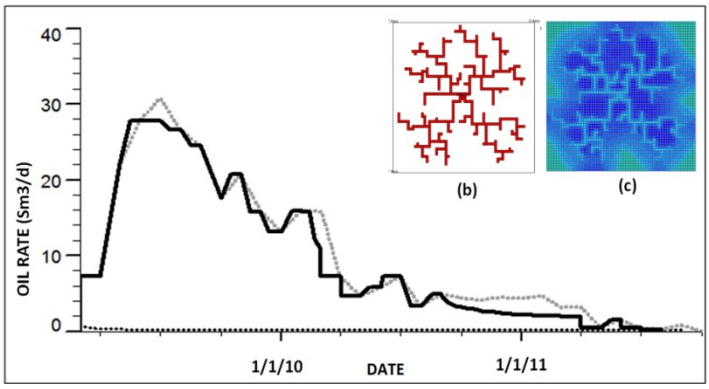

Figure 2- 5: Production profile of well 1 (a) Field oil production rate and matched simulation data for well 1 (dotted black line: well history; solid black line: step-by-step simulation results; dotted black line: CHOPS with no wormhole), (b) Fractal wormhole pattern, (c) Oil saturation profile.

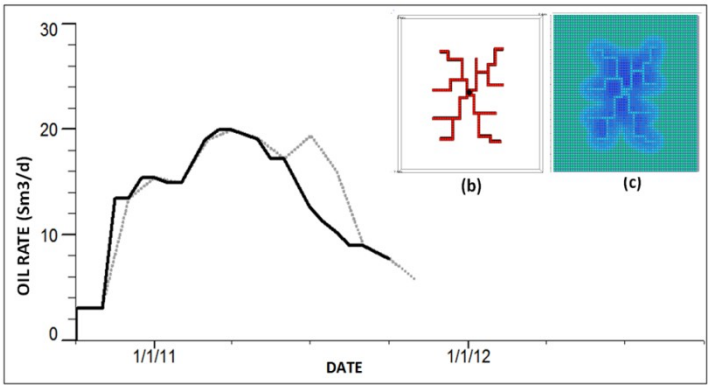

Figure 2- 6: Production profile of well 2 (a)Field oil production rate and matched simulation data for well 2 (dotted black line: well history; solid black lines: step-by-step simulation results), (b) Fractal wormhole pattern, (c) Oil saturation profile.

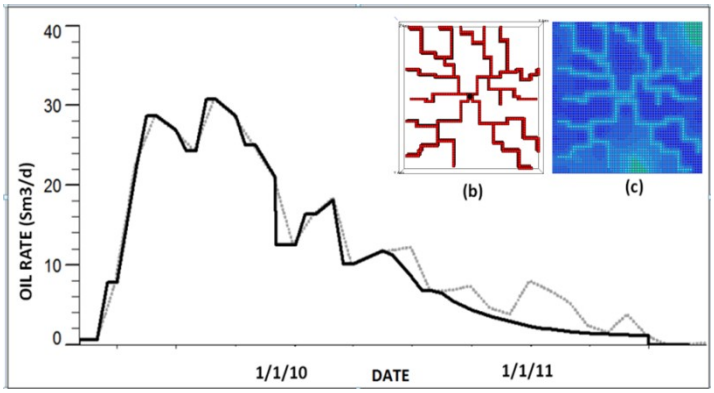

Figure 2- 7: Production profile of well 3 (a)Field oil production rate and matched simulation data for well 3 (dotted black line: well history; solid black lines: step-by-step simulation results), (b) Fractal wormhole pattern, (c) Oil saturation profile.

We also noticed that the step-by-step simulation technique is not a necessary task in single-well studies with low sand production and short histories. But when it comes to a field study with numerous wells, skipping this step is not recommended because it results in unrealistic saturation distribution. Introducing the whole wormhole network at once would be the first region to be depleted in a simulation study. Thus, a step-by-step simulation along with a growing wormhole network is needed for an accurate modelling of the process. This is the most consistent approach to coincide with what we already know about CHOPS and wormhole-network growth.

Wormhole Network Patterns. Sand production would eventually result in a network of high-permeability wormholes, and would most often create interconnections among the existing wells. The wormhole network is assumed to work efficiently in the same way as a possible multi-segment horizontal well; therefore, the detection of its distribution is critical in developing the field using EOR options or infill drilling. As stated earlier, the presence of a wormhole network is more reliable than a dilated region assumption. Conducting time-lapse-seismic surveys in some reservoirs showed that the sand production is not only sourced from near-wellbore regions, but has also shaped high-porosity high-permeability channels (Yale et al. 2012). In addition to numerical modelling, it is theoretically possible to use the dimensionless pressure-derivative curves to distinguish the behaviour between simple representation and fractal patterns (Liu and Zhao 2005b). However, in this study, no pressure-transient test was available and we were limited to numerical simulation. First, we studied three extreme cases, though some may not have sound physical evidence: a well-developed fractal pattern, a large-conduit pattern (assuming wormholes are like fracture corridors), and a distant-sand-sourcing pattern (assuming developed wormholes would be fed more from the sands of reservoir boundaries), as shown in **Figures 2- 8, 2-9, and 2-10,** respectively.

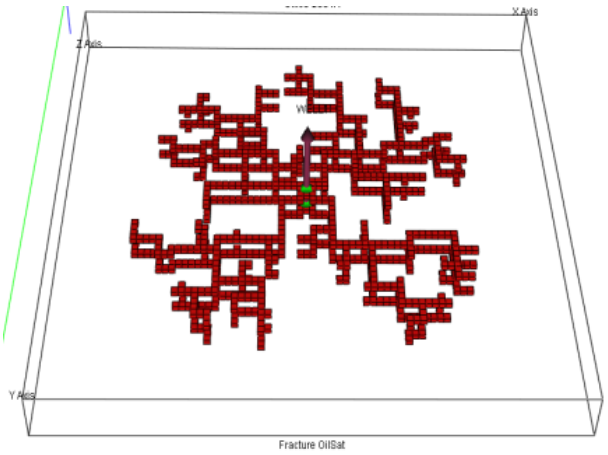

Figure 2- 8: Fractal pattern 01 for wormhole domain.

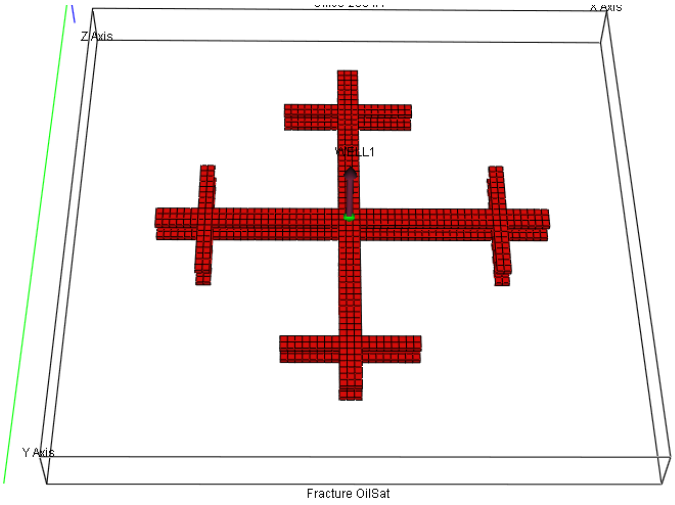

Figure 2- 9: Large-Conduit pattern for wormhole domain.

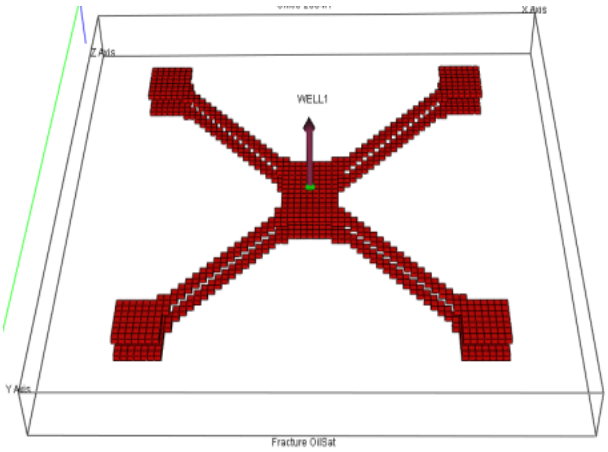

Figure 2- 10: Distant-Sand-Sourcing pattern for wormhole domain.

It was not practical to obtain a good history match on the patterns given in Figures 2-9 and 2-10. Even with the largest possible pressure drawdown, the reservoir is not able to deliver oil to the assumed well. Note that the wormhole cells were activated in accordance with sand mass balance. On the contrary, if a fractal pattern was selected to represent wormholes, the growth of wormholes would result in sufficient fluid production to match the production history **(Figure 2-11).** However, to obtain the best match, it was necessary to extend this pattern to reach farther regions near reservoir boundaries. The first observation was the impact of wormhole extension on oil recovery through more reservoir access, which resulted in a greater oil-production rate.

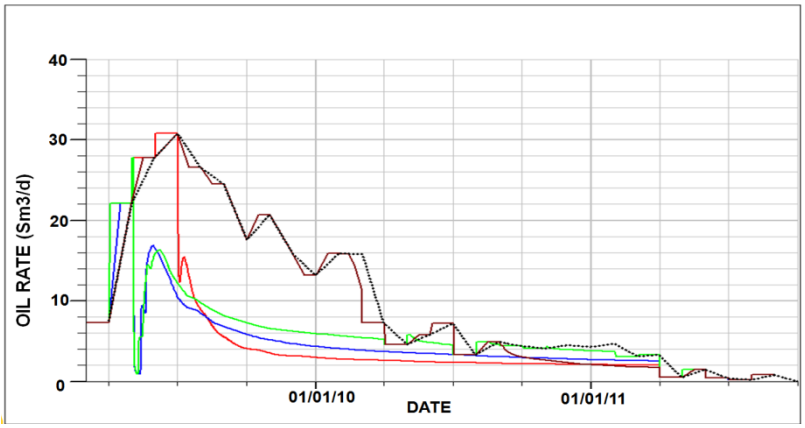

Figure 2- 11: Field Oil Production Rate (dotted black line: well history; solid red line: fractal pattern 01; solid blue line: large-conduit pattern; solid green line: distant-sand-sourcing pattern; solid brown line: extended fractal pattern 01).

We also studied numerous different fractal patterns, some depicted in **Figures 2-12 through 2-17. Figure 2-18** shows that different wormhole patterns would possibly give the same results if they had developed sufficiently to reach most of the reservoir regions. The effects of perforation on developing wormholes were assumed with a preferred growth direction for fractal patterns. The results show that the oil recovery would not be efficient if the wormholes were not developed in all directions. Moreover, the effect of branching or fractal configuration is not critical in primary production, but there may be fundamental issues in post-CHOPS applications. In primary production, it is sufficient that the reservoir be contacted by some wormholes in most regions, but when it comes to thermal or solvent injection, the provided contact area with wormholes for injected fluids would play an important role.

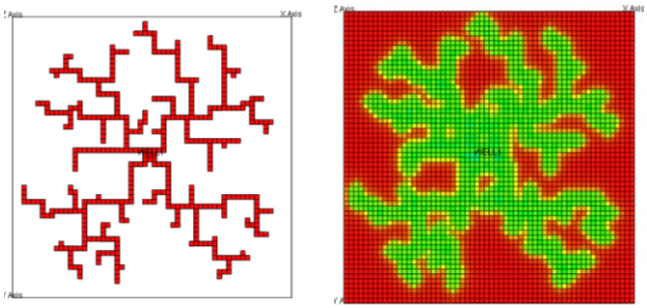

Figure 2- 12: Fractal pattern 01 and its resulted oil saturation profile.

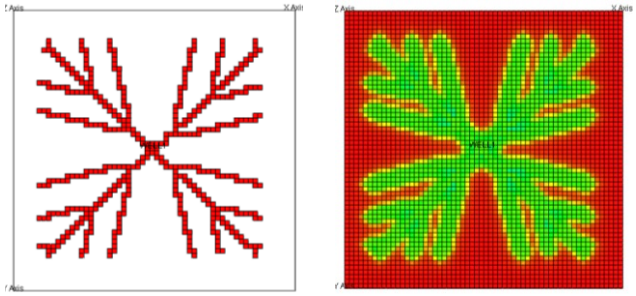

Figure 2- 13: Fractal pattern 02 and its resulted oil saturation profile.

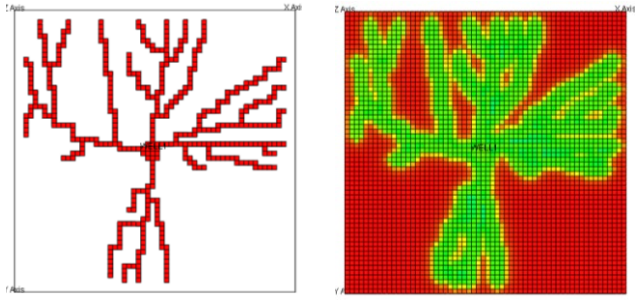

Figure 2- 14: Fractal pattern 03 and its resulted oil saturation profile.

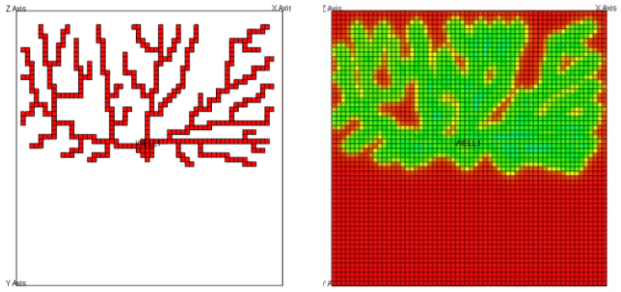

Figure 2- 15: Fractal pattern 04 and its resulted oil saturation profile.

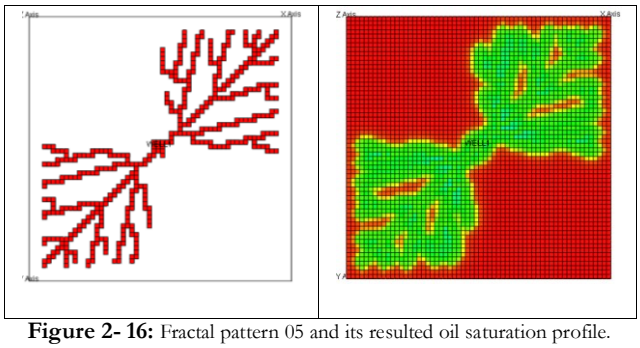

Figure 2- 16: Fractal pattern 05 and its resulted oil saturation profile.

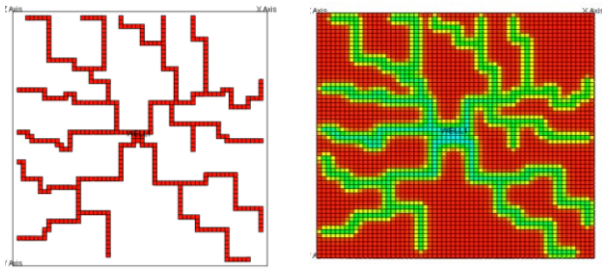

Figure 2- 17: Fractal pattern 06 and its resulted oil saturation profile.

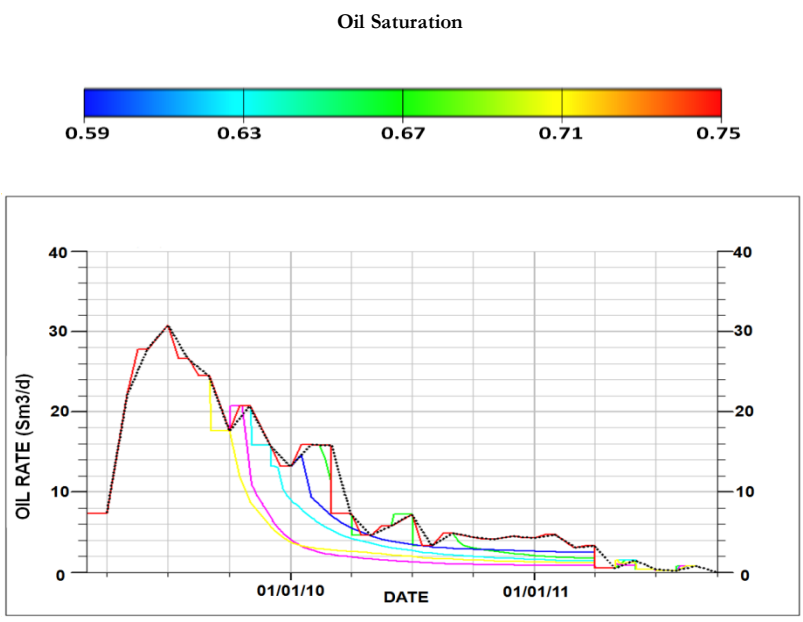

Figure 2- 18: Field oil production rate for several fractal patterns shown in Figures 2-12 through 2-17 (dotted black line: well history; solid green line: fractal pattern 01; solid dark blue line: fractal pattern 02; solid light blue line: fractal pattern 03; solid purple line: fractal pattern 04; solid yellow line: fractal pattern 05; solid red line: fractal pattern 06).

Gridblock Size Sensitivity. True representation of wormholes in simulation workflow is the main difficulty in modelling the CHOPS process. As mentioned previously, a DLA pattern is introduced to account for

wormhole growth; however, the box dimensions to analyze this fractal image would result in different binarized grids based on the required level of details of the study performed **(Figure 2-19).**

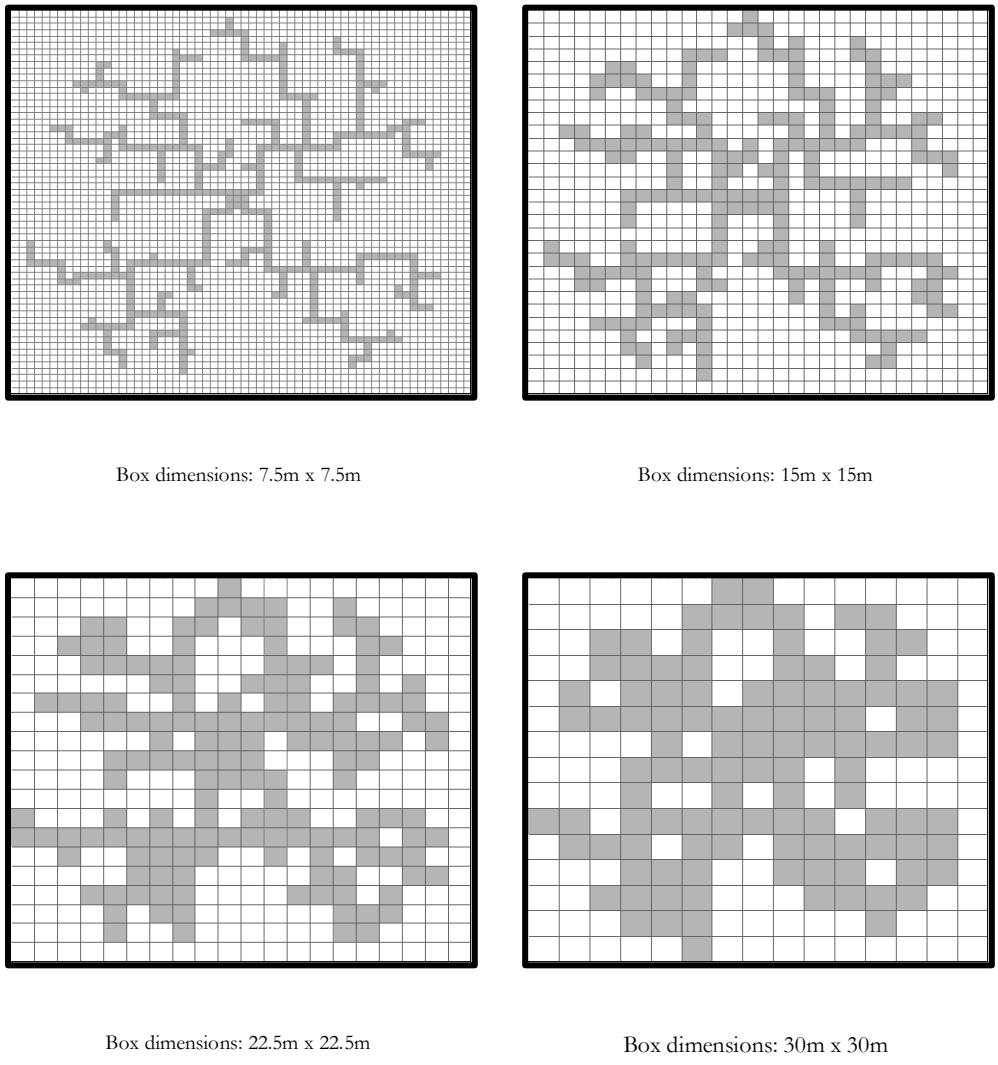

Figure 2- 19: A single fractal pattern for wormholes with different box dimensions.

Figure 2-19 shows that with an increase in the size of box dimensions, the wormhole pattern might not be represented in significant detail, but the simulation would be more cost-effective. With proper modification of the added porosity on the basis of gridblock size and integrated wormhole fractal model, it is feasible to obtain sufficiently accurate results in the history-matching process. The specifications and results of upgridding and uplayering a fine model for a single well are summarized and shown in **Table 2-2 and Figure 2-20,** respectively.

Table 2- 2: Specification of the Upgridded Wormhole Models.

Case	Grid Dimensions	Cell Size (m^3)	Total Active Cell Number		Legend Color in Figure 2-20
			Matrix	Wormhole	
Reference Model	60 x 60 x 20	7.5 x 7.5 x 0.35	36000	916	Black
Coarse 1	60 x 60 x 10	7.5 x 7.5 x 0.7	18000	916	Green
Coarse 2	30 x 30 x 10	15 x 15 x 0.7	9000	456	Red
Coarse 3	20 x 20 x 10	22.5 x 22.5 x 0.7	4000	308	Brown
Coarse 4	15 x 15 x 10	30 x 30 x 0.7	2250	216	Blue

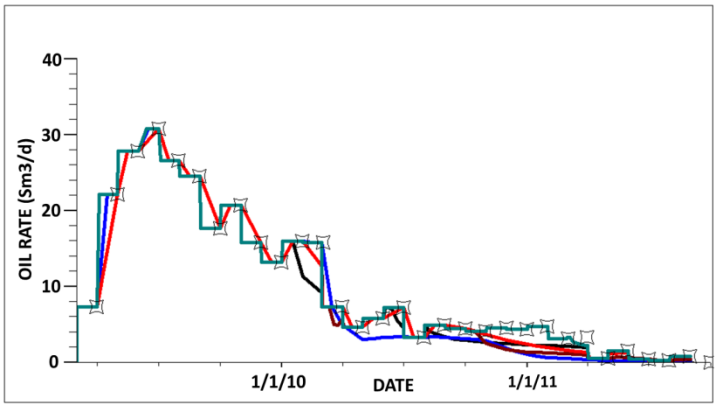

Figure 2- 20: Field oil production rate and matched simulation data for well 1 with different grid block sizes (See Table 2-3).

The results of simulation suggest that the upgridding process is possible in proposed CHOPS modelling, but it has a limitation. By coarsening the grid to a certain limit, the wormhole pattern may disappear into a dilation zone that covers most of the reservoir, thereby diminishing the role of wormholes. In this case, matching production history may not be of practical use. Therefore, keeping the grid size at a level able to represent the details of wormholes (shy of transitioning into a fully dilated zone) should be considered as a constraint of this approach.

Predicting the CHOPS Well Performance. The proposed CHOPS methodology is introduced mainly as a tool to provide a simulation restart file for further post-CHOPS studies assuming no or limited sand would be produced after CHOPS primary production. Hence, it should not be considered as a predictive tool that

governs the ongoing geomechanical effects and sand production on the basis of stress conditions. As long as no detailed data are available from the field (e.g., wormhole properties and their footprints), no methodology would be able to truly predict the CHOPS signature. However, we used the sand-production trend, allowing the wormholes to grow on the basis of a DLA pattern, and then, a single-rate constraint model was used to predict the flow behaviour. **Figure 2-21** shows that the model is able to predict the oil-production rate if proper data of wormholes are assumed. Note that Figure 2-21 is not a history-matching process; rather, it is obtained only with a single-rate constraint through the whole simulation time, providing a tuned growing wormhole pattern on the basis of available sand-production data.

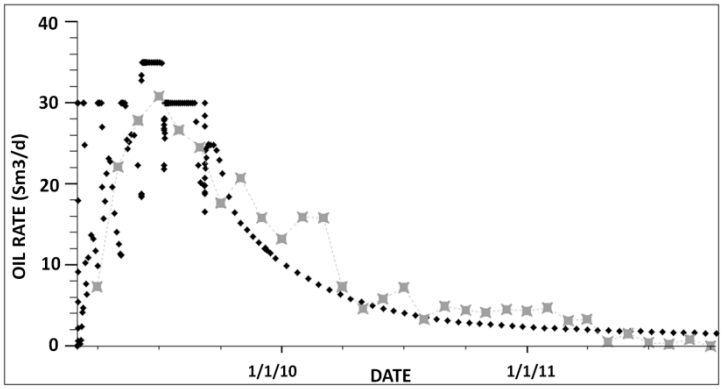

Figure 2- 21: Predicting oil production rate based on a tuned wormhole growth pattern (black dots: simulated oil rate, grey dots: oil rate history).

Post-CHOPS Applications

Model Options and Inherent Difficulties. The main difference between EOR modelling of CHOPS and non-CHOPS is that heavy oil lies in the presence of a growing wormhole network. To this end, EOR applications are basically expected to be modelled in the same way for both cases. Because of the nature of heavy oil and lack of compositional data, it is more reasonable to begin with a black-oil approach to an initial assessment on the potential of single-well post-CHOPS EOR. We propose two typical possible applications after CHOPS: steam and/or solvent injection. Once again, we will begin with the black-oil-type modelling to avoid the complexity and expense of using a compositional simulation.

The black-oil approach has its own limitations in modelling thermal and solvent injection. However, implementation of dual-porosity type structure of the wormhole system generated in the previous exercise for CHOPS modelling would be significantly simpler with the black-oil approach. The common practice for solvent modelling in a black-oil simulator is to implement the Todd-Longstaff empirical model. The effects of physical dispersion between the miscible components in the hydrocarbon phase would then be modelled through an empirical parameter ranging from zero (poor mixing) to unity (full mixing) that controls the degree of fluid mixing in each grid cell through fluid density, fluid viscosity, and relative permeability curves. This mixing parameter can be used in the history-matching process. It is important to mention that the compositional modelling of physical diffusion/dispersion processes during solvent injection calls for fine grids; otherwise, the numerical diffusion inherited in finite difference makes the model unreliable (Schlumberger 2011). However, a compositional approach might be used later in a segment model to study the governing mechanisms.

Thermal application also can be studied in heavy oil because of a large reduction of oil viscosity with an increase in reservoir temperature. The black-oil simulator has the ability to solve the energy-conservation equation at each time step and update the grid-block temperatures. The new temperatures will be used to calculate the oil and water viscosities for the subsequent time step. In this approach, the thermal properties of the rock and fluids should be provided for each study. The choice of grid size is more noticeable in thermal application because of the addition of energy-conservation equations. In short, the selection of black-oil or compositional simulation is based on the concerns and limitations caused by cost and time issues and the availability of the input data, grid block-size requirements for the representations of the wormhole grid system, and realistic representation of the governing mechanisms for accurate modelling.

Post-CHOPS EOR. A vast number of papers have been published in the literature on EOR applications for heavy oil, but none of them consider completely the presence of a wormhole network. The use of realistic physical models to represent the effects of sand production on post-CHOPS is rather difficult. In one of the

limited studies for post-CHOPS EOR, waterflooding, polymer flooding, gas injection, and gas pulsing were studied through a set of experiments, at both ambient and reservoir conditions, without considering the changes in in-situ stresses (Kantzas and Brook 2002). Air injection was also suggested for such thin reservoirs (Miller et al. 2002), but the success and applicability of the in-situ combustion method, even in a simple heavy-oil reservoir, is still in question because of the difficulty of monitoring and controlling of this process. The cyclic solvent injection showed some potential for post-CHOPS applications in the form of CO_2 injection in a long sand-pack system (Alshmakhy and Maini 2012). However, more efforts are needed for field-scale modelling of this kind of experimental approach on the realistic wormhole models to assess the effect of heterogeneous and unstable structure of the reservoir on the distribution of the injected material.

As observed, in addition to the inherent difficulties in experimental modelling, one of the main challenges in post-CHOPS applications is the assessment of the techniques through numerical simulations. In this paper, we propose and implement a post-CHOPS simulation approach based on the model developed for CHOPS presented. As a starting point, a huff 'n' puff cycle of only steam, solvent, and a hybrid combination of steam and solvent was considered in a single well. Obviously, the whole process is highly dependent on the wormhole patterns and parameters (Shandrygin et al. 2010), but the role of the wormhole network will be covered in this practice. Different single-well application scenarios, as listed in the following, were tested. Note that the cycles are arbitrary and may be later defined in practice through field optimization.

- Scenario 1: Steam (hot water) injection
    - 15 days: steam injection
    - 15 days: soaking (production well shut in)
    - 240 days: oil production
- Scenario 2: Solvent (miscible gas) injection
    - 15 days: solvent injection

- 15 days: soaking (production well shut in)
- 240 days: oil production

- Scenario 3: Steam and solvent injection
  - 7.5 days: steam injection
  - 7.5 days: solvent injection
  - 15 days: soaking (production well shut in)
  - 240 days: oil production.

The amount of total injected fluid is the same in all scenarios in order to compare with huff 'n' puff. **Figure 2-22** shows the simulation results, and it appears that solvent-over-steam injection would work more efficiently than steam injection or solvent injection individually. It is obvious that continuous steam injection is uneconomic in thin reservoirs, especially with the presence of a wormhole network. Solvent processes may overcome the costly steam generation, but recovering solvent back from a heterogeneous reservoir while a slow diffusion process is happening is a major issue. It seems that the main recovery mechanisms are a large reduction in oil viscosity caused by heating the reservoir and further dilution of heated oil by solvents. **Figure 2-23** presents the oil-saturation profile at the end of the first injection cycle of steam, solvent, and combination of steam/solvent in a layer located at the top of the the wormhole layer. **Figure 2-24** shows the same oil-saturation profile at the wormhole layer. Comparing them in each case, it indicates that the heated and diluted oils have a greater tendency to move downward to the wormhole network plane in the case of the combination of steam and solvent injection. It results in lower oil saturation at the top layer and higher oil saturation at the wormhole layers, which subsequently leads to more oil production. Further compositional studies are needed to describe the active mechanisms in more detail.

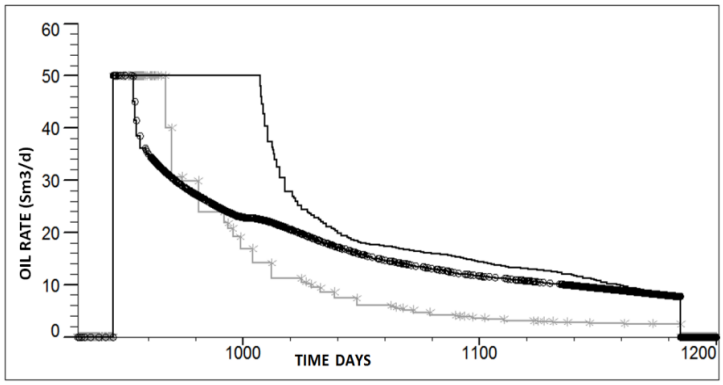

Figure 2- 22: Well#1 - Field oil production rate due to injection of (a) steam (hot water) (grey-line), (b) solvent (miscible gas) (thick-black), and (c) steam-over-solvent (thin-black).

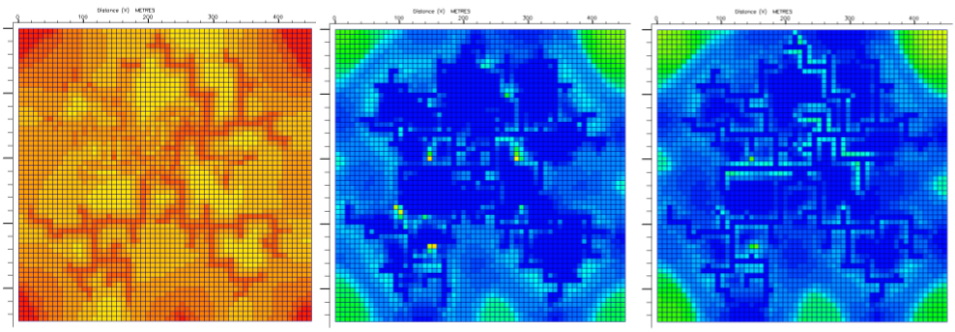

(a) **(b)** **(c)**

Figure 2- 23: Oil saturation profile from top view at the end of first cycle of (a) steam (hot water) injection, (b) solvent (miscible gas) injection and (c) steam-over-solvent injection over the wormhole plane.

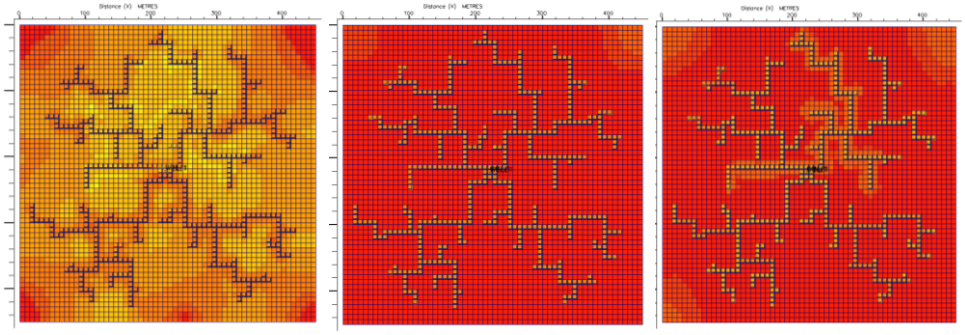

(a) **(b)** **(c)**

Figure 2- 24: Oil saturation profile from top view at the end of first cycle of (a) steam (hot water) injection, (b) solvent (miscible gas) injection and (c) steam-over-solvent injection in the wormhole plane.

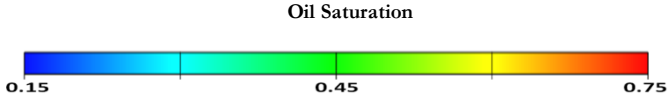

In addition to a large reduction in oil viscosity by heating or oil dilution with the help of solvents, providing the drive energy through injection is a major concern to be considered in post-CHOPS applications. Reservoirs are typically shallow and the pressure difference between reservoir and well is not sufficiently high to mobilize the heated or diluted heavy oil. The first simulation results indicate that the injection of the same amount of steam or solvent has a different impact on increasing the reservoir pressure. The solvent contributes more to provide drive energy than the steam because it also can be observed for steam over solvent injection. The reason behind this is that miscibility conditions could be achieved to some extent during cyclic solvent stimulation.

The pressure response to oil production after the first injection phase also behaves in a different way, as shown in **Figure 2-25.** It is worth noting that the cyclic well stimulation is considered in a single well with limited boundaries that results in a rapid pressure decrease during the production phase. Because the wormhole network is assumed among different wells in the field, studying more than a cycle for a single-well study is performed only for preliminary analysis and is not recommended for a field-development determination. In this case, cyclic times become more critical or the continuous-injection option using the connectivity among the wells through the wormhole network should be considered (Rangriz Shokri and Babadagli 2012b).

In a further attempt, the effect of soaking time on oil production was studied. **Figure 2-26** shows that the soaking period, indicated as Soak-01 (15 days), Soak-02 (30 days), and Soak-03 (60 days), did not change the ultimate oil-recovery factor, but it might accelerate the recovery process and eventually affect the economics of the project. The type of injected fluid is more critical on oil recovery than the soaking period time. The relative incremental oil recovery on the basis of the primary recovery factor, shown in **Figure 2-27,** confirms this statement. However, this shows that the combination of steam and solvent injection leads to higher oil production, keeping in mind that the amount of injected solvent or steam is reduced to half of its value compared with only solvent or only steam injection.

It should be highlighted once again that there are certain issues that cannot be analyzed through black-oil simulation because of its limitations in capturing uncertainties in the analysis of post-CHOPS applications involved in compositional changes. These issues should be addressed through a compositional study, which is our current effort (Rangriz Shokri and Babadagli 2013). Our preliminary observations from compositional models, with the inclusion of the wormhole system generated given in Figures 2- 3 through 6, indicate that a stability problem exists and defining the interaction between the matrix and wormholes require further work. Hence, the main contribution of this study, in addition to the CHOPS modelling proposed and tested on real field cases, is to introduce a practical framework for CHOPS modelling with respect to its compatibility with compositional, thermal, and geomechanical options to be used in field-scale post-CHOPS studies. The preliminary analysis performed provides an insight into the post-CHOPS potential of single-well-based EOR applications.

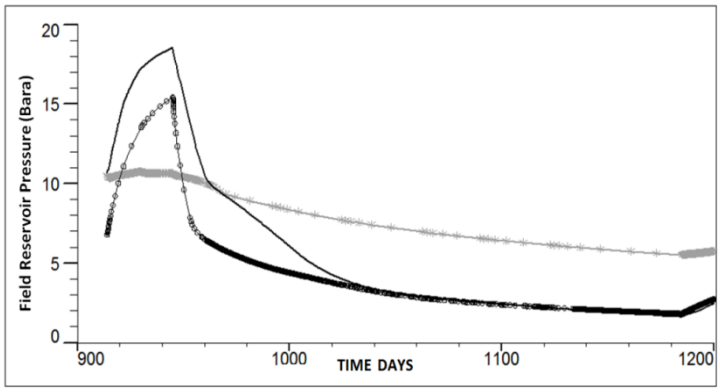

Figure 2- 25: Well#1 - Field reservoir pressure at the start of injection of steam (hot water) grey-line, solvent (miscible gas) thick-black and steam-over-solvent thin-black.

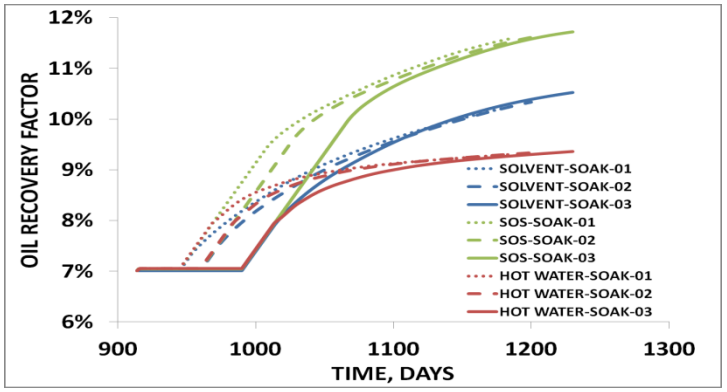

Figure 2- 26: Effect of soaking period and the injection fluid on oil recovery factor.

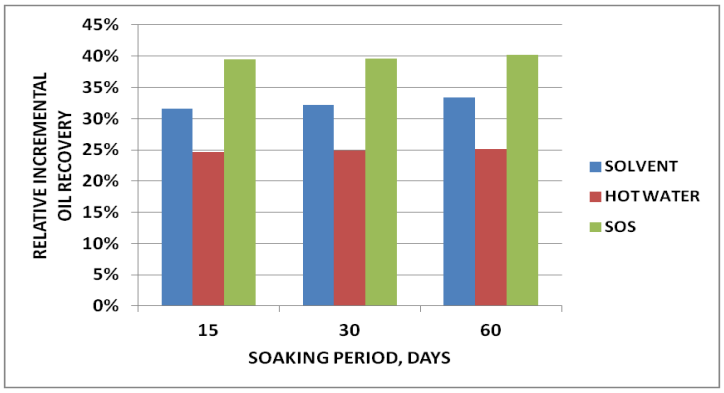

Figure 2- 27: Relative incremental oil recovery at the end of first cycle in a single well.

Conclusions

In this study, we defined a practical workflow for CHOPS modelling based on a step-by-step simulation technique and a fractal pattern for wormhole network. A DLA pattern was presented and may be implemented in a reservoir simulator with a partial dual-porosity approach. An integrated fractal wormhole model was introduced to help with the growing nature of wormholes based on reservoir properties and sand-production data. Moreover, foamy-oil flow was modelled with sufficient accuracy through a modified gas relative permeability. History matching was achieved in three single CHOPS wells. A fractal pattern was noted to be more reliable to represent wormholes. In addition, fractal configuration may not influence the primary production, but can affect the post-CHOPS recovery. The compatibility of our approach with thermal and compositional processes was studied through a simple huff 'n' puff process with cyclic injection of steam, solvent, or steam or solvent together. Such a process may later be considered as a technical possibility to increase the ultimate oil recovery from the CHOPS reservoir.

References

Alshmakhy, A. and Maini, B. B. 2012. A Follow-Up Recovery Method After Cold Heavy Oil Production. SPE157823-MS presented at the SPE Heavy Oil Conference Canada, Calgary, Alberta, 12-14 June.

Bayon, Y. M., Cordelier, Ph. R., Coates, R. M., et al. 2002.Application and Comparison of Two Models of Foamy Oil Behavior of Long Core Depletion Experiments. SPE paper 78961 presented at the SPE International Thermal Operations and Heavy Oil Symposium and International Horizontal Well Technology Conference, Calgary, Alberta, Canada, 4–7 November.

Coombe, D., Tremblay, B., Tran, D., et al. 2001. Coupled Hydro-Geomechanical Modeling of the Cold Production Process. SPE paper 69719 presented at the SPE International Thermal Operations and Heavy Oil Symposium,Porlamar, Margarita Island, Venezuela, 12-14 March.

Denbina, E.S., Baker, R.O., Gegunde, G.G., et al. 2001.Modeling Cold Production for Heavy Oil Reservoirs.*Journal of Canadian Petroleum Technology***40** (3).

Dusseault, M. 1993.Cold Production and Enhanced Oil Recovery. *Journal of Canadian Petroleum Technology* **32** (9): 16-18.

Dusseault, M. and El-Sayed, S. 1999. CHOP – Cold Heavy Oil Production. Paper presented at the 10th European Symposium on Imperial Oil Recovery, Brighton, UK, 18–20 August.

ECLIPSE Technical Manual, Schlumberger 2011.

Elkins, L.F., Morton, D., and Blackwell, W.A. 1972. Experimental Fireflood in a Very Viscous Oil-Unconsolidated Sand Reservoir, S. E. Pauls Valley Field, Oklahoma. Paper SPE 4086 presented at the 47th Annual Fall Meeting of the Society of Petroleum Engineers of AIME, San Antonia, Texas, 8–11 October.

Firoozabadi, A. 2001.Mechanisms of Solution Gas Drive in Heavy Oil Reservoirs.*Journal of Canadian Petroleum Technology*. **40** (3).

Huang, W., Marcum B., Chase, M.R., et al. 1998. Cold Production of Heavy Oil from Horizontal Wells in the Frog Lake Field.*SPE Reservoir Evaluation & Engineering*. **1** (6): 551-555.

Istchenko, C.M. and Gates, I.D. 2011.The Well-Wormhole Model of Cold Production of Heavy Oil Reservoirs.SPE150633-MS presented at the SPE Heavy Oil Conference and Exhibition, Kuwait, 12-14 December.

Kantzas, A. and Brook, G. 2002.Preliminary Laboratory Evaluation of Cold and Post-Cold Production Methods for Heavy Oil Reservoirs Parts A and B. CIPC Paper 2002-079 presented at the Petroleum Society's Canadian International Petroleum Conference 2002, Calgary, Alberta, Canada, 11-13 June.

Kobbe, W. 1997. AIME New York Meeting, American Institute of Mechanical Engineering Transactions, Vol. LVI, p. 814, February.

Lebel, J.P. 1994. Performance Implications of Various Reservoir Access Geometries. Document presented at the 11th Annual Heavy Oil & Oil Sands Technical Symposium "Challenges and Innovations" March 2nd.

Liu, X. and Zhao, G. 2004. Effects of Wormholes on Cold Heavy Oil Production. Paper presented at the Petroleum Society's 5th Canadian International Petroleum Conference (55th Annual Technical Meeting), Calgary, Alberta, Canada, 8 – 10 June.

Liu, X. and Zhao, G. 2005a. A Fractal Wormhole Model for Cold Heavy Oil Production.*Journal of Canadian Petroleum Technology***44** (9): 31-36.

Liu, X. and Zhao, G. 2005b. Transient Pressure Behavior of Cold-Heavy Oil Production Wells. SPE paper 97791 presented at the SPE/PS-CIM/CHOA International Thermal Operations and Heavy Oil Symposium, Calgary, Alberta, Canada, 1-3 November.

Loughead, D.J. and Saltuklaroglu, M. 1992. Lloydminster Heavy Oil Production: Why So Unusual. Paper presented at the 9th Annual Heavy Oil and Oil Sands Technology Symposium, Calgary, Alberta, Canada, 11 March.

Maini, B. B. and Sarma, H. K. 1993. Significant of Foamy-Oil Behavior in Primary Production of Heavy Oils.*Journal of Canadian Petroleum Technology***32** (9): 50-54.

Maini, B. B. 1999. Foamy Oil Flow in Primary Production of Heavy Oil under Solution Gas Drive. Paper SPE 56541 presented at the SPE International Conference, Houston, Texas, 3-6 October.

Mccaffrey, W. and Bowman, R. 1991. Recent Successes in Primary Bitumen Production. Paper presented at the 81st Annual Heavy Oil and Oil Sands Technical Symposium, 14 March.

Meza, B. 2001.Experimental Investigation of Sand Production into a Horizontal Well Slot.MSc Thesis, School of Mining and Petroleum Engineering, University of Alberta (Fall 2011).

Miller, K.A., Moore, R.G., Ursenbach, M.G., et al. 2002.Proposed Air Injection Recovery of Cold-Produced Heavy Oil Reservoirs.*JCPT***41** (3): 40-49.

Rangriz Shokri, A. and Babadagli, T. 2012a. Evaluation of Thermal/Solvent Applications withand Without Cold Heavy Oil Production with Sand (CHOPS). Paper SPE 158934 presented at the SPE Energy Conference, Developing Resources for Sustainability, Port-of-Spain, Trinidad, 11-13 June.

Rangriz Shokri, A. and Babadagli, T. 2012b. An Approach to Model CHOPS (Cold Heavy Oil Production with Sand) and Post-CHOPS Applications. Paper SPE 159437 presented at the SPE Annual Technical Conference and Exhibition, San Antonio, Texas, USA, 8-10 October.

Rangriz Shokri, A. and Babadagli, T. 2013. Modeling Thermal and Solvent Injection Techniques as Post-CHOPS Applications considering Geomechanical and Compositional Effects. Paper SPE 165534 presented at the 2013 SPE Heavy Oil Conf., Calgary, AB, Canada, 11-13 June.

Rivero, J. A., Coskuner, G., Asghari, K., et al. 2010. Modeling CHOPS Using a Coupled Flow-Geomechanics Simulator with Non-Equilibrium Foamy-Oil Reactions: A Multiwell History Matching Study. Paper SPE 135490 presented at the SPE Annual Technical Conference and Exhibition, Florence, Italy, 19-22 September.

Sanyal, T. and Al-Sammak, I. 2011.Analysis of the First CHOPS Pilot for Heavy Oil Production in Kuwait. Paper CSUG/SPE148966 presented at the Canadian Unconventional Resources Conference, Calgary, Alberta, Canada, 15-17 November.

Sawatzky, R. 2008-2009. Cold Production: Recovery Mechanisms and Field Performance. Presented as an SPE Distinguished Lecture in Calgary, Alberta, Canada.

Sawatzky, R.P., Lillico, D.A., London, M., et al. 2002.Tracking Cold Production Foot Prints. Paper 2002-086presented at the Petroleum Society's Canadian International Petroleum Conference 2002, Calgary, Alberta, Canada, 11–13 June.

Shandrygin, A., Dinariev, O., Mikhailov, D.,et al. 2010.Enhancing Efficiency of Steam-Thermal Treatment of Formations with High Viscosity Oil. Paper presented at the SPE Russian Oil and Gas Conference and Exhibition, Moscow, Russia, 26–28 October.

Sheng, J.J., Maini, B.B., Hayes, R.E., et al. 1997. Experimental Study of Foamy Oil Stability. *Journal of Canadian Petroleum Technology* **36** (4): 31–37.

Smith, G.E. 1986. Fluid Flow and Sand Production in Heavy Oil Reservoir under Solution Gas Drive. Paper SPE 15094 presented at the 56th California Regional Meeting of the Society of Petroleum Engineers, Oakland. CA, 2–4 April.

Squires, A. 1993. Inter-Well Tracer Results and Gel Blocking Program. Technical paper presented at the 10th Annual Heavy Oil and Oil Sands Technical Symposium, 9 March.

Tan, T., Slevinsky, R., and Jonasson, H. 2003.A New Methodology for Modeling of Sand Wormholes in Field Scale Thermal Simulations.Paper presented at the Canadian International Petroleum Conference, Calgary, Alberta, 10–12 June.

Tang, G.Q., Firoozabadi, A. 2003. Gas- and Liquid-Phase Relative Permeabilities for Cold Production from Heavy Oil Reservoirs.*SPE Reservoir Evaluation and Engineering***6** (2): 70-80.

Tremblay, B. Sedgwick, G. and Forshner, K. 1996. Imaging of Sand Production in a Horizontal Sand Pack by X-Ray Computed Tomography.*SPE Formation Evaluation***11** (2): 94-98.

Tremblay, B. Sedgwick, G., Forshner, K. 1997.Simulation of Cold Production in Heavy-Oil Reservoirs: Wormhole Dynamics.*SPE Reservoir Evaluation & Engineering* **12** (2): 110–111.

Tremblay, B. Sedgwick, G., and Vu, D. 1998a. CT Imaging of Sand Production in a Horizontal Sand Pack Using Live Oil. Paper 98-78 presented at the 49th Annual Technical Meeting of the Petroleum Society, Calgary, Alberta, Canada, 8–10 June.

Tremblay, B. Sedgwick, G., and Forshner, K. 1998b. Modeling of Sand Production from Wells on Primary Recovery.JCPT **37** (3): 41–50.

Tremblay, B. Sedgwick, G., and Vu, D. 1999a. CT Imaging of Wormhole Growth under Solution Gas Drive. *SPE ResEval&Eng***2** (1) 37-45.

Tremblay, B., Sedgwick, G., and Vu, D. 1999b.A Review of Cold Production in Heavy Oil Reservoirs. Paper 2008 presented at the 10th European Symposium on Improved Oil Recovery, Brighton, UK, 18-20 August.

L'Université de Franche-Comté. 2014. Fractalyse - Fractal Analysis Software 2.4. http://www.fractalyse.org/fr-home.html

Urgelli, D., Durandeau, M., Foucault, H., et al. 1999. Investigation of Foamy Oil Effect from Laboratory Experiments. Paper SPE 54083 presented at the SPE International Conference, Bakersfield, California, USA, 17-19 March.

Wang, Y. Chen, C., and Dusseault, M.B. 2001. An Integrated Reservoir Model for Sand Production and Foamy Oil Flow during Cold Heavy Oil Production.Paper SPE 69714 presented at the SPE International Thermal Operations and Heavy Oil Symposium, Palomar, Margarita Island, Venezuela, 12–14 March.

Wang, Y. and Chen, C. Z. 2002. Simulating Cold Heavy-Oil Production with Sand by Reservoir-Wormhole Model. Paper presented at the Canadian International Petroleum Conference, Calgary, Alberta, Canada, 11-13 June.

Wong, R.C.K. 2003.Sand Production in Oil Sand under Heavy Oil Foamy Flow.*JCPT***42** (3).

Yale, D. P., Hoda, N., and Wang, J. 2012. Enhancing the CHOPS Process through Reservoir Conditioning, World Heavy Oil Congress, Aberdeen, UK, 10-13 September.

Yeung, K. 1995.Cold Flow Production of Crude Bitumen at the Burnt Lake Project, Northeastern Alberta. Paper presented at the 1995 UNITAR International Conference on Heavy and Tar Sands, Houston, Texas, 12-17 February.

Yuan, J.Y, Tremblay, B., and Babchin, A. 1999. A Wormhole Network Model of Cold Production in Heavy Oil. Paper SPE 54097 presented at the SPE International Thermal Operations and Heavy Oil Symposium, Bakersfield, California, 17–19 February.

Yuan, J.Y., Babchin, A., and Tremblay, B. 2002. A Model for Sand Transport through a Partially-Filled Wormhole in Cold Production. *JCPT* **41** (4): 25-32.

Chapter 3: Field Scale Modeling of CHOPS and Solvent/Thermal Based post CHOPS EOR Applications Considering Non-Equilibrium Foamy Oil Behavior and Realistic Representation of Wormholes

A version of this chapter was accepted for presentation at the SPE Annual Technical Conference and Exhibition held in San Antonio, Texas, US, 8-10 October 2012, and was also submitted to the Journal of Petroleum Science and Engineering.

Abstract

Due to its lower cost, the cold heavy oil production with sands (CHOPS) method is a common primary production recovery technique, not only in Canada where it originated, but also in many other countries including Venezuela, Kuwait, Russia and China. However, this method has several practical limitations. It continuously changes the geomechanical and petro-physical properties of the reservoir due to the sand produced, resulting in high permeability channels known as wormholes. In addition, this method has a low oil recovery factor (5-15 %) and this entails further recovery techniques.

Thermal methods after CHOPS are not usually favorable due to heterogeneity and reservoir instability. In addition to this, CHOPS wells are not completed for thermal (steam) operations. The CHOPS method is typically applied in thin formations in which heating by injected steam is characteristically inefficient. Solvent injection possesses similar problems caused by heterogeneity and cost. An option could be the hybrid application of steam/solvent. Assessment of this technique first requires a realistic modeling of the CHOPS process. Due to dynamic changes in reservoir properties, no valid model was available to accurately simulate field-scale CHOPS production.

Our main focus in this paper is to present a quick workflow for CHOPS modeling to investigate efficient EOR/IOR methods after CHOPS. To achieve this, we first propose a partial-dual porosity approach coupled with algorithms for wormhole generation to create a realistic static reservoir model. After generating fractal wormhole patterns of different kinds using a diffusion limited aggregation (DLA) algorithm, they were introduced into a reservoir model. It is assumed that wormhole's properties are a function of its radius and can be controlled along its length and pattern, which facilitates the history matching process. Based on fractal analysis, novel upgridding procedures for wormhole network in partial dual porosity models were introduced. After validation of the models using data obtained from a field in Alberta, several preliminary post-CHOPS scenarios including thermal, solvent and thermal/solvent hybrid applications were simulated.

The new modeling workflow, proposed and validated to model the CHOPS process with realistic wormholes representations along with a simple mathematical wormhole network growth model, are the primary contributions of this paper. Secondarily, hybrid steam/solvent applications were evaluated from technical and economics points of view using this validated static model and compared with the sole application of steam and solvent.

Key words: CHOPS modeling, fractal wormholes, upscaling, post CHPOS EOR, solvent injection, field scale application.

Introduction

CHOPS is a common primary cold recovery technique in Canadian unconsolidated sand reservoirs. In this technology, sand is allowed to be produced along with oil. This co-production of oil and sand increases the oil production rate in a dramatic fashion. Recent literature revealed the successful application of the technique at the field scale as well as in laboratory experiments and numerical simulations. An extensive review of the published data can be found in our recent publication (Rangriz Shokri and Babadagli, 2014). Two issues, however, are to be addressed: (1) very low ultimate recovery of CHOPS that definitely requires challenging further EOR applications, and (2) understanding the physics of the wormhole growth process and representing it accurately in the simulation model for further assessment applications.

The production of sand, leading to a wormhole network, is absolute evidence of all the changes happening in the reservoir. The most probable explanation is that the sand production leads to the generation of a network of wormholes which continues to grow and develop in the vicinity of the wellbore or far beyond it, within the reservoir. This means that, as long as the sand production occurs, the fundamental geological parameters such as permeability, porosity and formation compressibility are altered. Therefore, any model which utilizes a time-independent static model for its flow simulation shall not be considered a suitable one. This phenomenon, known as wormhole growth, provides high-permeability channels for fluid to flow and is accounted for a higher oil production rate.

The foamy oil behavior ranks probably as the second significant contributing parameter. Foamy oil, which is usually discussed with heavy oil, is the reluctance of small gas bubbles to coalesce to create a continuous phase. Thus, the small bubbles preferentially remain as dispersed in the oil rather than being a free phase. This phenomenon causes the oil to swell which provides more drive energy and, as long as the free-gas saturation is still zero, the dispersed gas moves with the same velocity as the oil phase, i.e. there is no free gas movement. One may compare this fact with conventional oil in which the emergence of free-gas saturation decreases the oil mobility due to a higher gas relative permeability and lower viscosity.

As mentioned above, the key question is a very low recovery factor of CHOPS. Therefore, one of our main objectives in this paper is to investigate possible ways to recover this remaining oil using efficient EOR methods. To do so, there is a need to understand CHOPS and to illustrate the changes in the reservoir caused by this technology. For the time being, no unique solution has been reported to model CHOPS in practice, hence, there is no "CHOPS" option in any commercial simulator software. Like in all other parts of the petroleum world, there is a huge amount of uncertainty, which should be captured and addressed realistically. We extend our previous efforts with the new simulation technique that is believed to take the network wormhole growth and foamy oil behavior into account. We first show how the knowledge of a naturally fractured reservoir can play an astonishing role by integrating fractal patterns to represent CHOPS wormholes. This mathematical model shows how far the wormhole can develop from the wellbore in a homogeneous reservoir while the effects of all stresses are considered the same.

After demonstrating the validity of our wormhole modeling approach using the field data obtained from a field in Alberta, different steam and solvent based EOR schemes in this thin and loose reservoir are evaluated. A hybrid combination of steam and solvent turned out to be a good candidate as the discussion unfolds.

CHOPS Flow Behaviour

The production of a typical CHOPS well is initiated with an increase in the oil rate as well as sand. The oil production reaches a peak-value and then it decreases gradually. This peak-value is expected in the sand trend, too. If the foamy-oil flow behavior is a sound theory of gas evolution within the reservoir and possibly the wellbore, the gas-to-oil ratio should be considered constant and the gas rate would follow the same trend as the oil. The behavior of oil, gas, and sand of a CHOPS well is depicted in **Figure 3-1**, as reported by Rangriz Shokri and Babadagli (2014). Note that gas production may not necessarily follow this trend in a highly depleted pressure region, for instance around the wellbore, where free gas phase might have been created. When a single well study is performed, it is assumed that the wormholes do not reach the boundaries. But in real field cases, the wormholes of each well may meet each other, so that the wells would be connected through a high-permeability wormhole domain. Therefore, the well behavior should be considered with regard to the whole field rather than as an independently acting unit.

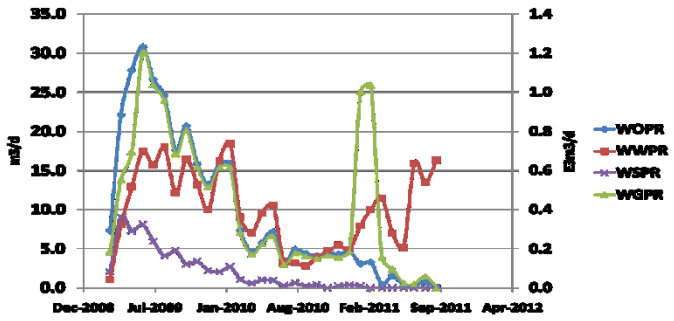

Figure 3- 1: CHOPS well signature: WOPR (Well Oil Production Rate); WWPR (Well Water Production Rate); WSPR (Well Sand Production Rate); WGPR (Well Gas Production rate) of a typical CHOPS well.

CHOPS Modeling Workflow

Challenges in CHOPS Modeling

As explained, continuous sand production leads to a dynamic alteration in reservoir properties like porosity, permeability and formation compressibility. This necessitates a dynamic geological model for simulation studies. A negative skin around wells (Sanyal and Sammak, 2011), use of multi-segment wells (Istchenko and Gates, 2014) or a moving dilation region to improve well productivity index were previously proposed simplifications to model the CHOPS process. Modeling of the wormhole growth is the key parameter that makes a distinction among these models. In general, wormhole growth can be modeled using probabilistic methods or alternatively, a failure criterion at wormhole's tip such as a critical pressure gradient. Both approaches were used in the literature; however, it was observed that the latter approach to be a time-consuming process (Liu and Zhao, 2004). In addition, one should notice that modeling each wormhole individually needs accurate details about CHOPS formation which is impossible to achieve in practice. For instance, to predict the wormhole growth based on a critical pressure gradient at its tip, one needs huge and precise information of geomechanical properties (cohesion of the grains at each point, true failure criteria considering impact of fluid saturation on strength properties, impact of bubble nucleation on rock cohesion, and ...) in field-scale. Providing such meticulous information is practically impossible even in a single-well study, because the resolution of seismic/microseismic activity, well logging, and ... is not sufficiently high to provide such information. In addition, the uncertainty associated with true representation of CHOPS reservoir conditions would prevail accuracy of any data obtained from laboratory experiments. To this end, Rangriz Shokri and Babadagli (2014) proposed to integrate the probabilistic approaches with available field data such as sand production history, porosity or density map to adjust and update the wormhole network as a whole and not each individual wormhole as an independently acting unit.

Apart from wormhole growth, modeling the wormholes as pipes/multi-segment wells brings many unknown parameters into account. Defining a connection factor for each well segment with simulation grids, pressure drop along segments, at the connection of segments to each other and to the well, well production control of each segment, wellbore friction options, representation of multi-phase and slurry flow along segments, segment-to-segment crossflow, and crossflow within the individual segments and ... are some other concerns which necessitates additional experimentation. Also, representing wormholes with pipes/multi-segment wells is not able to consider the geomechanical effects of the reservoir, which could be a critical issue in the post-CHOPS applications.

In the present study, we preferred the approach previously tested by Tan et al. (2003) and Wang and Chen (2002), assuming that the wormhole network should be a fractal pattern, extending from the wellbore to the reservoir boundaries. The reasons behind adopting this approach were the many field evidences and reported experiments supporting this idea. While a moving dilation region suggests that the wormholes should be extended up to ~50 meters away from the well at time t_1, a well drilled just some 100 meters away encountered mud loss due to meeting the wormhole domain in some field cases. The uncertainty is a yet-unknown kind of pattern gap and type and its growth mechanism. Capturing these dynamic reservoir alterations, wormhole growth, foamy oil behavior, and discovering the governing physics are the main challenges in modeling the CHOPS process.

Methodology Followed for Simulation

Following our previous work (Rangriz Shokri and Babadagli, 2014), we propose an integrated approach combining fractal theory, fractured reservoir modeling and simulation, and the history matching process to model CHOPS. A partial dual porosity model is preferred to a single porosity, a standard dual porosity, or a dual porosity-dual permeability approach. "Partial" in this context means that all parts of the reservoir are considered a single porosity medium, but the wormhole network corresponds to the fracture domain by attaching a selected dual porosity model to a single porosity model. This was achieved using ECLIPSE and PETREL software (ECLIPSE Technical Manual, 2011). This approach reduces the CPU time significantly

compared to regular dual porosity or dual porosity-dual permeability approaches. In our previous study (Rangriz Shokri and Babadagli, 2014), we reached the conclusion that the wormhole network may be best represented with a fractal pattern using DLA or other fractal generating methods. Public domain Fractalyse 2.4 (http://www.fractalyse.org/fr-home.html) was the software used for fractal analysis.

The fractal pattern was then binarized with different box dimensions to incorporate the wormhole network into the numerical simulation model. The sand production data was used to control/adjust the wormhole network growth. The entire simulation time was divided into certain periods based on production trends followed at different life spans of a well, but not necessarily equal intervals. The wormhole was allowed to grow for the first period based on sand production history, and then the flow model started to match the fluid production history. Wormhole extent and its permeability are usually the first matching parameters. Once a match was obtained, the second sand production period allowed its growth and this continued until the simulation covered the entire field history. The interested reader is referred to (Rangriz Shokri and Babadagli, 2014) for more details. The results for a single CHOPS well taken from Rangriz Shokri and Babadagli (2014) are shown in **Figure 3-2**. As seen, the wormhole network was extended at each step based on the DLA/fractal theory as indicated by the red circle. This methodology is flexible enough to be compatible with any kind of black-oil, compositional or thermal approaches. Upgridding and upscaling procedures for this method will be defined later in this paper.

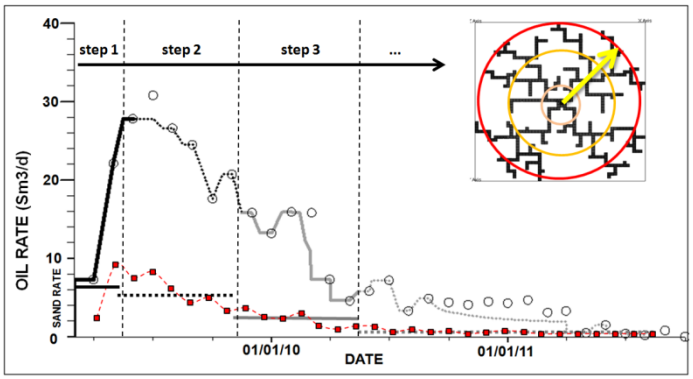

Figure 3- 2: Step-by-step simulation technique to match oil and sand production based on a growing wormhole-fractal pattern (black circles: oil rate history; red squares: sand rate history; lines: simulation rates). Note the growing nature of wormhole based on sand production history indicated at each step.

Assigning Reservoir Properties to Flow Model

We used a uniform random distribution function to assign the porosities and permeabilities to the field-scale case. The reference model is a very-fine grid with millions of cells to capture the on-going physical parameters in our later applications (mainly the post-CHOPS EOR process). The absolute permeability of the matrix-domain is between 1500 to 4500 md, with an average of 3000 md. The porosity of the matrix-domain varies between 0.15 and 0.40 with an average of 0.35. The assigned value to the wormhole network (fracture-domain) is mainly a function of the wormhole diameter using the laminar flow theory in capillary tubes (equality of Darcy and Poiseuille's laws), as $k = 12.67*10^6 r^2$ where *k* is permeability in Darcy and *r* is pipe radius in cm. A permeability of about 67,000 Darcy was assigned to the wormhole domain. However, the permeability of the wormholes may be used as a matching parameter. Fracture porosity is about 0.65 which is high enough for a realistic representation of the wormhole network. The matrix-wormhole transfer function was a low value close to 0. The reservoir thickness is from 2.8 m to 5 m which is not sufficient to have significant gravity effects. Moreover, a vertical anisotropy of 0.5 was considered. The relative permeability curves were generated using Wyllie and Gardner correlations for the unconsolidated well-sorted sands and P_c was ignored due to high permeability. **Table 3-1** summarizes the data used in simulation.

Table 3- 1: Reservoir Properties used in the Field-Scale Simulation.

Partial Dual Porosity		**Reference model**	**Upscaled case 1**	**Upscaled case 2**	**Upscaled case 3**	**Upscaled case 4**
Grid dimension		333*333*20	333*333*10	166*166*10	83*83*10	41*41*10
Total active cells	Non-wormhole	1108890	554445	137780	34445	8405
	Wormhole	6738	6738	3346	1644	756
Grid size	X-direction	7.5 m	7.5 m	15 m	30 m	60 m
	Y-direction	7.5 m	7.5 m	15 m	30 m	60 m
	Z-direction	0.35 m	0.7 m	0.7 m	0.7 m	0.7 m
Initial reservoir pressure		2,590 kPaa				
Formation depth		425 mTVD				
Average reservoir porosity		0.35	0.35	Multiple realizations (average of porosity = 0.35; average of		
Average reservoir permeability		3,000 md	3,000 md	permeability =3,000 md).		
Dead oil viscosity (15ºC)		65,000 cP		Ln (Ln (μ, cP)) = 22.2018 -3.5098 Ln (T, ºC + 273)		
Initial solution GOR		8-11 m3/m3				
Average wormhole porosity		0.65	0.325	0.164	0.083	0.0415
Average wormhole permeability		On the order of 10,000s D, an increasing variable during history match based on sand production data.				

In single well study, black-oil model was selected to include the effect of wormhole patterns through a sensitivity analysis. Foamy oil flow was modeled through the modification of gas relative permeability and the primary values of the wormhole properties were determined by matching the simulation results with field production history. In this approach, PVT data was provided through tables and no equation of state or K-values were used. Rangriz Shokri and Babadagli (2013) implemented a compositional approach for a segment model of this field. The main difference between the two approaches would be the addition of an energy variable and an energy equation as well as temperature dependence of the properties. In addition to black oil approach, we developed a thermal model. With this option, instead of an equation of state, the K-values were provided to determine equilibrium and densities, viscosities and enthalpies for each component in each phase. The main properties of thermal simulation are summarized in **Table 3-2**. For brevity, the interested reader is referred to ECLIPSE technical description manual for relevant formulations to calculate equilibrium conditions and viscosity-temperature relation (ECLIPSE Technical Manual, 2011).

Table 3- 2: Fluid Properties for Foamy Oil Flow and Solvent Injection.

Component name	Heavy	Dissolved C1	Trapped C1	Free C1	C2	C3	C6	C10
Component volatility type	Dead	Dead	Dead	Gas	Live	Live	Live	Live
Component compressibility type	Oil	Oil	Gas	Oil	Oil	Oil	Oil	Oil
Molecular weight (kg/kg-Mole)	450	16.04	16.04	16.04	30.07	44.09	84	134
Critical temperature (K)	783	190.6	190.6	190.6	305.4	369.8	507.5	626
Critical pressure (kPa)	970	4600	4600	4600	4880	4250	3010	2410
K-value correlation:	*K (P, T) = (A + B/P + C.P) exp [-D/(T-E)] P (pressure) in barsa and T (temperature) in K*							
A, dimensionless	212	0	0	0	0	0	0	0
B (barsa)	10714.5	11650	11650	11650	11748	36440	47360	83740
C (1/bars)	0	0	0	0	0	0	0	0
D (K)	2222	1058	1058	1058	1701	2539	3666	5537
E (K)	266	0	0	0	0	0	0	0
	Ln (Ln (μ, cP)) = 22.2018 -3.5098 Ln (T, °C + 273)							
Oil viscosity at 15 °C (cP)	65000	2.3	2.3	0.205	0.335	0.408	0.611	1.002

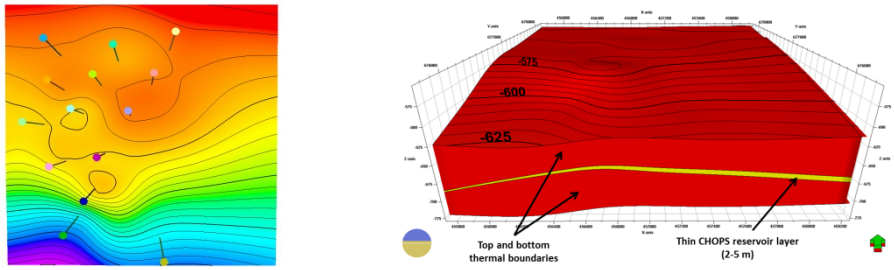

Figure 3- 3: Inclusion of heat loss to adjacent layers (a) Top view of the CHOPS field and well locations (b) Thin CHOPS layer (2-5 m) and thermal boundaries for heat loss.

Due to very thin layer of the CHOPS reservoir under consideration, the heat loss to the overburden, underburden and sides of the reservoir was also considered in the post-CHOPS simulations (**Figure 3-3**). The rock type for heat loss can be identified based on initial temperature, rock conductivity, volumetric heat capacity and temperature dependence of heat capacity. A numerical method was adopted to calculate the heat loss rate per unit area based on rock conductivity and temperature gradient outside the reservoir. These properties are summarized in **Table 3-3**.

Table 3- 3: Thermal Properties for Heat Loss Calculations.

Thermal conductivity of reservoir rock (kj/m/day/°C)	210
Heat capacity of rock (kj/m^3/K)	2350
Thermal conductivity of base and cap rock (kj/m/day/°C)	150
Heat capacity of rock (kj/m^3/K)	2350
Initial temperature (°C)	15
Heat loss calculation method	Numerical

Capturing the Foamy Oil Flow Behavior

Foamy oil occurs in heavy oil reservoirs during cold production. It is believed that high viscosity oil traps small gas bubbles as they come out of the solution, making them reluctant to coalesce to form a continuous gas phase (ECLIPSE Technical Manual, 2011). This reduces the flow rate of the gas and provides drive energy for more oil production. A mathematical description of this flow is quite complex and simplifications are needed. To model foamy oil flow, we followed two approaches. In the black oil approach, we postulate that foamy oil effect can be modeled with an increase in critical gas saturation. Based on the significance of foamy oil flow, this method can be used in single well study, but it does not simulate the dynamic process of formation and dispersion of the trapped gas. Another option is to use different kinetic reactions for this phenomenon. In the kinetic model, three gas components were used to represent the gas in the oil phase (solution gas), foamy oil phase (dispersed gas) and gas phase (free gas). In the foamy oil phase, the trapped gas was modeled as an oil-phase component to ensure that the trapped gas moves with the oil phase. Two first-order kinetic reactions were used to represent the liberation of gas from (1) dissolved gas to trapped gas and from (2) trapped gas to free gas. These reactions have the advantage of allowing non-equilibrium effects to be modeled and replacing the flash. However, we found that in a field-scale study with tens of millions cells, these models increase CPU time compared to modified gas relative permeability in practice.

We also performed a sensitivity analysis on the critical gas saturation in the black oil approach to mimic the foamy oil effect. A quarter of a single well was selected and three models were studied. The first one was a simple black oil model without any modification for critical gas saturation and gas relative permeabilities. The

second one was a black oil model with increased critical gas saturation and no kinetic reactions. The third model includes two kinetic reactions as detailed above without any modification in critical gas saturation. **Figure 3-4** shows a similar trend (and reasonably good match) of oil and gas production for the second and third approaches confirming that foamy oil effect can be modeled using the kinetic reaction approach or modifying the gas relative permeability and critical gas saturation.

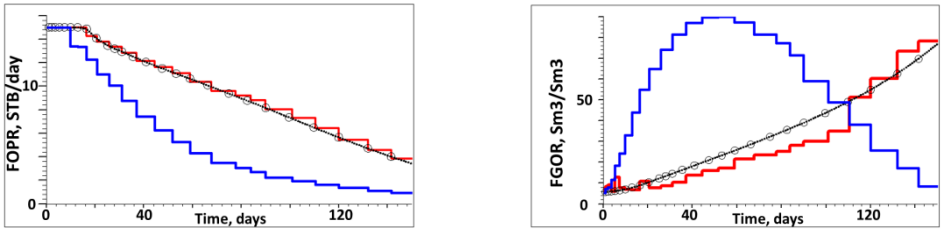

(a) Oil production rate, STB/day

(b) Gas-oil ratio, Sm3/Sm3

Figure 3- 4: Comparison of different approaches to capture foamy oil effect in a single well study (1) using kinetic reactions (circles - dotted black line) (2) no kinetic reaction, but an increase in critical gas saturation (red line) (3) no kinetic reactions and no increase in critical gas saturation (blue line).

Application of Integrated Fractal-Wormhole Model

It was observed that different wells may produce different amounts of sand and at different times. Also, the same amount of sand production may be obtained from very different wormhole growth processes. The radius at which a wormhole may develop around a well is critical in the history matching process. It is not difficult to find a simple model to predict the radius which the wormhole network grows from each individual well as a function of an effective sand production time in 2D plane. In a perfect model, this radius would be a function of reservoir properties, mainly porosity, permeability and formation compressibility, sand production history and geomechanical properties. In this part, we implemented a simple mathematical model for wormhole network growth based on sand mass balance (Rangriz Shokri and Babadagli, 2014) which can be defined separately for each fractal wormhole pattern to match sand production history. **Figure 3-5-(a)** shows

the cumulative sand production on a well basis for 15 wells in an Albertan CHOPS reservoir. The integrated fractal-wormhole model was implemented in this field to predict the wormhole network growth. The resulted network at six time steps is depicted in **Figure 3-5-(b)**. Note that if more appropriate data such as porosity or density map are available, these patterns must be modified.

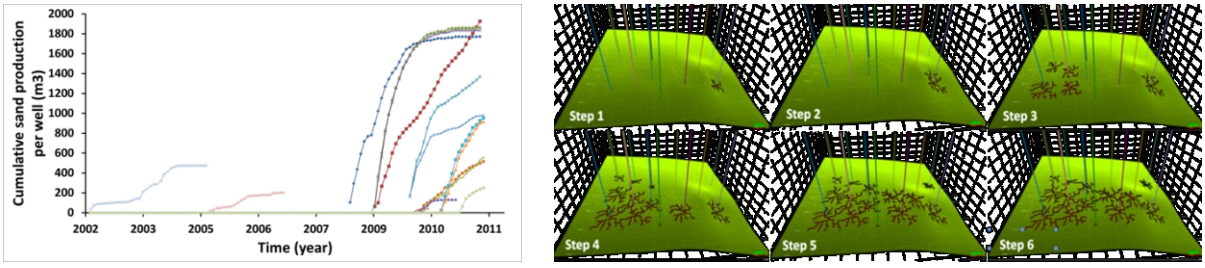

(a) Cumulative sand production history per well. (b) Developed wormhole network based on available sand production data.

Figure 3- 5: Field-scale application of fractal-wormhole model.

Post-CHOPS Modeling

Due to the limitations of dual porosity models for thermal and miscible applications that are needed for post-CHOPS performance assessments, we firstly used a black-oil simulator. Post-CHOPS refers to any EOR/IOR methods used after a CHOPS well reaches its ultimate recovery by cold primary production. In fact, sand production could reach almost zero as seen in Figure 3-1. Therefore, it was assumed that during post-CHOPS, no more sand is produced and the formation is almost stable. As a consequence of this, we assumed the wormhole network remains open during any EOR applications.

The existence of a wormhole rejects any continuous injection of steam or solvent since almost all the wells are connected to each other through a wormhole network. Therefore, initially, the Huff'n'Puff method was considered in the preliminary EOR evaluation. A reduction in oil viscosity due to a thermal injection and diluting heavy oil with solvents are the main active mechanisms. It should be noted that any kind of injection will increase the reservoir pressure and provide the drive energy. This is very critical in motivating the remaining oil to be displaced towards wells during oil production phase. The common procedure is to inject steam or hot water and solvent or miscible gas into the wormhole domain followed by a soaking period while

the wells are shut. Then the wells are allowed to produce the oil. It can be assumed as a blow down period in a single well. The cycles could possibly be repeated.

It is worth mentioning that handling the data, conversion of a black-oil model to a thermal model, use of appropriate data and compatible models are essential at this step and should be considered very carefully. For example, the wormhole network would be regarded with zero heat conduction as no rock was available for this domain, but not in the non-wormhole domain. The need for a three phase relative permeability curve is another issue to be considered.

Results and Discussions

Implementation of Methodology for Field-Scale Study

We implemented this methodology into a field-scale model with a very fine grid. The modeling approach proposed in this paper makes it possible to model CHOPS at a larger scale with multiple wells. Note that some wells started production years later than others; hence, assigning sand production data to each well at different time steps becomes a vital issue as the growth of wormholes is affected by the history of the other wells due to interference. In **Figure 3-6**, the effect of wormhole network growth on oil saturation profile is shown at different simulation times. It should be noted that some of the wells show connections to others through the wormhole network, while some of them remain almost detached from this network. This fact is crucial in any EOR studies to design the injection/production pattern.

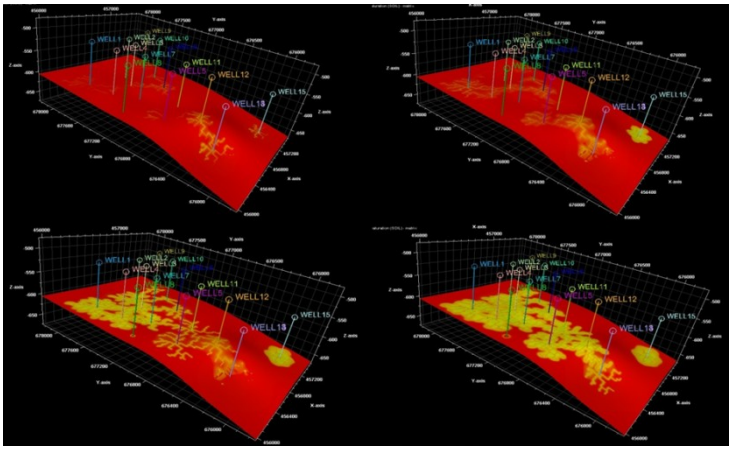

Figure 3- 6: Field scale wormhole-growth model at time t_1 to t_4 in a wormhole network plane.

Upgridding of Fractal Patterns in Partial Dual Porosity Model

To represent the wormhole, a 2D fractal pattern was introduced in simulation grids as dual medium. A more detailed representation of this pattern is constrained to grid block size. In the field-scale study, smaller box dimensions may be used to characterize wormhole network pattern, but it would result to a very fine grid model with millions of cells, eventually increasing the CPU time in fluid flow calculations. We define two new algorithms to upgrid the fractal patterns to compensate for simulation efficiency. These two algorithms may be used in any kind of simulations with a partial dual porosity option. In the first approach, called regular upgridding, the box dimension for fractal analysis was increased. The absence and presence of fractals in a box was represented by 0 and 1, respectively. The upgridded boxes containing the trace of fractals would be assigned 1 while any other boxes with no fractals would be assigned 0. In the second approach, called special upgridding, the number of fractal traces in the new upgridded box would be summed up and the resulted number would be given to the new upgridded cell. Other cells lacking the fractal traces would be assigned 0. These upgridding procedures are summarized in **Figure 3-7-(a)**.

Special upgridding may be preferred to regular one because it considers the properties of fractal traces which in our case are the wormhole porosity and permeability. New upgridded cells with higher values indicate that

wormhole plays a more significant role in these cells compared to other cells with less value in the wormhole network. However, the regular approach is more practical when the details of very fine fractals are not confirmed through experiments or field experience such as micro-seismic activity, tracer tracking, and porosity map. We implemented the regular upgridding in our developed wormhole network at different levels. Note that the non-wormhole (non-fractal) domain must be upgridded to the wormhole network accordingly. **Figure 3-7-(b)** shows how this upgridding procedure simplifies the wormhole network pattern.

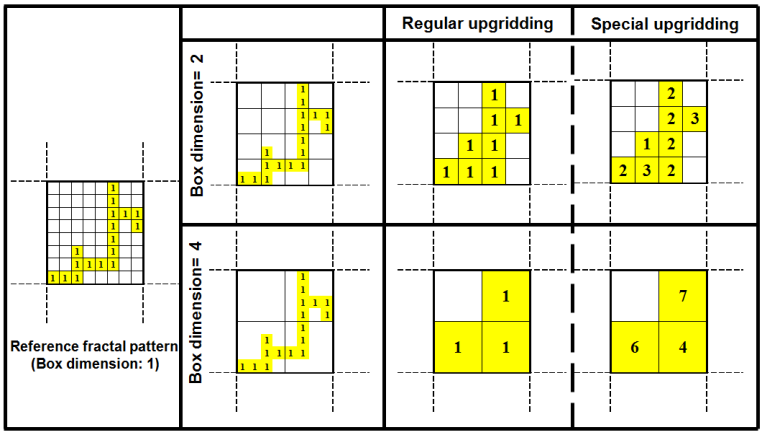

(a) Upgridding procedure in partial dual porosity for fractal-wormhole network.

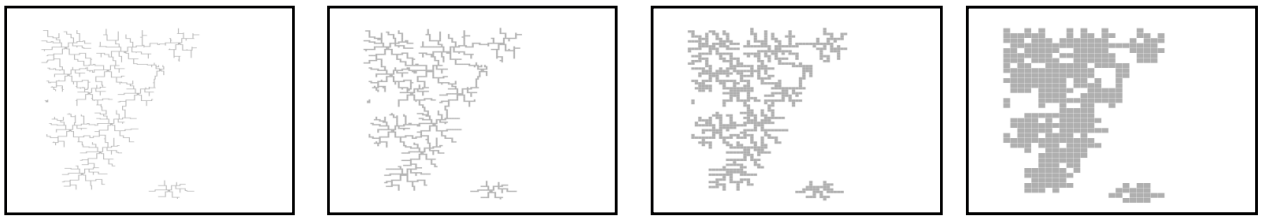

Wormhole network pattern | 2 times upscaled | 4 times upscaled | 8 times upscaled

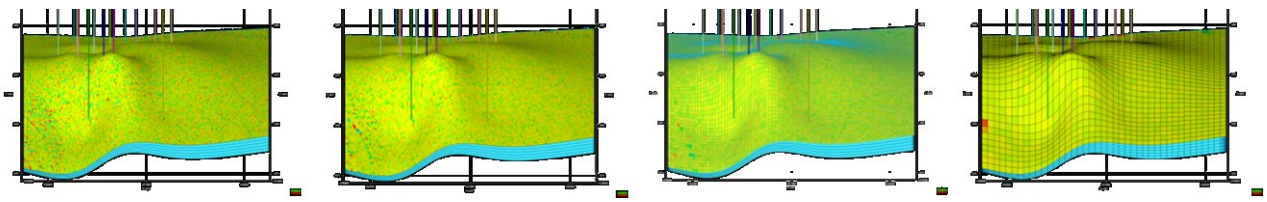

Upscaled matrix static model | 2 times upscaled | 4 times upscaled | 8 times upscaled

(b) Representation of regular upgridding procedure in a field-scale model.

Figure 3- 7: Field-scale wormhole upgridding.

Prior to implementing the upgridding procedure at the field scale, several cases including a simple huff and puff process were considered in a quarter of a single CHOPS well at different levels **(Figure 3-8**). In the first step, the production profile of single porosity and partial dual porosity approaches were compared without any upscaling. **Figure 3-9-(a)** and **(b)** confirm that both approaches result in the same oil and gas production rates. In this case, one may conclude that dual porosity without upgridding can represent very fine single porosity model. Next, the upgridding procedure was conducted in partial dual porosity up to 5 times upscaling in structure. It was noted that upscaled models are able to represent the same production profile as the very fine grid model, however, with an increase in the degree of upscaling, gas production rate tends to increase, which in turn decreases the accuracy of the upscaled models (**Figure 3-9-(c)** through **(e)**). With notion to a significant decrease in CPU time as shwon in **Figure 3-9-(f)**, the upscaling process is recommended. However, for detalied EOR analysis, a refinement around the wormhole may increase the accuracy of the complex injection processes.

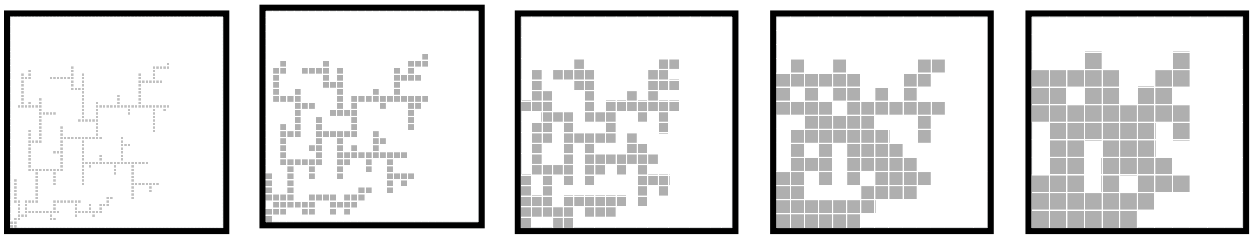

1m x 1m x 0.6m (36000 cells) | 2m x 2m x 0.6m (9000 cells) | 3m x 3m x 0.6m (4000 cells) | 4m x 4m x 0.6m (2250 cells) | 5m x 5m x 0.6m (1440 cells)

Figure 3- 8: Different levels of upgridding for Huff'n'Puff in a quarter of a single CHOPS well.

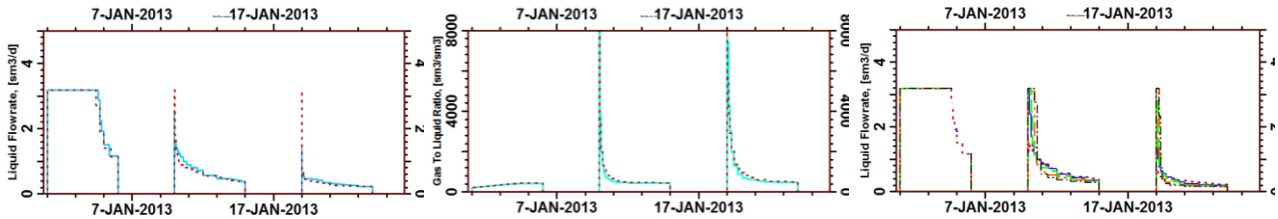

(a) Oil production rate of single porosity (dotted red) and partial dual porosity (solid blue)

(b) Gas-Oil ratio of single porosity (dotted red) and partial dual porosity (solid blue)

(c) Oil production rate of 1X to 5X upscaling schemes. The curves almost overlay each others.

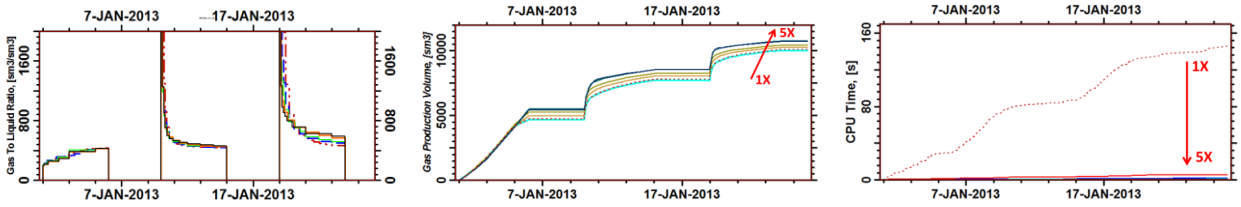

(d) Gas-Oil ratio of 1X to 5X upscaling schemes.

(e) Cumulative gas production of 1X to 5X upscaling schemes.

(f) CPU time of 1X to 5X upscaling schemes.

Figure 3- 9: Justification of upgridding procedure during huff 'n' puff process in a quarter of a single CHOPS well. Note the significant decrease in CPU time. The difference in CPU time of 2X to 5X upscaled models is negligible that could not be recognized in this figure.

Upscaling Properties and Generating/Testing Multiple Realizations

With upgridding the model both in the wormhole and non-wormhole domains, the properties of both domains should be upscaled individually. For example, the matrix porosity should be upscaled by standard techniques, while the wormhole network porosity should be modified in a way that the total pore volume of wormhole network before and after upgridding are equal to the total sand production. This is mainly due to an increase in the box dimension for upgridding, as explained earlier.

The wormhole permeability may be used as a matching parameter. Because the properties of the reference case were generated with random distribution functions, multiple realizations at different scale were generated and the results were simulated. **Figure 3-10** shows permeability distribution examples with a mean value of 3000 md in the non-wormhole domain. Some resulted models are also illustrated in Figure 3-10. We noticed the difference in properties of non-wormhole domain does not play any significant role in primary production of CHOPS as long as wormhole network develops in accordance to sand production history. However, the propagation of wormhole network is highly dependent on non-wormhole properties, especially porosity distribution. The wormholes prefer to grow in higher porosity clean sand layers than tight zones with shale breaks. This dependency would not be covered in this paper.

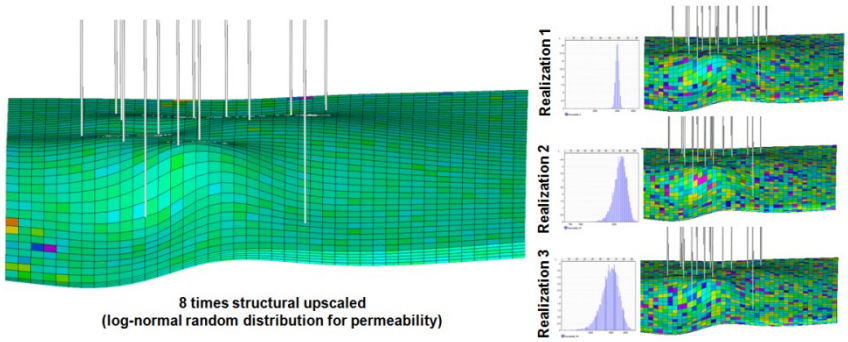

Figure 3- 10: An example of multiple realization and resulted permeability distribution in the upscaled model.

Field-Scale History Matching

The first attempt was to history match the production data of the very fine grid model incorporating a developing wormhole network based on sand production. In this approach, black-oil simulation option was adopted. Different colors in **Figure 3-11-(a)** illustrate the steps that wormhole network was developed. At each step, simulation was restarted based on new developed wormhole network. **Figure 3-11-(b)** shows a comparison of the history matching of the upscaled models to the reference model. Using the proposed upgridding procedure, no significant inconsistency was observed in field oil production rate of reference and upscaled models. Although the field oil production curves are following almost the same trend, the evolution of gas production in **Figure 3-11-(c)** is different. The early constant GOR is mainly due to foamy oil flow, but an increase in the grid size results in a decrease in the efficiency of foamy oil, especially around wells where pressure drop is higher. In the thermal approach, kinetic reactions were used to capture the foamy oil phenomenon. As observed with a kinetic model in **Figure 3-11-(d)**, a good history matched can be obtained for both oil and gas production rates.

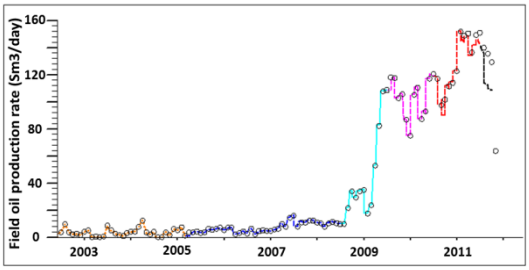

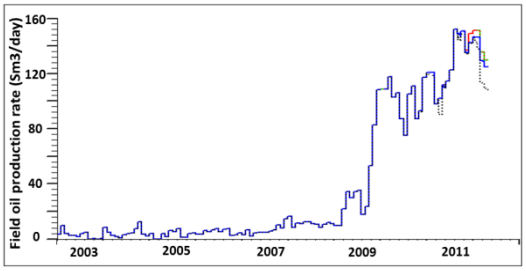

(a) Field oil production rate of reference model: Simulation results at different steps in solid colored lines and observed data in black circles.

(b) Field oil production rate of reference model (dotted black), 2 times upscaled (blue), 4 times upscaled (red) and 8 times upscaled (green). Note that in most parts, the curves overlay each other.

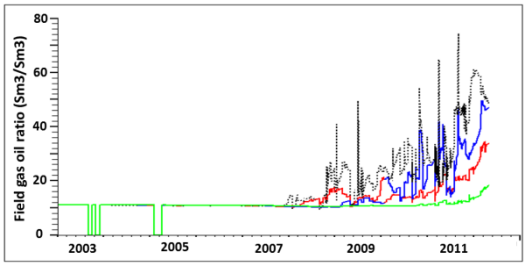

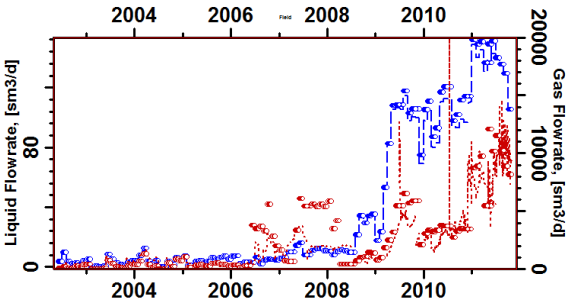

(c) Field gas-to-oil ratio assuming foamy oil flow, reference model (green), 2 times upscaled (red), 4 times upscaled (blue) and 8 times upscaled (dotted black).

(d) History matched field production data, simulated oil data (blue line), historic oil data (blue circles), simulated gas data (red line), historic gas data (red circles).

Figure 3- 11: History matched field oil production rate.

The history matched oil and gas production rates of 15 wells are shown in **Figure 3-12**.

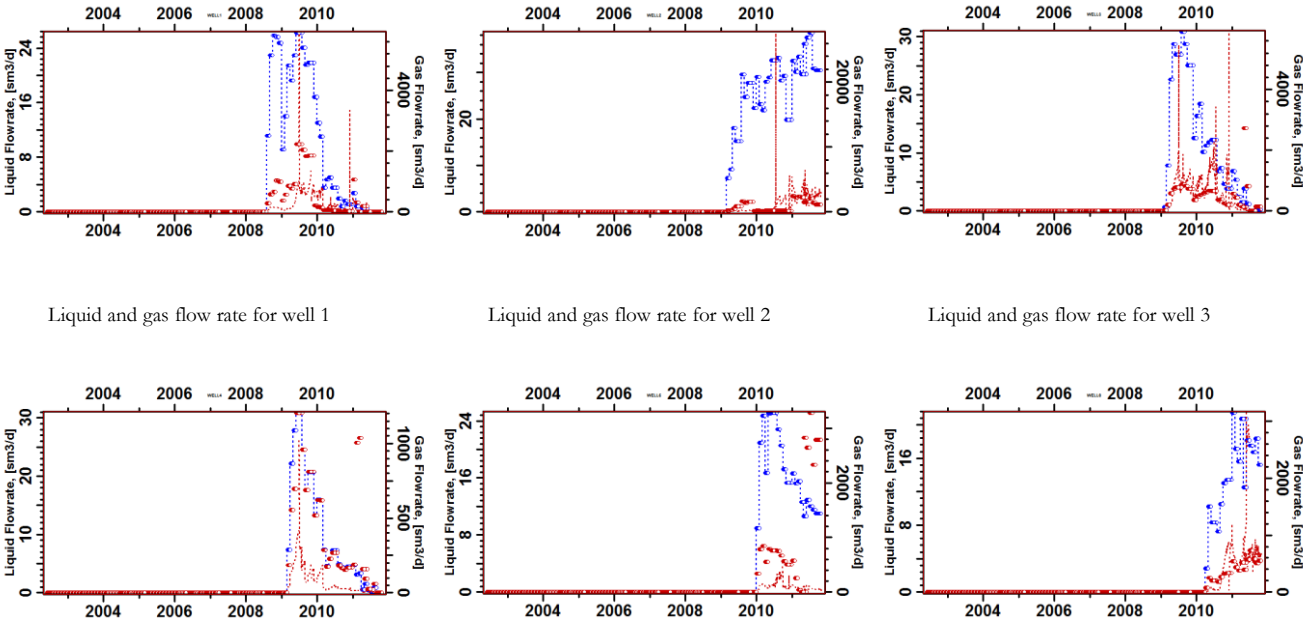

Liquid and gas flow rate for well 1

Liquid and gas flow rate for well 2

Liquid and gas flow rate for well 3

Liquid and gas flow rate for well 4

Liquid and gas flow rate for well 5

Liquid and gas flow rate for well 6

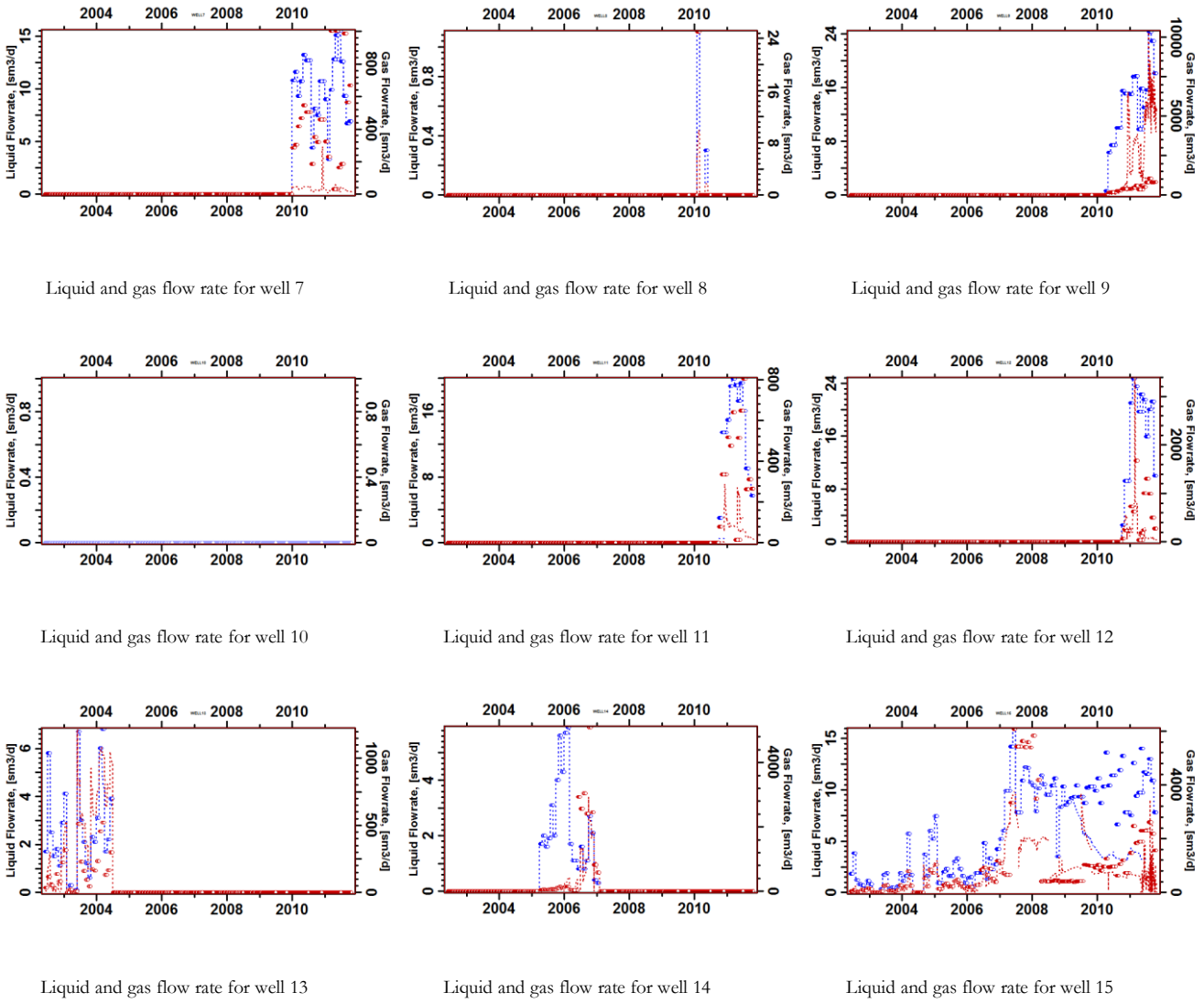

Figure 3- 12: History matched oil and gas production rate on a well basis.

Figure 3-13 shows the oil saturation distribution at the end of production history in different upscaled models. The top view in one layer is also included in Figure 3-13. As seen, upscaling the wormhole pattern reduces the details of the wormhole role in oil production. This might be very significant in the following EOR processes. With notion to lack of data such as porosity or density map to build the wormhole network, the decrease in simulation cost due to upgridding scheme is favorable for early uncertainty analysis at the field scale. We suggest that fine grids are used only in small scale studies such as a segment model of the field when the details of EOR studies are very crucial.

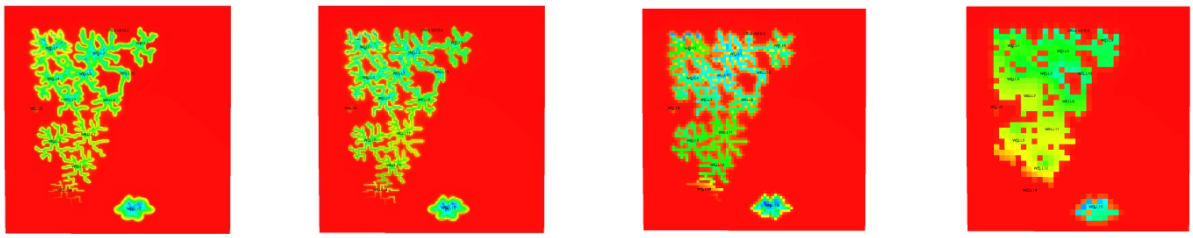

reference fine grid (7.5m x 7.5m) 2X upgridded model (15m x 15m) 4X upgridded model (30m x 30m) 8X upgridded model (60m x 60m)

Figure 3- 13: Effect of upgridding on oil saturation of non-wormhole domain in a layer close to wormhole network (top view).

Post-CHOPS Applications

A typical CHOPS reservoir offers very low recovery factor of 5-15% which means a huge amount of oil would remain unrecovered. At the end of CHOPS primary production, the developed high permeability network (wormholes) among several wells decreases the efficiency of water/polymerflooding due to early water breakthrough. The reservoir has been already depleted and the current reservoir pressure is not sufficiently high to support more oil production. Therefore, one of the key factors to enhance oil production from CHOPS reservoirs is to increase the reservoir pressure, which is not viable through continuous injection due to the presence of wormholes.

Increasing reservoir temperature is another key factor to enhance oil recovery; however, thermal EOR approaches are not practical in thin CHOPS reservoirs (2-5 m) since they suffer from huge amount of heat loss to surrounding formations. Oil dilution with solvent mixture could be an option, but due to the complexity and unknown nature of the developed wormhole network, the chance to lose the injected solvent would be significant. Since the complexity of CHOPS reservoirs and fractured reservoirs are comparable, we propose the modification of SOS-FR method (Steam-Over-Solvent in Fractured Reservoir) developed by Al-Bahlani and Babadagli (2009). SOS-FR method consists of three phases: (1) initial thermal phase in order to heat the reservoir with steam or hot water injection and to prepare the reservoir for the next phase (2) solvent phase which may include several solvent injection, soaking and oil production periods, and (3) final thermal phase with the aim to recover the injected solvents back from the reservoir when the expected ultimate oil recovery is achieved. In a recent study, Coskuner et al. (2013) noticed that the first thermal phase might be

neglected in heavy oil cases since it reduces the light components of heavy oil in the early life of the reservoir, hence, it decreases the efficiency of solvent phase. In this section, we mainly deal with field application of the second phase in which different cycles of solvent injection and oil production are considered.

To include the modified SOS-FR as post-CHOPS, the history matched model was considered to experience a period of pressure depletion until the reservoir pressure can no longer support more oil production. This may not be the optimum time to start the post-CHOPS EOR scheme as emergence of solution gas would leave dead oil behind in reservoir. However, with such an option, one is able to show that the incremental oil is only caused due to implementation of proposed post-CHOPS schemes. As shown in the earlier sections, the wormhole network was generated based on sand production and field reports. It connects some wells to each other while some may remain detached. The field development strategy is then to convert some of the production wells into injectors. Solvents (C1, C3, and C6) are injected through these injectors into the wormhole network. This increases the reservoir pressure in addition to the possibility of oil dilution. All wells in the field are then shut in a soaking period for a certain time that could be optimized. In production phase, oil is produced from remaining wells. This mimics a huff'n'puff process, but in a field scale by replacing a single well with the whole field. The cycles potentially can be repeated.

The solvent injection may be conducted at reservoir temperature, especially with lack of interest in use of thermal in thin layers. We refer to this strategy as cold post-CHOPS option. An alternative option is to use steam along with solvent. As steam is not continuously injected into reservoir, instead of steam-to-oil ratio, we define steam-to-solvent ratio. Such ratio can later be considered in economical aspects of post-CHOPS strategies. Laboratory experimental studies have shown that more than 80% of solvent can be retrieved back using a final thermal phase (Mohammed and Babadagli, 2013). Therefore, economical analysis of this process should be assessed when solvent retrieval phase is considered.

Figure 3-14 shows different stages of modified SOS-FR for post-CHOPS in three phases: (1) injection (30 days), (2) soaking (15 days), and (3) production (300 days). In wells that were not connected to the wormhole network, a simple huff'n'puff process was implemented. 6 cycles of solvent injection including C1, C3, and

C6 were considered. 3 Production wells were converted to injectors at reservoir temperature (25ºC) with a control of 100 Sm3/d per well and injection bottomhole pressure of 35 bars for 30 days, followed by a soaking period of 15 days. To complete the huff'n'puff process, the remaining wells were allowed to produce the oil with a minimum bottomhole pressure of 1-2 bars for 300 days. The cycles were repeated for 6 years. **Figure 3-15** shows the field oil production rate for C1 injection at reservoir temperature. **Figure 3-16-(a)** shows the incremental oil production for different solvents. Note that the effect of produced solvent was removed in the figure. As can be seen, the use of heavier solvents results in higher oil production with additional cost of associated solvents. It should be mentioned that possible asphaltene precipitation is currently ignored. Asphaltenes might precipitate during solvent injection. Considering high permeability wormholes, positive effect of in-situ upgrading of the heavy oil may prevail the negative impact of permeability reduction due to asphaltene precipitation.

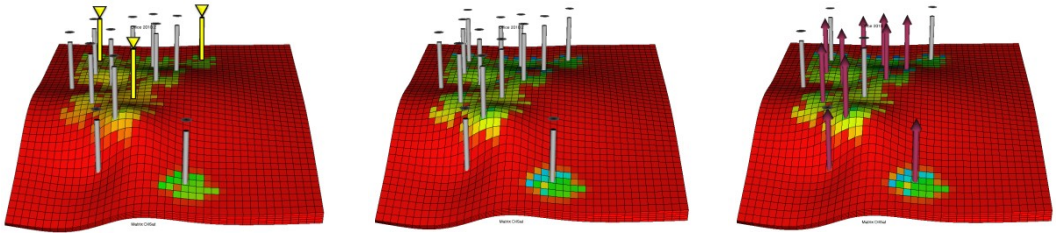

Figure 3- 14: Solvent injection in wormhole network as post-CHOPS option (a) converting some production wells into injectors (b) soaking period (c) production phase.

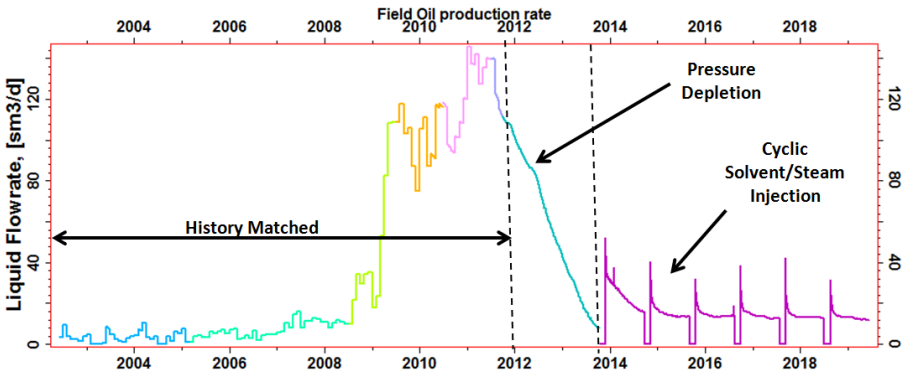

Figure 3- 15: Field oil production rate, history matched model followed by aggressive pressure depletion and solvent stimulation.

To compare the impact of temperature on the overall process, a high quality steam was injected at 225ºC followed by solvent injection as explained. The steam-to-solvent ratio was considered as 0.1. Cumulative steam-to-oil ratio after 6 cycles is also less than 0.1. One should bear in mind the cyclic nature of huff'n'puff process compared to continuous steam injection which results in such low steam-to-oil ratio. Nevertheless, the emphasis is on the hybrid application of thermal-solvent EOR options rather than sole application of thermal methods. It was noticed that the addition of steam would increase total oil production through a decrease in oil viscosity. As shown in **Figure 3-16-(b)**, the use of C1 and steam will almost provide the same amount of oil production using cold heavier solvents, C6 in this case, providing equal amount of solvent injected. Also, we performed a high-pressure C1 injection with 100 times increasing injection rate. The incremental oil production is comparable with C6 case and hybrid C1+steam; however, it is by far less than hybrid application of C6+steam. The question is then availability of the solvents and feasibility of converting CHOPS wells to thermal injection wells. The reader should also note that CHOPS wells are not suitable for thermal injection unless they are completed after primary production that brings workover procedure into economical assessment.

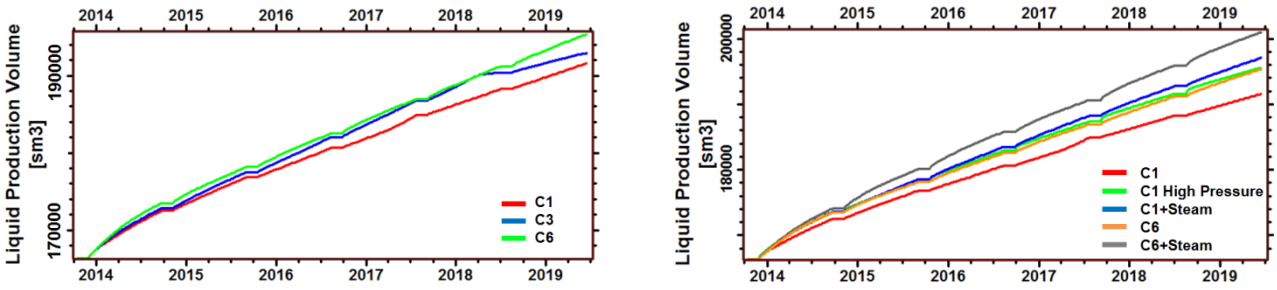

(a) (b)

Figure 3- 16: Field total oil production at the end of primary production followed by (a) cold solvent stimulation and (b) thermally-aided solvent stimulation.

Economic Analysis

A method to evaluate the project costs (solvent/steam injection, oil production/upgrade and the cost associated with solvent loss) and the revenue obtained (from incremental oil production) was adopted for economic analysis. Such approach yields an estimate of recovered money after 6 cycles of solvent stimulation. Note that royalty, taxes, price inflation and discounting are not considered. The base prices are summarized in **Table 3-4**.

Table 3- 4: Base Prices used in Economic Analysis.

Oil price ($/STB)	75
Oil production/upgrade cost ($/STB)	7.1
C1 price ($/STB) equivalent water injection	1.5
C3 price ($/STB) equivalent water injection	80
C6 price ($/STB) equivalent water injection	120
Steam price ($/STB) equivalent water injection	3

Table 3-5 summarizes the total fluid injection and production volumes associated with 6 cycles of solvent/steam stimulation. Also, the economic indicator of money recovered is shown for each case. It is worth mentioning that the produced gas volumes of C1 and C3 were not included in the economic analysis. The base prices, shown in Table 3-4 for oil production/upgrade and fluid (equivalent water) injections, take account of operational costs and infrastructure expenses. Notice that these values are not unique and could vary based on many factors such as operating companies, government regulations and field location. Bearing all of this in mind, it can be seen that heavier solvent and additional steam result in higher oil production volumes, but at the expenses associated with solvent/steam costs. Although the money recovered term is highly dependent on the economic input values (oil and solvent prices), this simple economic analysis indicates that the use of lighter component is more economically viable.

In short, it can be stated that there is a potential to use the wormhole network as a medium to deliver different solvents to depleted CHOPS reservoirs in a similar manner to huff'n'puff process. Based on the preliminary results, solvent injection may be applied at reservoir temperature as a modification to SOS-FR method and would result in considerable oil recovery after CHOPS. Considering the possibility of solvent

retrieval phase, reservoir optimization tools should then be used for further field-scale post-CHOPS applications to assess the added values of oil recovery with optimal operating conditions.

Table 3- 5: Total injection and production volumes and estimated money recovered after 6 cycles of solvent/steam stimulation.

Injection Stream	Total Fluid Injection Volume (SM3)	Solvent Injection Volume (SM3)	Steam Injection Volume (SM3)	Incremental Oil Production Volume (SM3)	Incremental Liquid Solvent Production (SM3)	Money Recovered (million $)
C1	18000	18000	0	25825	0	1.73
C1 + Steam	18000	16362	1638	31696	0	2.12
C3	18000	18000	0	27186	0	0.41
C6	18000	18000	0	29741	2686	0.18
C6 + Steam	18000	16362	1638	35882	2978	0.83

Conclusions

A new workflow for quick CHOPS simulation at field scale was implemented. It combines a step-by-step simulation technique with a partial dual porosity approach and is able to capture the growing nature of wormholes during CHOPS, confirmed with available field data. In this workflow, an integrated fractal-wormhole model incorporated sand production history and wormhole network in the numerical simulations. It was shown that foamy oil flow can be easily modeled in practice using a modified version of gas relative permeability curve, or alternatively, with first-order kinetic reactions to replace the in-situ flash process. Regular and special upgridding procedures in partial dual porosity were also defined and implemented at field scale. Multiple realizations of upscaled models were used to check the quality of history matching process.

After history matching of the CHOPS performance in the selected field, several post-CHOPS scenarios as modified versions of SOS-FR (Steam-Over-Solvent in Fractured Reservoirs) technique were studied at field scale. It was observed that in an iso-thermal process, additional oil can be produced from wormhole network. The use of hot fluids as well as solvent-aided process would be effective in increasing oil recovery from non-wormhole domain, but at the expenses associated with solvent cost. Considering the potential of solvent

retrieval, the use of optimization tools is then recommended at the final step for assessment of EOR post-CHOPS applications.

References

Al Bahlani, A. M. M., and Babadagli, T. 2009. Laboratory and Field Scale Analysis of Steam Over Solvent Injection in Fractured Reservoirs (SOS FR) for Heavy Oil Recovery. Paper SPE 124047 presented at the SPE Annual Technical Conf. and Exh., New Orleans, Louisiana, 4-7 October.

Coskuner, G., Naderi, K. and Babadagli, T. 2013. An Enhanced Oil Recovery Technology as a Follow Up to Cold Heavy Oil Production with Sand. Paper SPE 165385 presented at the SPE Heavy Oil Conf., Calgary, Alberta, Canada, 11-13 June.

ECLIPSE TECHNICAL MANUAL, Schlumberger, 2011.

Istchenko, C. M., and Gates, I. D. 2014. Well/Wormhole Model of Cold Heavy-Oil Production with Sand. *SPE J.* 19 (2), 260-269.

Liu, X., and Zhao, G., 2004. Effects of Wormholes on Cold Heavy Oil Production, presented at the Petroleum Society's 5th Canadian International Petroleum Conference (55th Annual Technical Meeting), Calgary, Alberta, Canada, June 8 – 10.

Mohammed, M. and Babadagli, T. 2013. Efficiency of Solvent Retrieval during Steam-Over-Solvent Injection in Fractured Reservoirs (SOS-FR) Method: Core Scale Experimentation. Paper SPE 165528 presented at the SPE Heavy Oil Conf., Calgary, AB, Canada, 11-13 June.

Rangriz Shokri, A. and Babadagli, T. 2014. Evaluation of Thermal/Solvent Applications with and without Cold Heavy Oil Production with Sand (CHOPS). *JCPT* **53** (2), 95-108.

Rangriz Shokri, A. and Babadagli, T. 2013. Modeling Thermal and Solvent Injection Techniques as Post-CHOPS Applications considering Geomechanical and Compositional Effects. Paper SPE 165534 presented at the 2013 SPE Heavy Oil Conf., Calgary, AB, Canada, 11-13 June.

Sanyal, T. and Al-Sammak, I., 2011. Analysis of the First CHOPS Pilot for Heavy Oil Production in Kuwait, CSUG/SPE148966, SPE-CURC Canadian Unconventional Resources Conference in Calgary, Alberta, Canada, 15-17 Nov.

Tan, T., Slevinsky, R., Jonasson, H., 2003, A New Methodology for Modeling of Sand Wormholes in Field Scale Thermal Simulations, Canadian International Petroleum Conference, Calgary, Alberta, 10 – 12 June.

Wang, Y. and Chen, C. Z., 2002. Simulating Cold Heavy-Oil Production with Sand by Reservoir-Wormhole Model, Canadian International Petroleum Conference, Calgary, Alberta, 11 – 13 June.

Chapter 4: Field-Scale Deformation Analysis of Cyclic Solvent Stimulation in Thin Unconsolidated Heavy Oil Reservoirs with Developed Wormhole Network

A version of this chapter was accepted for presentation at the A version of this chapter is presented at the SPE Heavy Oil Conference Canada held in Calgary, Alberta, Canada, 11–13 June 2013 and was also submitted to Journal of Canadian Petroleum Technology.

Abstract

With the current interest in exploiting thin unconsolidated heavy oil reservoirs, cold heavy oil production with sand (CHOPS) can be considered to be a promising primary recovery technique. However, it offers low recovery factors (~10%) and creates a complex network of high-permeability channels known as wormholes, while simultaneously changing formation compressibility and in-situ stress conditions. Eventually, development of such a network would lead to a softer layer within the shallow unconsolidated reservoir, which can carry less of the overburden stress. Further development of such reservoirs is usually achieved through enhanced oil recovery applications in the form of cyclic solvent stimulation within an economic framework. Cyclic loading and unloading of this EOR technique makes it even more difficult to predict the recovery performance.

In this study, a 3D geomechanical model was used to calculate the stress distribution in a history matched field in Alberta with fifteen producers. The fractal patterns generated based on Diffusion Limited Aggregation (DLA) algorithm were used to represent the wormhole network with different strength properties. Foamy behavior of heavy oil was modeled with the help of a set of kinetic reactions. The hydro-geomechanical model was then used for field development planning, reservoir management and assessment of near wellbore regions during cyclic injection and production. The field-wide deformation and stress changes were analyzed in deep overburden, cap rock, and reservoir to show the influence of local stress orientations in soft and stiff layers.

Next, we considered a sector model with a single well. The model introduced was used to assess EOR processes with different solvent streams. While light hydrocarbon components help to re-pressurize the formation, the heavier components seem more effective in heavy oil dilution. This occurred while stress arching re-distributed the cyclic injection-production induced stresses to flow around soft inclusions. Although it is difficult to obtain data to calibrate the 3D hydro-geomechanical model, it allows for reliable

investigation of reservoir performance and gives deeper insight than using flow simulation alone. The assessment of the potential of geomechanics can ascertain whether a more detailed modeling is necessary.

Introduction

Heavy oil production with sand from shallow, loose, and thin unconsolidated sand reservoirs in the Alberta region is mostly implemented through the cold production technique. In this technique, known as CHOPS, a huge pressure drawdown with the aid of Progressive Cavity Pump (PCP) in the production well forces the heavy and viscous oil to be produced along with sands from the reservoir. The co-production of the sand and oil increases the daily oil production rate 10-50 times and keeps the well at an economic state. However, it creates high-porosity high-permeability regions in the form of channels –wormholes– or cavities and dilated zones around the wellbore and possibly further in the reservoir (Rangriz Shokri and Babadagli 2014). Moreover, the heavy oil with very low GOR tends to have a foamy behavior. The very first gas bubbles are reluctant to coalesce until they reach a certain saturation (critical gas saturation), which is higher than critical gas saturation in the conventional oil.

Characteristically, CHOPS' primary production is only ruled by the geology and the nature of the heavy oil. Increasing the number of wells with aggressive pressure drawdown and allowing more sand production would possibly lead to higher oil recovery factor, but remains in the range of 5-15%. With this in mind, post-CHOPS is referred to all EOR/IOR strategies that improve the oil recovery of CHOPS reservoirs beyond this recovery factor range. The difficulty of modeling post-CHOPS applications lies in the unknown and disturbed structure of the reservoir due to sand production and existence of wormhole or dilated regions. Presence of a wormhole network among different wells has been reported in many field observations (Loughead and Saltuklaroglu 1992; Coombe et al. 2001; Dusseault 1993; Lebel 1994; Meza 2001; Tremblay et al. 1996, 1997, 1999; Squires 1993; Elkins et al. 1972; Yeung 1995; Smith 1986; Loughead and Saltuklaroglu 1992). Experimental and numerical models have also shown the possibility of channel-like structures

(Mccaffrey and Bowman 1991; Squires 1993; Tremblay et al. 1996, 1997, 1999). For an extensive literature review on these modeling approaches, the reader is referred to Rangriz Shokri and Babadagli (2014).

Apart from fluid interactions, such unconsolidated reservoirs suffer from mechanical changes in their strength properties. Abrupt pressure depletion due to sand production eventually leads to the development of a softer material in reservoir layers, which can carry less of the overburden stress. Then the question arises whether the altered formation is still able to support the overburden load. This is where the geomechanics plays its role to provide insight into the subsurface stress state. With the help of a finite element simulator, a 3D Mechanical Earth Model (MEM) was constructed to capture the complex interplay of pore pressure depletion, re-pressurization and loading process, reservoir geometry, and material properties. Despite a relatively simple geometry, the resulting deformation, stress and strain fields were noticeably heterogeneous. This paper also presents the steps to build the 3D MEM and to analyze its complex behavior. The emphasis is on deep overburden and cap rock region where changes in stress tensor are significantly different from reservoir and wormhole network regions.

One of the practical outcomes of this study is the possibility of stress arching effect in less stiff layer of reservoir, which in turn might lead to proper field development planning of cyclic solvent stimulation. With a close look at reservoir compaction, overburden subsidence and underburden rebound, one may notice how the stiff layers accumulate stress while soft layers enable the stress to flow around. A sector model of full field reservoir was adopted to demonstrate this behavior. To complete the work, several fluid streams for injection in the sector model were simulated and both fluid and geomechanical response were analyzed. The simulation study was performed using the ECLIPSE/PETREL/VISAGE software packages (ECLIPSE Technical Manual 2013; VISAGE Technical Manual 2013).

Description of Reservoir Fluid Flow Model

Field overview. The full field model was built based on the information provided from a Canadian oil company. The reservoir is located at depth of 425 mTVD. The upscaled 3D model consists of 41, 41 and 5 grids in x, y and z-directions, respectively. Each single grid has dimensions of 60 m x 60 m x 1 m with notion to the fact that the wormhole layer in reservoir is 10 cm thick. It was assumed that the wormhole network is laterally developed in one layer. The sector model is 8 times refined around one of the selected wells. Initial reservoir pressure is 2583 kPa.

A uniform random distribution function is used to assign the porosity and permeability data for the full field model keeping the absolute permeability and porosity of the non-wormhole domain as an average value of 3,000 mD and 35%, respectively. The assigned value of the wormhole network is mainly a function of the assumed wormhole diameter. The permeability is assumed to be $k = 12.67*10^6 r^2$, based on the laminar flow theory (equality of Darcy and Poiseuille's equations) where k is permeability in Darcy and r is pipe radius in cm, a value of 67,000 Darcy in this study. However, the absolute permeability of wormholes may be treated as a history matching parameter. Wormhole porosity is about 65% in full field model and 85% in refined sector model, which is sufficiently high for a realistic representation of the wormhole network. Reservoir is as thin as 2.8 to 5 m with a vertical anisotropy of 0.5, implying the inefficiency of gravity drainage. Relative permeability curves in the matrix domain were generated by Wyllie and Gardner correlation in unconsolidated well-sorted sands (Wyllie and Gardner 1958). Due to high permeability and porosity, the capillary pressures are assumed to be zero. Typical cross fracture relative permeability curves were assigned in wormhole domain. **Table 4-1** summarizes the data used in simulation.

Table 4- 1: Reservoir Properties used in Fluid Flow Simulation Models

Porosity	0.35
Horizontal permeability	3000 md
Vertical permeability	1500 md
Initial reservoir pressure	2583 kPa
Initial reservoir temperature	25 ºC
Reference depth at top of reservoir	425 mTVD
Initial oil saturation	0.75
Initial water saturation	0.25
Kro at connate water	1.0
Krw at irreducible oil	0.3
Krg at connate liquid	0.3
Krog at connate gas	1.0
Relative permeability correlations	Wyllie-Gardner
Three-phase relative permeability model	Stone's model II
Formation compressibility	1.8E-5 1/kPa
Reservoir rock heat capacity (Butler 1997)	2600 kJ/m^3 ºC
Reservoir rock thermal conductivity (Butler 1997)	660 kJ/m day ºC
Over/underburden rock heat capacity (Butler 1997)	2600 kJ/m^3 ºC
Over/underburden rock thermal conductivity (Butler 1997)	660 kJ/m day ºC
Bitumen thermal conductivity (Butler 1997)	11.5 kJ/m day ºC
Water thermal conductivity	1500 kJ/m day ºC
Gas thermal conductivity (Yazdani et al. 2011)	2.89 kJ/m day ºC

Wormhole network growth. A comprehensive review of work done on numerical and experimental modeling of CHOPS in thin unconsolidated sand reservoirs is reported by Rangriz Shokri and Babadagli (2014). Most of the existing models attempted to predict or to represent the wormhole growth during sand production on the basis of certain criteria for its growth; for instance, the pressure gradient at the tip of each individual wormhole. These models are difficult to use in practice because of difficulties in verification. In addition, they require a true representation of a large (and accurate) body of input data from a field, which is quite impossible to achieve even for a single-well study. An alternative is to use probabilistic methods to generate the wormhole network on the basis of a fundamental assumption that the wormhole network can represent a random behaviour (Rangriz Shokri and Babadagli 2014). Our proposed method treats the wormhole as a network rather than modeling each wormhole individually, simply due to lack of data

collection from wormhole trails. One or more DLA patterns are selected to represent the wormhole network and its growth is controlled by the sand production data obtained from the field for each well, and then imported as the wormhole network at different stages into the reservoir grid. A simple mathematical model is also used to predict the radius in which a wormhole can grow away from production well based on the DLA-fractal pattern and sand material balance.

It is worth noticing that the pressure drop is believed to be higher parallel to the reservoir bedding considering very thin reservoir; hence, the wormholes would possibly grow laterally in the direction of higher pressure drawdown. At a selected time step, the wormhole growth is predicted and fluid flow simulator matches the production data. Then, the wormhole can grow more in accordance with sand production data and fractal pattern in the next time step, followed by production history matching. This technique is referred to as "step-by-step" simulation. This procedure is repeated until it covers the whole production time or until it reaches a specified time by the user. The interested reader is referred to our earlier publications listed in references.

Foamy oil behavior. The foamy oil behavior can be treated with available kinetic models that use the kinetic reactions from nucleation of gas bubbles until they are connected and form a single gas phase (Maini and Sarma 1993). During cold production, high viscosity oil traps small gas bubbles as they come out of solution, reducing the potential of bubble coalescence to form a continuous gas phase. This reduces the flow rate of the gas and provides drive energy for more oil production (ECLIPSE Technical Manual 2013). In the lab scale with a black oil approach, it is recommended to modify the gas relative permeability data. Foamy oil is usually indicated by higher critical gas saturation and a depressed gas relative permeability curve. Another approach adopted for this study is to use three gas components to represent the gas in the oil phase (dissolved gas), foamy oil phase (dispersed gas), and gas phase (free gas). The trapped gas in foamy oil phase would then be modeled as an oil phase component to ensure that the trapped gas moves with the oil phase.

Finally, two first-order kinetic reactions are used to represent the liberation of gas from (1) dissolved gas to trapped gas and from (2) trapped gas to free gas. Rangriz Shokri and Babadagli (2014) recommended the use of the second approach with the upscaled models.

Fluid characterization. Based on current literature on the subject of heavy oil properties in the Alberta regions (Sawatzky 2008, 2009; Maini and Sarma 1993; Maini 1999; Urgelli et al. 1999), a fluid model was created to match the black oil PVT data including oil formation volume factor (FVF), solution GOR, oil density, and oil viscosity using the PVTi software, Schlumberger. Pure streams of C1, C2, C6, and a mixture stream (25mole%C10 + 25mole%C6 + 50mole%C1) were considered as the primary injection fluids to re-pressurize the reservoir and dilute the oil to a lower viscous status. The Peng-Robinson equation of state with shift-volume was selected for compositional analysis to fit the Crookston coefficients. The main fluid properties are summarized in **Table 4-2**.

Table 4- 2: Fluid Properties for Foamy Oil Flow and Solvent Injection.

Component name	Heavy	Dissolved C1	Trapped C1	Free C1	C2	C3	C6	C10
Component volatility type	Dead	Dead	Dead	Gas	Live	Live	Live	Live
Component compressibility type	Oil	Oil	Gas	Oil	Oil	Oil	Oil	Oil
Molecular weight (kg/kg-Mole)	450	16.04	16.04	16.04	30.07	44.09	84	134
Critical temperature (K)	783	190.6	190.6	190.6	305.4	369.8	507.5	626
Critical pressure (kPa)	970	4600	4600	4600	4880	4250	3010	2410
K-value correlation:	$K(P,T) = (A + B/P + C.P)\exp[-D/(T-E)]$ P (pressure) in barsa and T (temperature) in K							
A, dimensionless	212	0	0	0	0	0	0	0
B (barsa)	10714.5	11650	11650	11650	11748	36440	47360	83740
C (1/bars)	0	0	0	0	0	0	0	0
D (K)	2222	1058	1058	1058	1701	2539	3666	5537
E (K)	266	0	0	0	0	0	0	0
	$Ln(Ln(\mu, cP)) = 22.2018 - 3.5098\, Ln(T, ^\circ C + 273)$							
Oil viscosity at 15 °C (cP)	65000	2.3	2.3	0.205	0.335	0.408	0.611	1.002

3D geomechanical model construction. Mechanical Earth Model (MEM) or three-dimensional reservoir geomechanical model is essential to describe the stress field in the reservoir and under/over/sideburdens. This includes building a structural model, grid generation, assigning elastic and strength properties, and model calibration (Herwanger and Koutsabeloulis 2011).

Geometric description of MEM and coupling schemes. An embedded grid was made by adding overburden, underburden, and sideburden grid cells to the existing reservoir grid (**Figure 4-1**). By adding 10 cells with a geometric factor of 1.5, the overburden was extended to surface to reduce the impact of boundary constraints. 5 cells were added to construct a limited underburden zone. The model is assumed to be relatively thick so that the stress model does not significantly buckle. However, too much thick grid cells in underburden should be avoided as it would lead to unrealistic stress concentration in the lower areas and poor response in the top of the model where reservoir is located (VISAGE Technical Manual 2013). Towards the lateral boundaries of the grid, large grid blocks were employed to keep the number of grid blocks manageable. It is also recommended to keep the aspect ratio of MEM less than 3:1. Inclusion of stiff plates at sideburdens will also help to better distribute the imposed boundary stresses. Note that the modeled stress results of a coarse MEM can be used as boundary conditions for the detailed sector or near wellbore models (Herwanger and Koutsabeloulis 2011). In this study, one-way coupling scheme was adopted.

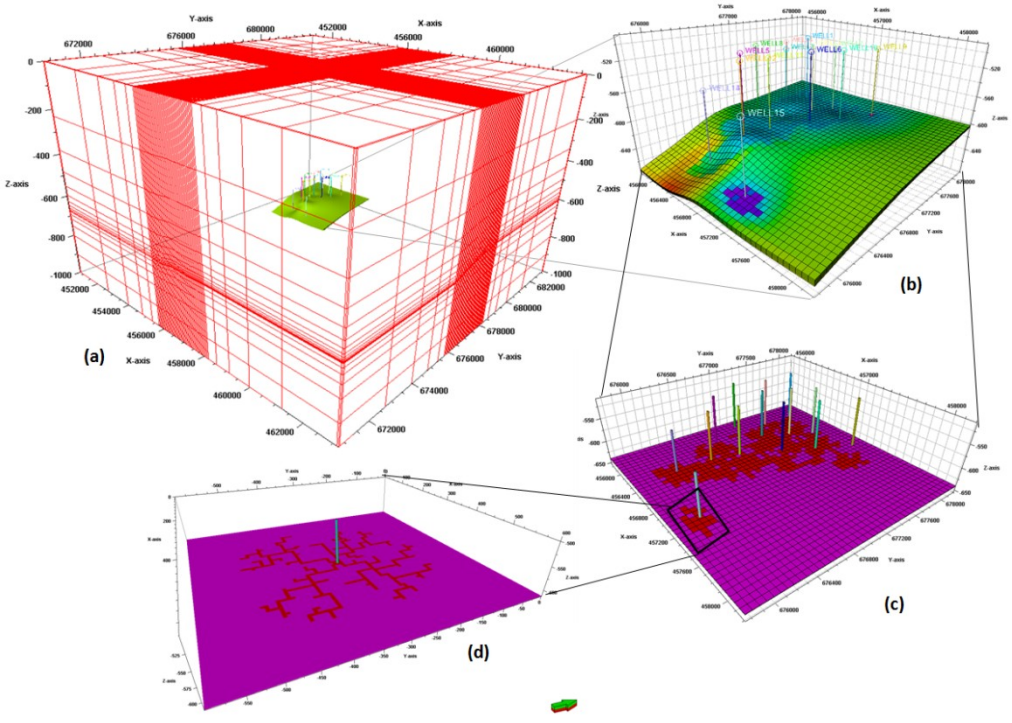

Figure 4- 1: Mechanical Earth Model Construction (a) embedded grid contains full field flow model (b) Full field model for fluid simulation (c) upscaled wormhole network within full field flow model (d) refined sector model around a single well.

Material properties and failure criterion model. With lack of detailed geological information, material properties were selected from Petrel library (2013). Reservoir was assumed to be made of loose uniform sand. A layer of shale was assumed to separate reservoir from overburden. Dense uniform sand was assigned to over/under and sideburden. The Mohr-Coulomb failure criteria chosen for all segments of MEM. The full description is summarized in **Table 4-3**.

Table 4- 3: Description of Material Properties and Failure Criteria Models.

Material Name	**Loose Uniform Sand**	**Dense Uniform Sand**	**Shale**
Material Type	Intact Rock	Intact Rock	Intact Rock
Elasticity Model	Isotropic	Isotropic	Isotropic
Young Modulus (kPa)	18000	51500	3.60E+07
Poisson Ratio	0.3	0.38	0.2
Rock Density (kg/m3)	2160	2680	2520
Biot Coefficient	1	1	1
Thermal Expansion Coefficient (1/°C)	1.30E-05	1.30E-05	1.30E-05
Porosity	0.3	0.3	0.3
Yield Criteria	Mohr-Coulomb	Mohr-Coulomb	Mohr-Coulomb
UCS (kPa)	0	0	125000
Friction Angle (deg)	32	32	14.4
Dilation Angle (deg)	10	12	7.2
Tensile Strength (kPa)	0	0	6000
Hardening/Softening	0	0	0

Boundary conditions and stress initialization. The numerical solution of the stress equations requires the application of boundary conditions to simulate the correct physical conditions. It can be argued that production induced deformation would not extend to the lateral boundaries if the lateral section of MEM extends far beyond the reservoir section (Herwanger and Koutsabeloulis 2011). In this case, roller boundary (zero-lateral boundary) was implemented at sideburdens, which enables the free movement in z-direction. No-displacement boundary was imposed for the underburden. The included overburden in the model provides loading effect on reservoir section, which should be calibrated in the initialization step. It is assumed that at initial equilibrium step, the loads caused by gravity, pore pressure, and the applied boundary conditions (tectonic loads if present in the region) are balanced so that no deformation would appear in the model. If any undesirable deformation is observed at initial equilibrium step, virtual stresses can be used to remove the

effect. Note that virtual stresses are not a part of stress field and they are only used to remove the deformation during equilibration of the loads (Herwanger and Koutsabeloulis, 2011).

Results and Discussions

Full field history matching. The proposed CHOPS modeling was implemented in a heavy oil reservoir in Alberta with 15 wells. The sand production data was fed into the fractal-wormhole model to predict the wormhole network growth at every 4 to 6 months. The cumulative sand production data per well and the resulting wormhole network in several periods are reported by Rangriz Shokri and Babadagli (2013) in the conference version of this paper. Assuming the kinetic reaction model for foamy oil flow, both gas and oil production rates were matched as shown in **Figure 4-2**. Once the match was obtained, the full field model was imported to VISAGE geomechanics simulator for further analysis.

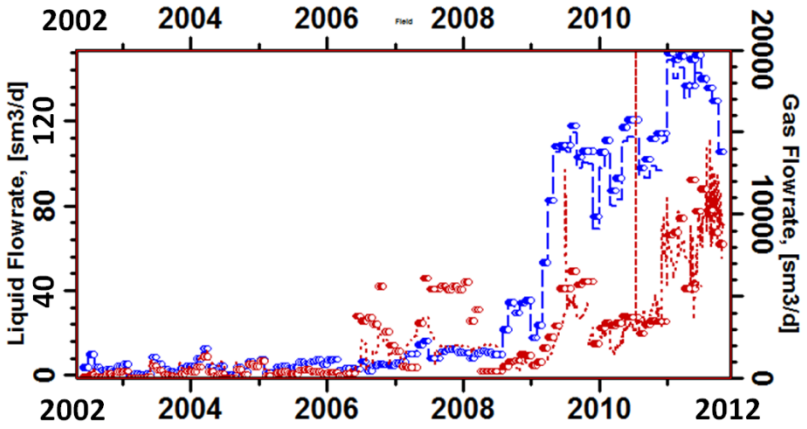

Figure 4- 2: History matched field production data, simulated oil data (blue line), historic oil data (blue circles), simulated gas data (red line), historic gas data (red circles).

Field-wide deformations and stress changes. During 10 years of reservoir production, average pressure in the reservoir decreased. The pressure drop is the largest in the vicinity of producing wells whereas the reservoir pressure far from wellbore and near reservoir boundaries does not show significant changes. This phenomenon might be more pronounced due to heavy nature of studied viscous oil. A decrease in pore

pressure will locally transfer the weight of overburden, previously supported in part by pore pressure, to the rock matrix and causes an increase in vertical effective stress in the reservoir (Herwanger and Koutsabeloulis 2011). The increase in compressive stress results in reservoir compaction. This compaction might be along with overburden subsidence or/and underburden rebound; i.e. overburden moves downward and underburden moves upward. These movements would make the rock in overburden and underburden become stretched and decreased the vertical effective stresses in these domains. Since the equilibrium equations should be honored in all directions, horizontal movement or an increase in subhorizontal stresses are predicted just above reservoir section, in deep overburden and cap rock regions. Details of this analysis are provided in cap rock (shale) and reservoir (loose uniform sand) segments.

Geomechanical analysis in reservoir segment and wormhole network. A decrease in pore pressure during 10 years of production has increased the effective vertical stresses, causing reservoir compaction with maximum of downward vertical displacement of 15 cm at the top layer and upward vertical displacement of 10 cm at the bottom layer. This localized compaction is more pronounced around the well location with largest pressure drawdown (Well 15). The top view of the upper and lower layers of full field reservoir is shown in **Figure 4-3 (b) and (d)**, respectively. Note the vertical downward displacement (negative values) around wells shown in purple color while red color is reserved to resemble vertical upward displacement (positive values). Green color shows zero or no significant displacement. Also, the displacement in wormhole layer is depicted in **Figure 4-3 (c)**. As seen, if the wormhole network layer (10 cm in thickness) was developed in the middle to lower layers of the reservoir, then the vertical displacement would not be very significant and probably more of compaction type during production phase. This issue should be studied with more accurate geological and mechanical information.

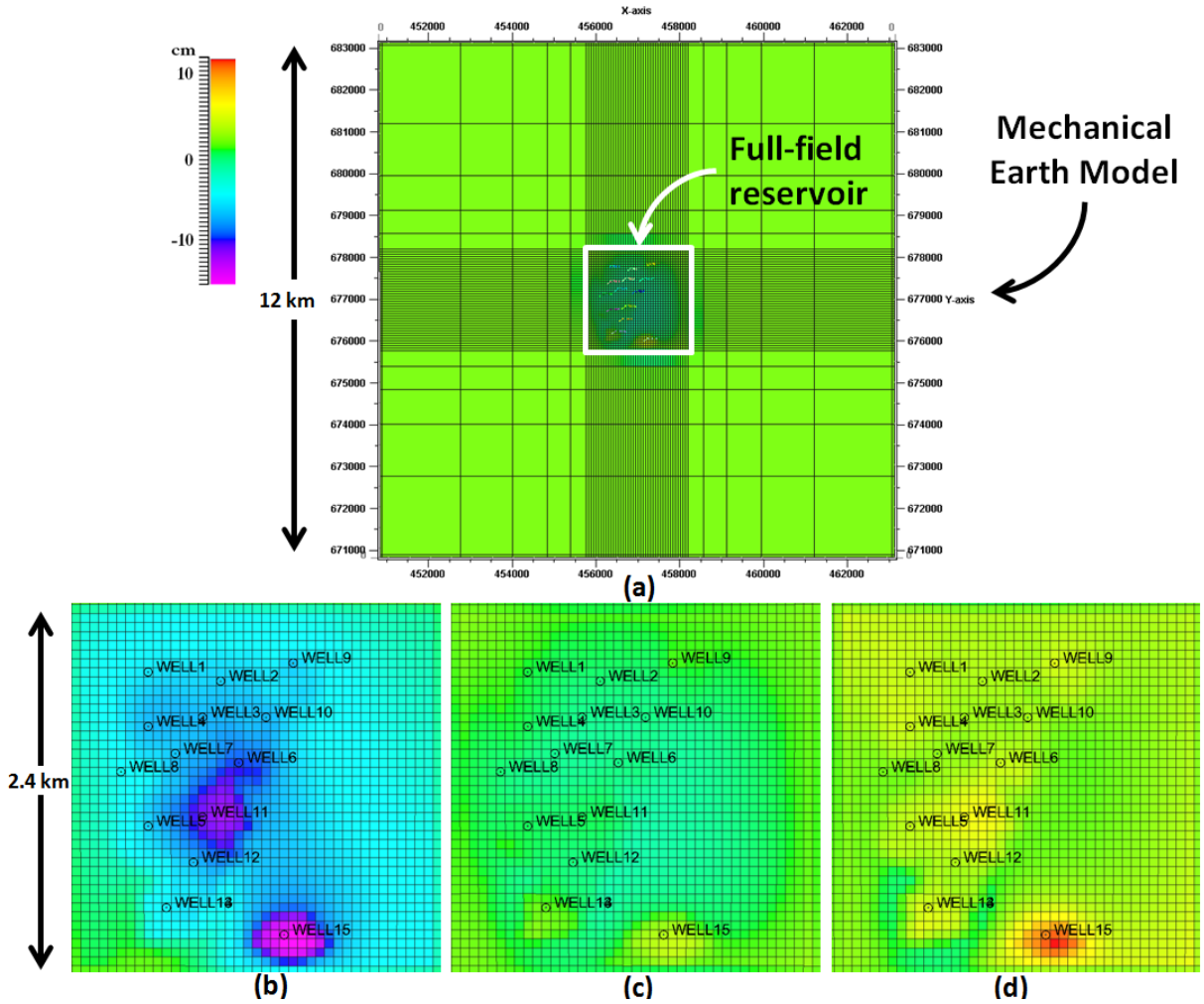

Figure 4- 3: Vertical displacement profile after primary production (a) top view of Mechanical Earth Model and location of reservoir section for further analysis (b) downward movement of upper reservoir layer shown with cold colors (c) no significant displacement in wormhole layer (d) upward movement of lower reservoir layer shown in warm colors.

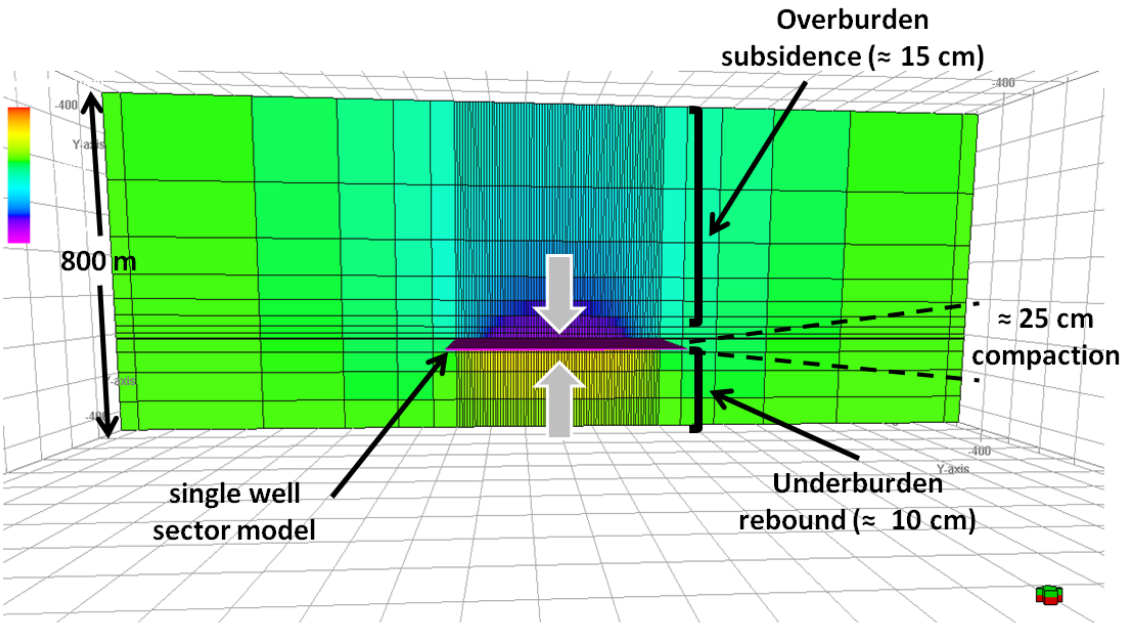

Figure 4- 4: Reservoir compaction, overburden subsidence and underburden rebound in the sector model.

We now focus on one of the wells with the largest pressure drop and, hence, the largest vertical displacement, as shown in **Figure 4-4**. When the localized stress tensor is considered within the reservoir section in **Figure 4-5**, the first point to notice is that effective stresses increase in all direction, but this increase is more pronounced in the vertical direction (note the change in vertical stress compared to horizontal components). This results in rock shortening in both vertical and lateral directions. However, the largest stress increase is observed in the vertical direction. The ratio of change in vertical and horizontal stress changes is governed by the Poisson's ratio. This ratio results in a larger displacement in vertical direction compared to horizontal movement, which is almost negligible.

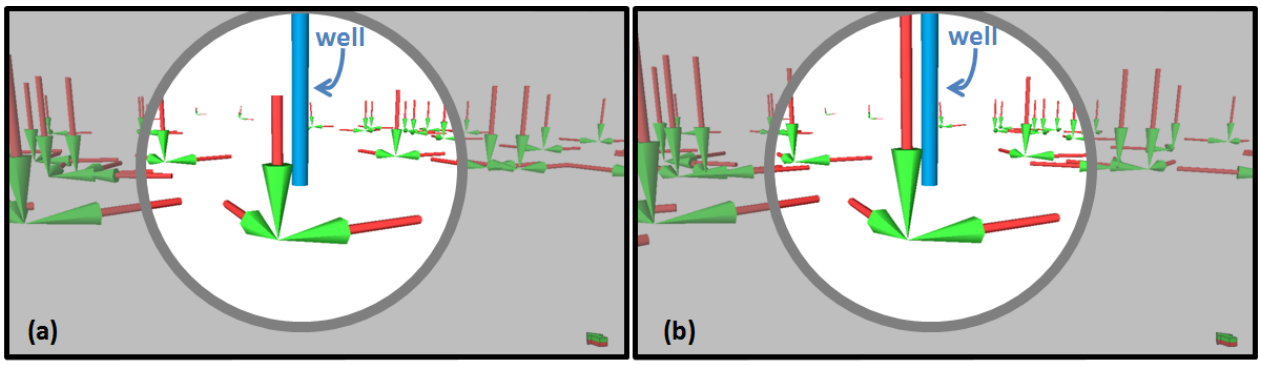

Figure 4- 5: Principal effective stress tensor (a) before and (b) after primary production. Note the increase in the vertical effective stress compared to changes in horizontal components.

Another interesting feature is the re-orientation of principal stresses shown in **Figure 4-6**. With oil production from a well, the principal stresses are re-orienting themselves towards the well in the direction of largest pressure drop. In the wormhole layer, however, pressure drop is perpendicular to the direction of the wormhole branches, which impedes localized stress re-orientation.

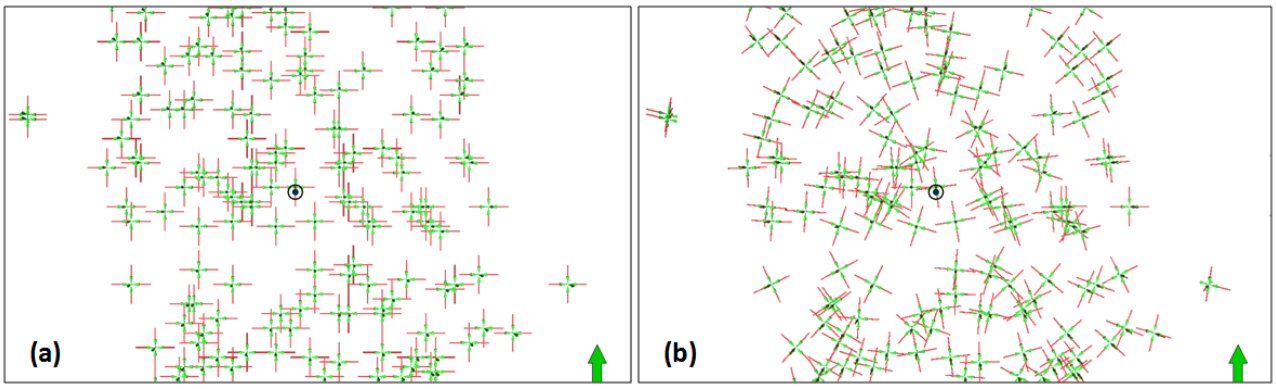

Figure 4- 6: Maps of effective stress change around a production well (a) before and (b) after primary production. Note the re-orientation of the stress components due to aggressive pressure depletion around well.

Geomechanical analysis in deep overburden and cap rock segment. A shale layer with material properties provided in Table 4-3 was assumed at the top of reservoir model. Although there is no fluid flow and pressure drop in this layer, the effect of pressure drawdown and associated reservoir compaction creates

small scale deformation features in this layer around wells. Overburden stretching along with reservoir compaction causes stress decrease in subvertical direction. In subhorizontal direction, the compressive principal stress changes are in radial and tangential direction in the vicinity of wellbore regions. If large shear stresses are experienced at reservoir-seal interface, the shear failure just above the reservoir would occur (Dusseault et al. 2001).

Figure 4-7 (a) shows the upscaled wormhole network in reservoir section. For details of the fractal-based upscaling, the interested reader is referred to Rangriz Shokri and Babadagli (2014). The resulted vertical displacement at the upper layer of reservoir is shown in **Figure 4-7 (b)**. Note the change in the vertical displacement around wells caused by localized compaction above the developed wormhole network. It is evident that the compaction features are well separated for large well spacing, for instance well 15 and well 11. As the reservoir compacts, the overburden stretches in vertical direction. This causes a decrease in vertical effective stress in overburden segment located at the top of wormhole network of reservoir region. As a requirement of the equilibrium equation, some of the vertical effective stress would transfer to the other parts of overburden. This phenomenon is known as stress arching. For densely spaced wells, the compaction features merge and stress arching is less pronounced (Herwanger and Koutsabeloulis 2011).

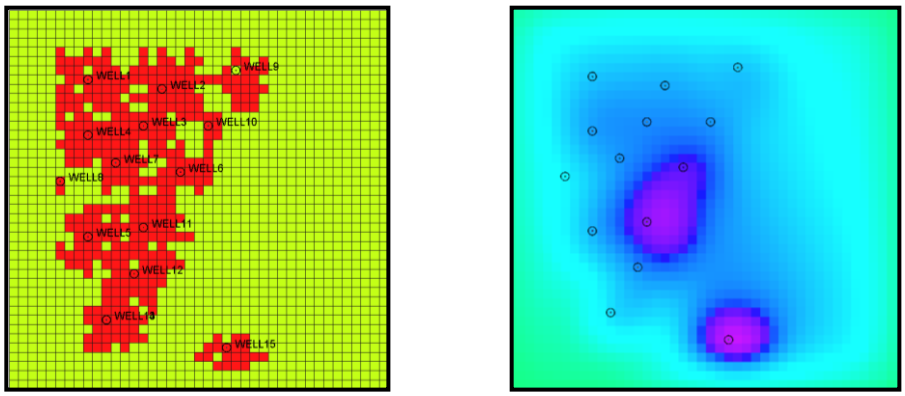

Figure 4- 7: Analysis of displacement with the presence of a wormhole network. (a) Upscaled wormhole network in field-scale simulation model (b) vertical displacement of the interface of reservoir layer and cap rock. Note the compaction features are well separated for large well spacing (well 15 and well 11).

Geomechanical response from cyclic loading and unloading due to solvent injection. Figure 4-8 demonstrates the variation of the vertical displacement of upper and lower layers of the reservoir during primary production and two cycles of injection and production. The pressure drop is only shown in two cycles of solvent stimulation. The first loading period is caused by early production and significant pressure drop. The upper layer of reservoir moves downward while the lower layer is displaced upward, which indicates the first reservoir compaction. After the first injection period, the average reservoir pressure increases and takes the reservoir into a loading state until the injection stops and the well is put on production. This is marked with a sudden movement of upper and lower layers upward and downward, respectively. In our analysis, no failure was experienced due to insignificant reservoir pressure increase. If the injection pressure increase continues above initial reservoir pressure, a short dilation process followed by tensile failure is predicted. However, keeping the loading and unloading process within a limited range, the simulator suggests no dramatic failure would occur.

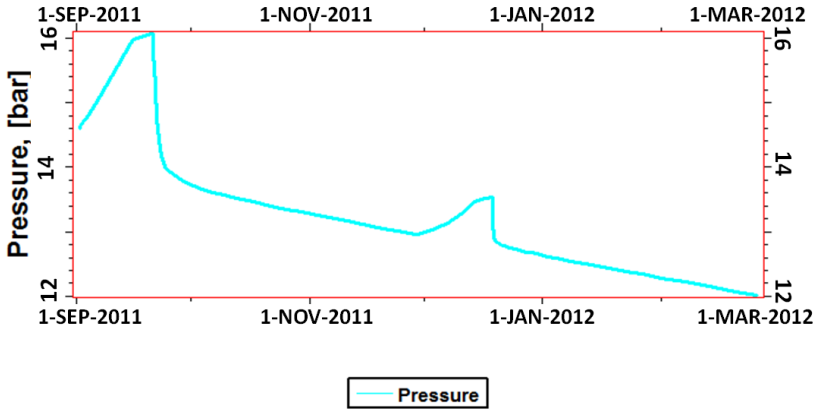

(a) Average reservoir pressure response during two cycles of cold solvent stimulation.

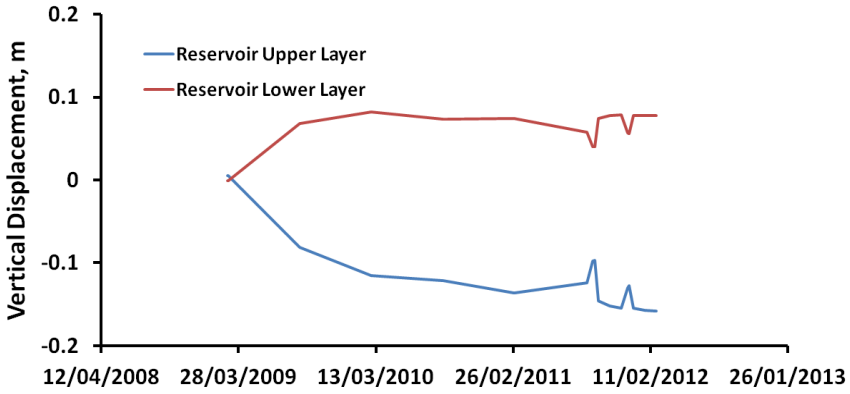

(b) Vertical displacement of upper and lower reservoir layers near a well subjected to cyclic solvent stimulation.

Figure 4- 8: Geomechanical response of cyclic solvent stimulation near wellbore region.

Impact of fluid injection stream. In the single well sector model, a quick study was done on the nature of injected solvent at isothermal reservoir conditions. C1, C2, C6 and a mixture of these single-component hydrocarbons were selected with identical operating constraints at the well face. It was first noticed that light hydrocarbons would increase the reservoir pressure more effectively than heavier components. Injection of light components shows more a swelling effect rather than changing oil properties. Therefore, in short cycles of 7 to 14 days of injection, re-pressurization of reservoir is more significant than oil dilution and diffusion. Heavier components, on the other side, show improvement in liquid production rate (**Figure 4-9**). Some part of the liquid production in each cycle is from the injected solvent. To observe the improvement, this effect was removed in Figure 4-9c. For the same injection volume at reservoir conditions (Figure 4-9b), the cumulative reservoir production was increased in the case of heavier hydrocarbon component in very short cycles of injection. This situation can possibly be explained through the time dependent diffusion process of solvents in the oil rather than the swelling effect. This could be enhanced by increasing the soaking periods when the wells were shut. Nevertheles, optimizing this cyclic injection is not considered here.

Although the injection of heavy components is not feasible in practice due to economic reasons, it gives a hint for possible combination of light and heavy components. Light components would help to increase reservoir pressure while a small batch of heavier component diffuses into the oil and changes the oil properties more effectively. The thermal injection option as well as its hybrid application with solvent was not considered in this paper due to inefficiency of thermal methods in thin layers.

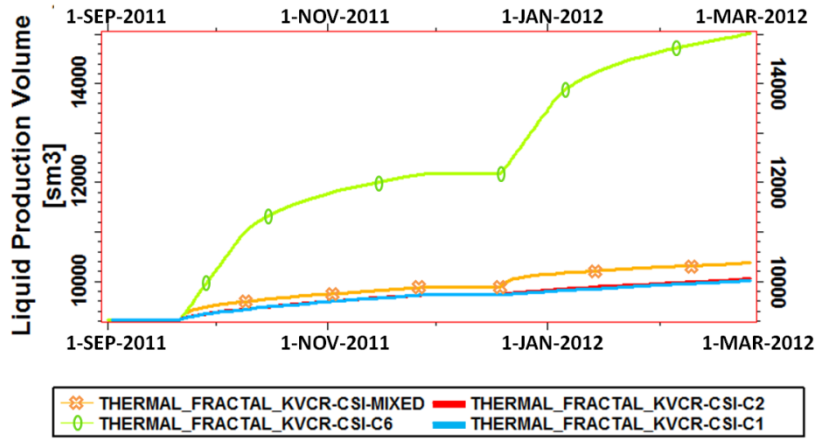

(a) Cumulative oil production of several solvent streams during two cycle of solvent stimulation.

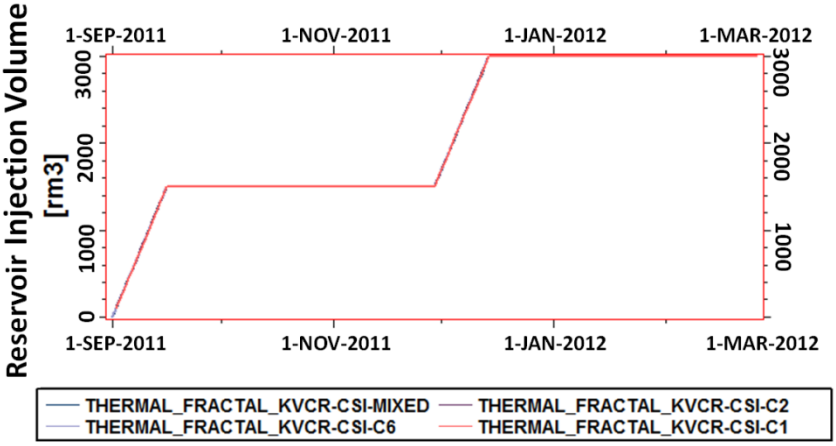

(b) Cumulative reservoir injection of several solvent streams during two cycle of solvent stimulation.

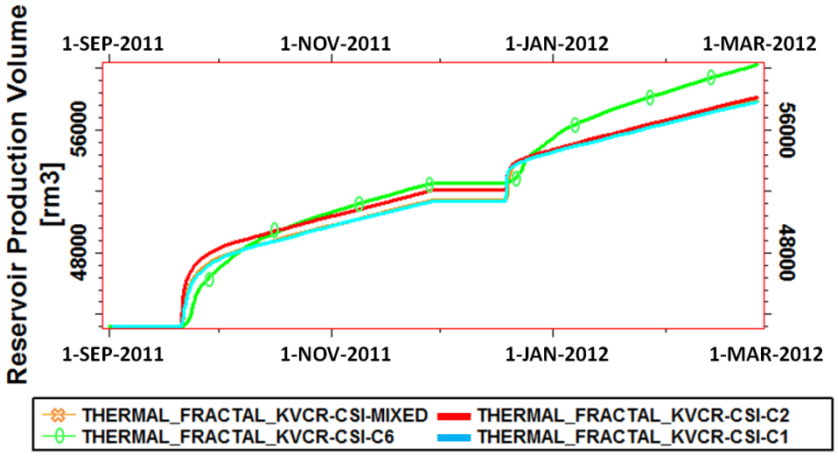

(c) Cumulative reservoir production of several solvent streams during two cycle of solvent stimulation.

Figure 4- 9: Reservoir performance during two cycles of solvent stimulation.

Porosity and permeability update in coupled cyclic solvent stimulation. To estimate the importance of possible porosity and absolute permeability change during cyclic solvent stimulation on fluid flow, we developed a simple interface using VBA programming language. For simplicity, we adopted a sequentially coupled scheme in which pressure and temperature data (if non-isothermal EOR is considered) are fed cell by cell into the geomechanics simulator at each coupling time step to calculate and update the stress and strain fields. The resulted volume strains are then used to update porosity and absolute permeability for fluid flow simulation (Longuemare et al. 2002) as:

$$\Phi = \frac{\Phi_0 + \varepsilon_v}{1 + \varepsilon_v} \qquad (4-1)$$

$$\frac{k}{k_0} = \frac{\left[1 + \frac{\varepsilon_v}{\Phi_0}\right]^3}{1 + \varepsilon_v} \qquad (4-2)$$

Subscript of "o" in **Eqs. 4-1** and **4-2** states the initial value of the specified parameter and ε_v is the volumetric strain to be defined as the summation of strains in x, y and z directions:

$$\varepsilon_v = \varepsilon_{xx} + \varepsilon_{yy} + \varepsilon_{zz} \qquad (4-3)$$

With notion to the presence of a layer containing high permeability wormhole network, it could be predicted that the effect of compaction on fluid flow is insignificant, unless the wormhole network locally collapses due to aggressive cyclic fluid injection and production. Bearing in mind the geomechanical simulation results in the preceding sections, the latter was not assumed to be an option in this study and wormholes were considered sufficiently stable during solvent stimulation. **Figure 4-10** demonstrates the results of coupled approach considering porosity and permeability changes compared to uncoupled approach excluding porosity and permeability updates. At this stage, no convergence criteria or stability analysis is performed in the sequentially coupled schemes. Figures 4-10 (a) and (b) indicate a significant decrease in porosity and permeability of non-wormhole domain around wellbore region rather than wormhole network. The changes in permeability and porosity of non-wormhole domain near wellbore region are in the order of 10% and 25%, respectively. Note that the changes in permeability and porosity of wormhole domain near wellbore region are about 3% and 2%, respectively. It should be also noticed that near wellbore region experiences the maximum changes in mechanical properties compared to other parts of reservoir, mainly due to larger pressure drop. In view of the fact that the wormholes are considered as the main fluid path from reservoir to wellbore, the effect on fluid production might be considered negligible. Figure 4-10 (c) suggests that the use of coupled approach slightly reduces the amount of oil production on the order of 0.5% to 3%. This reduction is probably caused by the earlier assumption of the way that wellbore communicates with wormhole network. It was assumed that wormholes are connected to the well through one layer, i.e. limited perforation. In reality, the wellbore region is highly affected with sand production and the well is connected to the wormhole layer through the whole perforation as a single unit of damaged zone, even with the assumption of wormhole network growth in one layer. Therefore, the discrepancy of the coupled and uncoupled approaches is related to non-wormhole domain in wellbore region. Proper use of a limited damage zone around well would make the discrepancy of coupled and uncoupled approaches practically negligible in restricted loading and unloading cycles when no significant sand production is exercised. If sand production occurs in large amount during solvent stimulation, the model should then be updated with new sand

production data to include the growth of wormhole network in a step-wise manner as practiced by Rangriz Shokri and Babadagli (2014).

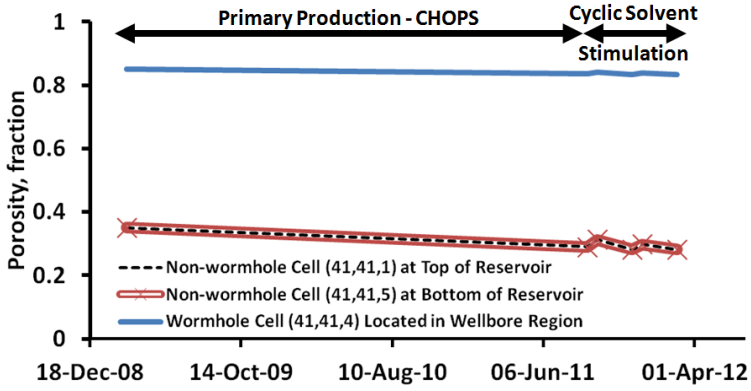

(a) Porosity change during primary production and two cycle of solvent stimulation.

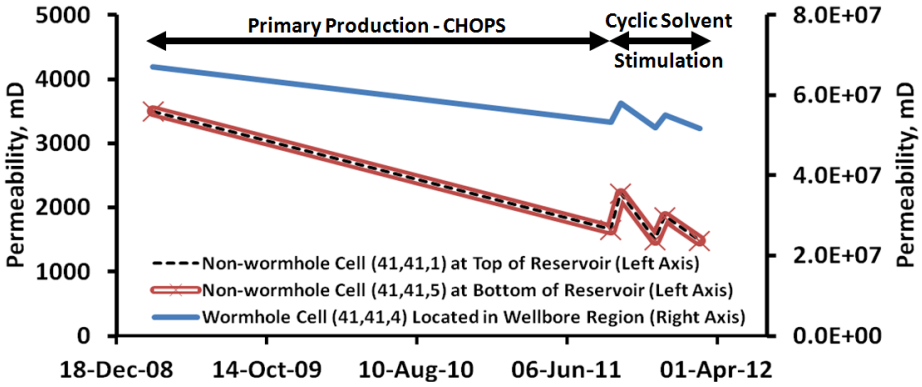

(b) Permeability change during primary production and two cycle of solvent stimulation.

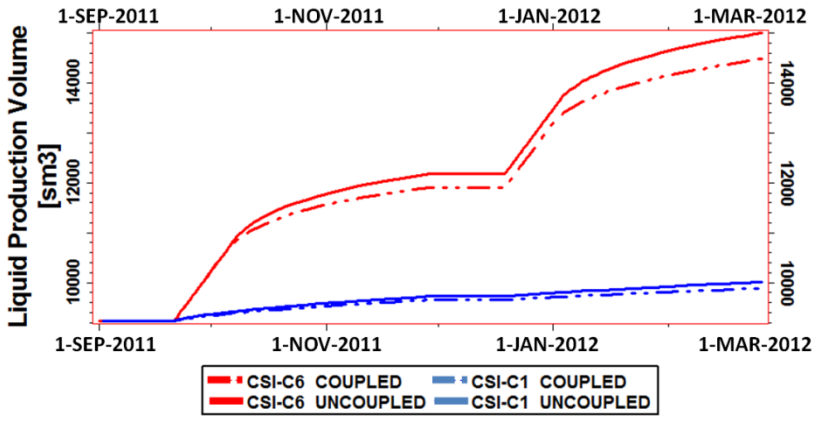

(c) Cumulative oil production of C1 and C6 solvent streams during two cycle of solvent stimulation.

Figure 4- 10: Comparison of coupled and uncoupled schemes during two cycles of solvent stimulation.

Conclusions

In this study, a 3D Mechanical Earth Model was constructed to understand the contribution of production schedule on stress changes on a thin unconsolidated heavy oil reservoir in Alberta. Prior to performing geomechanical analysis, a fluid flow modeling approach was proposed that takes into account the growing nature of the wormhole network through a DLA (fractal) pattern respecting the sand production data and foamy oil flow through kinetic reactions. The hydro-geomechanical model was then used for assessment of near wellbore regions during cyclic injection and production. The field-wide deformation and stress changes were analyzed in deep overburden, cap rock, and reservoir region to show the influence of local stress orientations in soft and stiff layers. It was shown how stress arching re-distribute the cyclic injection-production induced stresses to flow around soft inclusions in the suspected wormhole layer. The study was then focused on a sector model to assess EOR processes with different solvent streams. It was noticed that light hydrocarbon components are responsible to re-pressurize the formation while the heavier components are more effective to dilute the heavy oil through component exchange.

The discrepancy of coupled and uncoupled approaches was also studied in wellbore region. Because the wormholes are considered to be the main fluid path for reservoir to deliver the oil to wellbore region, it was argued that the coupling effect on fluid production might be considered negligible in restricted loading and unloading cycles with no significant sand production. However, if sand production occurs in large amount during solvent stimulation, the model should then be updated with new sand production data to include the growth of wormhole network in a step-wise manner.

This study also addresses how a 3D hydro-geomechanical model with very limited data can be used for reliable investigation of reservoir performance to give deeper insight than using flow simulation alone. The assessment of the potential of geomechanics can then ascertain whether a more detailed modeling is necessary.

References

ECLIPSE Technical Manual, Schlumberger. 2013.

VISAGE Technical Manual, Schlumberger. 2013.

Butler, R.M., 1997. Thermal Recovery of Oil and Bitumen. Prentice Hall.

Coombe, D., Tremblay, B., Tran, D., et al. 2001. Coupled Hydro-Geomechanical Modeling of the Cold Production Process. SPE paper 69719 presented at the SPE International Thermal Operations and Heavy Oil Symposium,Porlamar, Margarita Island, Venezuela, 12-14 March.

Dusseault, M. 1993.Cold Production and Enhanced Oil Recovery. *Journal of Canadian Petroleum Technology* **32** (9): 16-18.

Dusseault, M., Bruno, M.S., and Barrera, J.A. 2001. Casing Shear: Causes, Cases, Cures. *SPE Drill. & Prod. Prac. J.* **16** (2): 98-107.

Elkins, L.F., Morton, D., and Blackwell, W.A. 1972. Experimental Fireflood in a Very Viscous Oil-Unconsolidated Sand Reservoir, S. E. Pauls Valley Field, Oklahoma. Paper SPE 4086 presented at the 47th Annual Fall Meeting of the Society of Petroleum Engineers of AIME, San Antonia, Texas, 8–11 October.

Herwanger, J. and Koutsabeloulis, N. 2011. *Seismic Geomechanics: How To Build and Calibrate Geomechanical Models using 3D and 4D Seismic Data*. D.B. Houten, The Netherlands: EAGE Publications.

Lebel, J.P. 1994. Performance Implications of Various Reservoir Access Geometries. Document presented at the 11th Annual Heavy Oil & Oil Sands Technical Symposium "Challenges and Innovations" March 2nd.

Longuemare, P., Mainguy, M., Lemonnier, P., Onaisi, A., Gerard, C., Koutsabeloulis, N., 2002. Geomechanics in Reservoir Simulation – Overview of Coupling Methods and Field Case Study. Oil and Gas Science and Technology – Rev. IFP **57** (5): 471.

Loughead, D.J. and Saltuklaroglu, M. 1992. Lloydminster Heavy Oil Production: Why So Unusual. Paper presented at the 9th Annual Heavy Oil and Oil Sands Technology Symposium, Calgary, Alberta, Canada, 11 March.

Maini, B. B. and Sarma, H. K. 1993. Significant of Foamy-Oil Behavior in Primary Production of Heavy Oils. *JCPT* **32** (9): 50-54.

Maini, B. B. 1999. Foamy Oil Flow in Primary Production of Heavy Oil under Solution Gas Drive. Paper SPE 56541 presented at the SPE International Conference, Houston, Texas, 3-6 October.

Mccaffrey, W. and Bowman, R. 1991. Recent Successes in Primary Bitumen Production. Paper presented at the 81st Annual Heavy Oil and Oil Sands Technical Symposium, 14 March.

Meza, B. 2001.Experimental Investigation of Sand Production into a Horizontal Well Slot.MSc Thesis, School of Mining and Petroleum Engineering, University of Alberta (Fall 2011).

Rangriz Shokri, A. and Babadagli, T. 2012. An Approach to Model CHOPS (Cold Heavy Oil Production with Sand) and Post-CHOPS Applications. Paper SPE 159437 presented at the SPE Annual Technical Conference and Exhibition, San Antonio, Texas, USA, 8-10 October.

Rangriz Shokri, A. and Babadagli, T. 2013. Modeling Thermal and Solvent Injection Techniques as Post-CHOPS Applications considering Geomechanical and Compositional Effects. Paper SPE 165534 presented at the SPE Heavy Oil Conf., Calgary, AB, Canada, 11-13 June.

Rangriz Shokri, A. and Babadagli, T. 2014. Evaluation of Thermal/Solvent Applications with and without Cold Heavy Oil Production with Sand (CHOPS). *JCPT* **53** (2): 95-108.

Sawatzky, R. 2008-2009. Cold Production: Recovery Mechanisms and Field Performance. Presented as an SPE Distinguished Lecture in Calgary, Alberta, Canada.

Smith, G.E. 1986. Fluid Flow and Sand Production in Heavy Oil Reservoir under Solution Gas Drive. Paper SPE 15094 presented at the 56th California Regional Meeting of the Society of Petroleum Engineers, Oakland. CA, 2–4 April.

Squires, A. 1993. Inter-Well Tracer Results and Gel Blocking Program. Technical paper presented at the 10th Annual Heavy Oil and Oil Sands Technical Symposium, 9 March.

Tremblay, B. Sedgwick, G. and Forshner, K. 1996. Imaging of Sand Production in a Horizontal Sand Pack by X-Ray Computed Tomography.*SPE Formation Evaluation***11** (2): 94-98.

Tremblay, B. Sedgwick, G., Forshner, K. 1997.Simulation of Cold Production in Heavy-Oil Reservoirs: Wormhole Dynamics.*SPE Reservoir Evaluation & Engineering* **12** (2): 110–111.

Tremblay, B. Sedgwick, G., and Vu, D. 1999a. CT Imaging of Wormhole Growth under Solution Gas Drive. *SPE ResEvale&Eng***2** (1) 37-45.

Tremblay, B., Sedgwick, G., and Vu, D. 1999b.A Review of Cold Production in Heavy Oil Reservoirs. Paper 2008 presented at the 10th European Symposium on Improved Oil Recovery, Brighton, UK, 18-20 August.

Urgelli, D., Durandeau, M., Foucault, H., et al. 1999. Investigation of Foamy Oil Effect from Laboratory Experiments. Paper SPE 54083 presented at the SPE International Conference, Bakersfield, California, USA, 17-19 March.

Wyllie, M.R.J., and Gardner, G.H.F. 1958. The Generalized Kozeny-Carmen Equation - Its Application to Problems of Multi-Phase Flow in Porous Media. World Oil, 146, 121.

Yazdani, A., Alvestad, J., Kjonsvik, D., Gilje, E., Kowalewski, E., 2011. A Parametric Simulation Study for Solvent Co-injection Process in Bitumen Deposits. Paper SPE 148804 presented at the Canadian Unconventional Resources Conference, Calgary, Alberta, Canada, November 15-17.

Yeung, K. 1995.Cold Flow Production of Crude Bitumen at the Burnt Lake Project, Northeastern Alberta. Paper presented at the 1995 UNITAR International Conference on Heavy and Tar Sands, Houston, Texas, 12-17 February.

Chapter 5: Laboratory Measurements and Numerical Simulation of Thermally-Aided Cyclic Solvent Stimulation in the Presence of Wormholes after CHOPS

A version of this chapter was submitted to Journal of Canadian Petroleum Technology.

Abstract

In this study, an experimental set-up consisting of a sand-pack with different configurations of complexity of wormhole patterns was designed. These different configurations have the same WCI (wormhole coverage index) determined by our earlier field scale history match studies. After saturating the model with heavy oil, three different solvents (CO_2, heptane, and diluents) were introduced into the wormhole structure inside the sand-pack (injection phase), then left for a period of time (soaking phase). Next, the resulted mixture (solvent and oil) was allowed to be produced (production phase). The experiment was aimed to mimic cyclic solvent stimulation at reservoir conditions and several cycles were run for each experiment. At each cycle, the amounts of collected oil and solvent were determined and the resulted mixture was analyzed through gas chromatography and refractometry. It was observed that some of the injected solvent was trapped inside the sand-pack. Therefore, in the final step, a solvent retrieval attempt was made by injecting different -low-temperature hot water based on the solvent type. The aim was to observe how much additional solvent could be retrieved from the sand-pack at reservoir conditions.

Next, the sand-pack experiments were numerically simulated and effective diffusion coefficients were obtained through history matching. To generate accurate predictions in field-scale simulation, an up-scaling procedure from laboratory results of the cyclic solvent injection process was suggested. In this study, we observed that the use of light solvents (CO_2) could maintain the sand-pack pressure for a longer period (attributed to foamy oil phenomenon) compared to liquid solvent during production phase. But the oil recovery from sole application of light solvent was not as considerable as with the heavier solvents (heptane and diluents). These observations suggest that an improved heavy oil recovery could be achieved using hybrid application of solvents and hot water in CHOPS reservoirs. A post-flush hot-water was found to play a positive role in solvent retrieval; however, the scale-dependency of solvent retrieval behaviour needs to be investigated. The findings of this paper can be used in a later study to optimize the field-scale solvent injection schemes considering the economics of the process tested.

Key words: Post-CHOPS EOR experiments, cyclic solvent injection, solvent retrieval thermally, wormhole/non-wormhole volume ratio

Introduction

A huge amount of heavy oil is located in thin and shallow unconsolidated reservoirs of Western Alberta, Canada. Due to its cheap operating cost, cold production of oil with deliberate initiation of sand influx (method called CHOPS –cold heavy-oil production with sands) has been preferred as a primary method. Although this gives early high production rates, it suffers from poor overall recovery. Meanwhile, this aggressive co-production of sands generates wormhole structures and eventually results in a heterogeneous reservoir. Continuous sand production causes the wormholes to grow more, resulting in a high permeability network, which may even connect the wells to each other. This is the main reason why waterflooding in CHOPS reservoirs experiences early breakthrough. In addition, the heterogeneous structure obscures an efficient application of solvent injection and the performance of thermal processes in 2-5m pay zone is economically impeded due to heat losses.

However, the development of high-permeability channels in the reservoir could be beneficial as they provide a network serving as a natural multi-branched system among the wells to deliver the injected and produced fluids to and from reservoir to surface facilities. To this extent, the similarity of CHOPS and naturally fractured reservoir (NFR) is quite astonishing, not only because the less permeable non-wormhole (matrix) domain contributes significantly to fluid storage, but also because it is the high permeable wormhole (fracture) domain that provides the path for fluid mobilization. It is therefore not a surprise, as will be revealed in this paper, if classical NFR studies are utilized for implementation of EOR options in CHOPS reservoirs.

The implementation of these EOR methods are limited as post-CHOPS options. Kantzas and Brook (2004) considered water/polymer-flooding in sand-packs saturated with heavy oil, and later, gas injection and gas

pulsing were suggested. Later, Alshmakhy et al. (2012) performed cyclic CO_2 injection modelling for post-CHOPS EOR. In a separate work, the potential of cyclic solvent injection in gas-phase as a post-CHOPS EOR option was experimentally studied by Ivory et al. (2010). They showed an increase of more than 50% oil recovery at lab conditions assuming the wormhole was located at the very bottom of their model, or equivalent producing formation. Therefore, most of recovery was attributed to gravity drainage. Based on current CHOPS literature, it is more favorable for wormholes to develop at the top of the formation (less overburden weight, higher probability of bubble nucleation, which are governing mechanisms for wormhole to overcome the critical pressure gradient at its tip to grow and allow for more sand production [Tremblay et al. 1997, 1999]).

Coskuner et al. (2013) and Naderi and Babadagli (2014) used hot water and solvent injection as a follow-up CHOPS recovery technique. They concluded that an initial hot water phase prior to solvent injection did not produce any appreciable amount of oil, but it may help to condition the reservoir in order to maximize oil recovery in solvent phase. Be aware that none of the above studies considered the physical presence of wormholes in their experiments.

In a recent study, Du et al. (2013) considered the presence of wormhole in a set of experiments. They selected propane as the solvent in gaseous phase and studied the effects of wormhole length, vertical location and model diameter in attempt to suggest an up-scaling procedure for CSI and an analogy of vapour chamber rise as in VAPEX. They did not observe the foamy oil behavior of oil and propane mixture, probably since they used a low viscous oil (4330 cP at 15ºC).

With notion to the potential use of solvents in post-CHOPS, more experimentation is required to study the interactions between wormhole and non-wormhole domains based on different wormholes/non-wormhole volume ratios and solvent types. We introduce the wormhole coverage index, WCI, as follows based on our simulation work done for a real field case (Rangriz Shokri and Babadagli 2012, 2014):

$$WCI = \frac{Wormhole\ Volume}{Total\ Sandpack\ Volume} \tag{5-1}$$

It is evident that the dimensionless WCI is a function of wormhole diameter, wormhole configuration, and the extent that wormhole network might have developed. In field scale, WCI can be related to a fractal number associated to the developed wormhole network (Rangriz Shokri and Babadagli 2014).

In this study, an experimental set-up consisting of a sand-pack with different configurations of complexity of wormhole patterns was designed. These experiments would be a "scaled model" based on our previous field model study (Rangriz Shokri and Babadagli 2012). These different configurations have the same WCI determined through history matching of sand production of 15 wells in an Albertan CHOPS field, which yielded fractal type wormhole patterns (Rangriz Shokri and Babadagli 2014). The experimental model was initially saturated with heavy oil. Three different solvents (CO_2, heptane, and diluents) were first introduced into the wormhole structure inside the sand-pack (injection phase), then left isolated for a period of time (soaking phase). Next, the resulted mixture (solvent and oil) was allowed to be produced (production phase). The experiment was aimed to mimic cyclic solvent stimulation at low and high pressure conditions and several cycles were run for each experiment. At each cycle, the amounts of collected oil and solvent were determined and the resulted mixture was analyzed through gas chromatography and refractometry. In the final step, a solvent retrieval attempt was made by injecting different -low- temperature steam/hot water based on the solvent type. The aim was to observe how much solvent could be retrieved from the sand-pack considering different boiling points of the solvents at reservoir conditions. Finally, these five experiments were numerically simulated and effective diffusion coefficients were obtained that could be used in our later field-scale optimization schemes.

Fluid Characterization and Modeling

Crude oil characterization is mainly based on boiling point distribution. One can characterize crude oil fractions in terms of pseudo-components defined by an average boiling point (Kariznovi et al. 2010). Most

heavy oil studies only consider two components to represent heavy oil: a light component (usually methane) and a lumped heavy component. This is not recommended when more elaborate behavior, such as asphaltene precipitation or near miscible floods, needs to be modeled. On the other hand, including all or most components is computationally expensive and an optimum number of pseudo-components should be selected.

In this study, the original oil and diluents (one of the liquid solvents) were characterized with the help of gas chromatography. The cumulative mass distribution of both original oil and diluents are shown in **Figure 5-1a** vs. true boiling point, and in **Figure 5-1b** through **Figure 5-1d** vs. single carbon number up to C_{120+}. **Figure 5-1e** shows one of the most computationally efficient characterizations, which honors the wide range of hydrocarbon components in both original oil and diluents with a residue of C_{30+}. Since CO_2 and C_7 are used as separate solvents during CSI experiments, they are also included as separate components. Also note that CO_2 has the extraction capability up to C_{30}.

The Peng-Robinson EOS with volume translation was adopted to match saturation pressure and GOR of dead oil mixture with C_1 and CO_2, separately (**Table 5-1**).

Table 5- 1: Fluid Properties of Original Dead Oil.

Parameter	Value
Dead oil viscosity (cP) @ 25 °C	67400
Oil density (kg/m3) @ 25° C	1004
Saturation pressure with C1 (bars)	25.3
GOR at P_{sat} with C1	10-11
Saturation pressure with CO_2 (bars)	24.1
GOR at P_{sat} with CO_2	10-11
Saturated content (%)	25.57
Aromatic content (%)	31.17
Resin content (%)	26.77
Asphaltene content (%)	16.30

In the first step, the molecular weight of pseudo-components was estimated from true boiling points. The Lee-Kesler correlation was selected to determine critical properties of the pseudo-components since this correlation has shown to produce considerably better results than other correlations in Athabasca, Wabasca, Peace River, and Cold Lake bitumen with different solvents (Kariznovi et al. 2010). However, the critical

properties of pseudo-components were slightly adjusted as primary tuning parameters. The minimization of saturation pressures variance was considered as the criteria to obtain optimal values of binary interaction coefficients. The acentric factors were estimated by the Twu correlation. Volume shifts were employed to match liquid density. To complete the characterization, the Lohrenz-Bray-Clark (LBC) model was used to correlate the oil viscosity. Full description of PVT modeling is summarized in **Table 5-2** through **Table 5-4**.

Table 5- 2: Full Description of EOS Parameters.

Components	Mol Weight	Critical Pressure (bar)	Critical Temperature (K)	Omega A	Omega B	Acentric Factor	Parachors	Critical Volume (m3 /kg-mole)	Critical Z-factor	Critical Volume for Viscosity (m3 /kg-mole)	Critical Z-factor for Viscosity	Boiling Temperature (K)	Reference Density (kg / m^3)	Reference Temperature (K)
CO2	44.01	73.866	304.7	0.45724	0.077796	0.225	78	0.094	0.27408	0.094	0.27408	194.7	777	293
C1	16.04	46.042	190.6	0.45724	0.077796	0.013	77	0.098	0.28473	0.098	0.28473	111.6	425	111.7
C2-6	72.15	33.589	465.9	0.45724	0.077796	0.2413	228.9	0.31	0.26881	0.31	0.26881	305.9	623.6	293
C7	96	29.384	548	0.45724	0.077796	0.3	312.5	0.392	0.25281	0.392	0.25281	365.05	722	289
C8-29	258.34	16.066	763.58	0.45724	0.077796	0.64768	664.86	0.92632	0.23442	0.5253	0.13294	584.55	848.26	289
C30+	620	5.8238	1502.1	0.45724	0.077796	1.671	1556	2.5001	0.11658	4.5116	0.21038	953.34	936.14	288.71

Table 5- 3: Fluid Compositions of Original Oil and Solvents.

Components	Composition (weight percent)			
	Original oil	C7	Diluents	CO2
CO2	0.00	0.00	0.00	100
C1	0.00	0.00	0.00	0.00
C2-6	3.20	0.00	23.37	0.00
C7	0.12	100	14.14	0.00
C8-29	24.05	0.00	44.71	0.00
C30+	72.64	0.00	17.79	0.00
TOTAL	100	100	100	100

Table 5- 4: Binary Interaction Coefficients (BICs).

Component	CO2	C1	C2-6	C7	C8+	C30+
CO2	0					
C1	0.1	0				
C2-6	0.1	0	0			
C7	0.1	0.03308	0	0		
C8+	0.1	0.050756	0	0	0	
C30+	0.1	0.06306	0	0	0	0

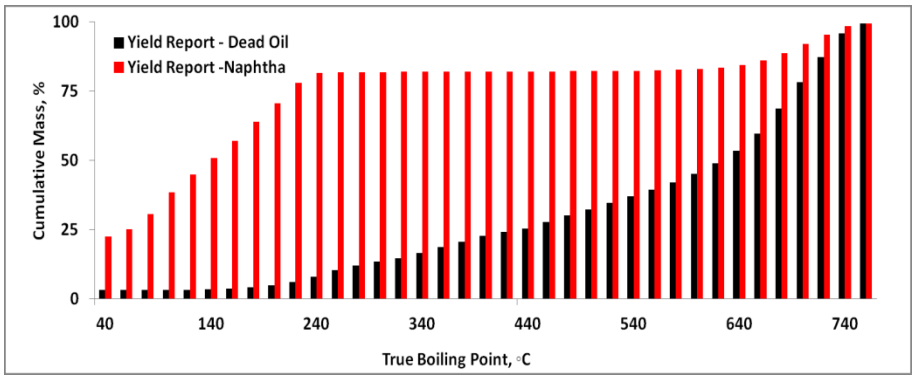

(a) Yield report for diluents and original dead oil.

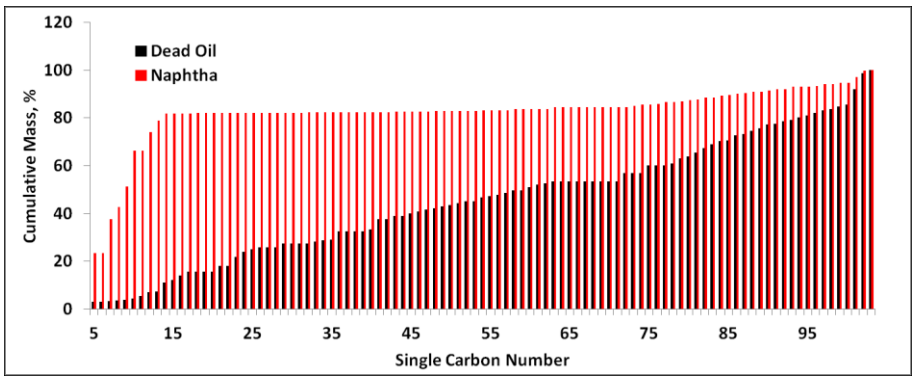

(b) Cumulative mass distribution of diluents and original dead oil.

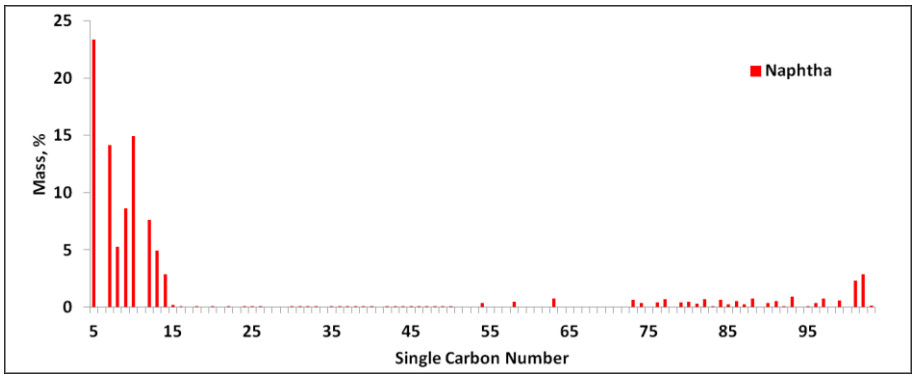

(c) Weight fraction of diluents up to C_{120+}.

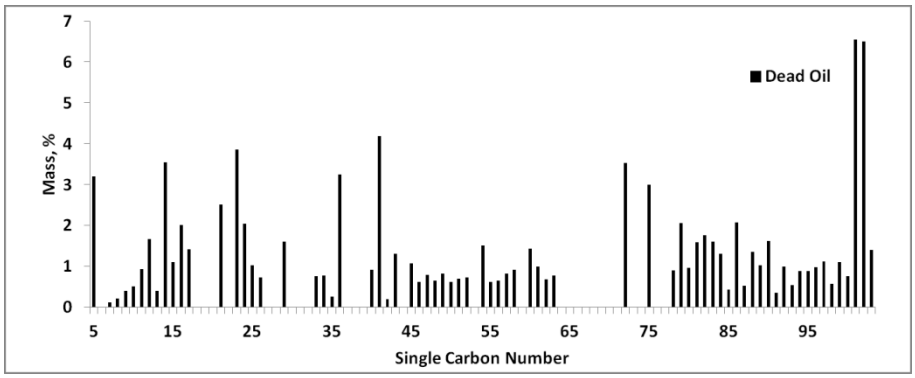

(d) Weight fraction of original dead oil up to C_{120+}.

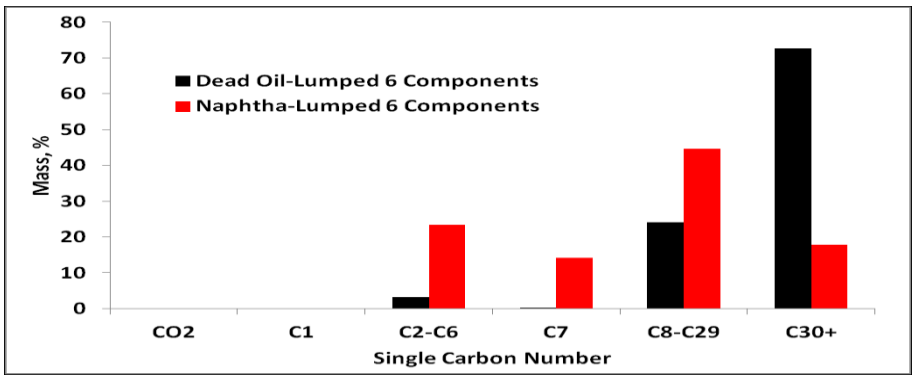

(e) Lumped pseudo-components of diluents and original dead oil.

Figure 5- 1: Gas chromatography characterization of diluents and original dead oil.

The changes in heavy oil density and viscosity with different solvents and temperature are shown in **Figure 5-2a** through **Figure 5-2d**.

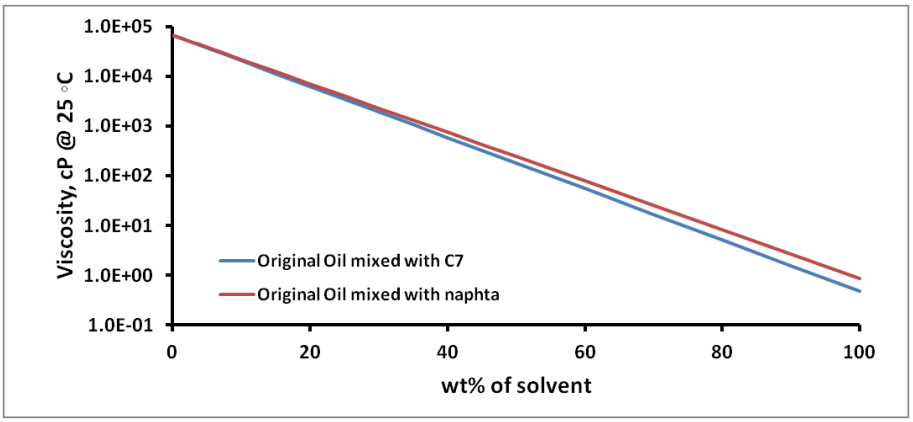

(a) Mixture viscosity of original dead oil with C7 and diluents at 25ºC.

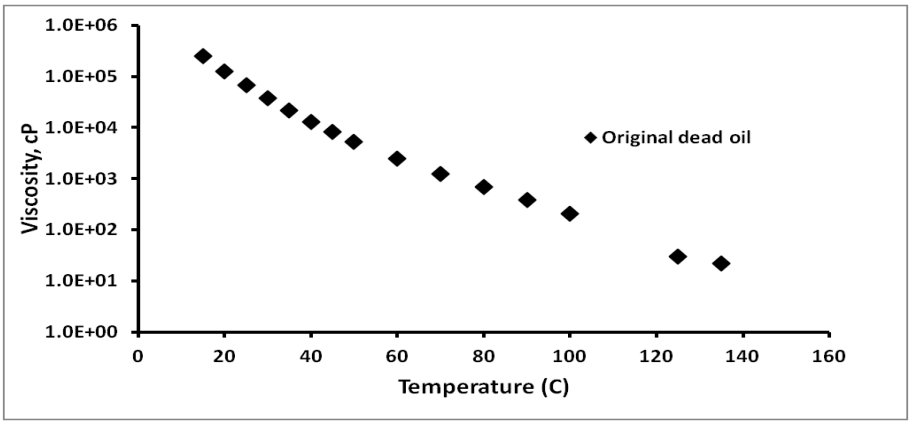

(b) Dead oil viscosity variation with temperature.

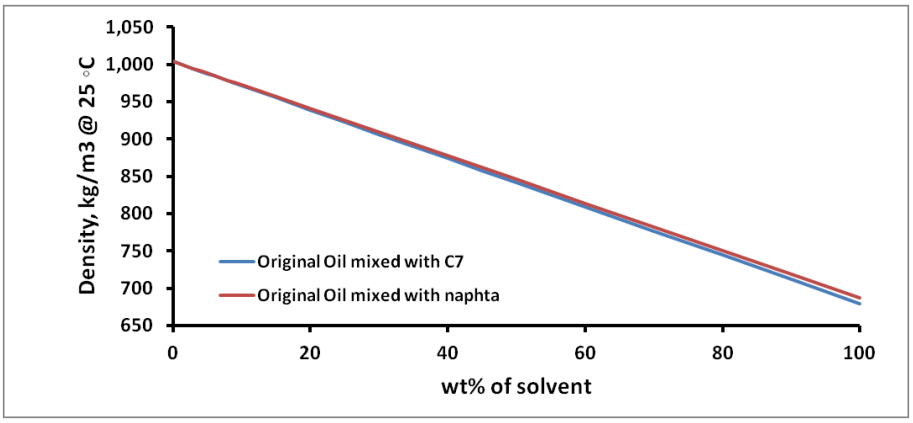

(c) Mixture density of original dead oil with C7 and diluents at 25ºC.

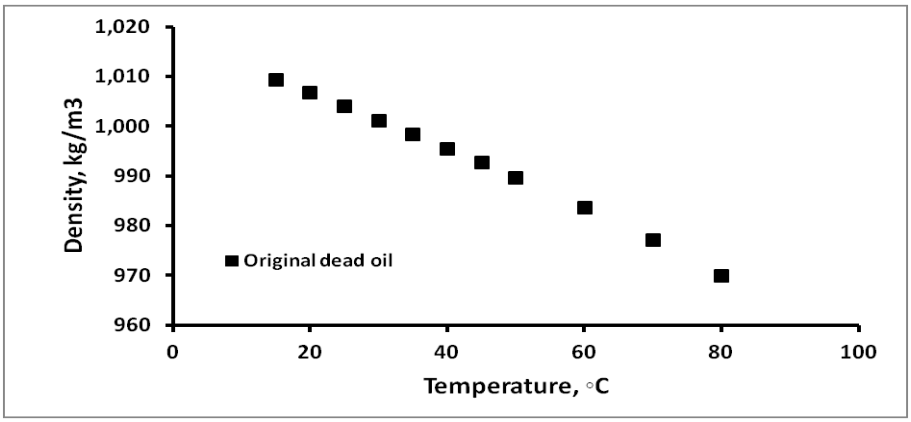

(d) Dead oil density variation with temperature.

Figure 5- 2: Density and viscosity variations of heavy oil with solvent content and temperature.

During the experiments, mixtures of dead oil with C_7 and diluents showed asphaltene precipitations. C_7, when mixed with original oil, was proved to produce higher amounts of asphaltene precipitation compared to diluents. Asphaltene particles are believed to form complex aggregated structures to different degrees in different solvents. Polarity, aromaticity, concentration of a given solvent, asphaltene type and the mixing temperature are the key factors to determine the extent of aggregation (Kariznovi et al. 2010). In this study, asphaltene precipitation is not addressed.

Post-CHOPS CSI: Experiments and Simulation

In this section, we will consider five cyclic solvent injection experiments with a follow-up solvent retrieval phase (hot water at 50ºC) and their numerical simulations. A full description of each experiment is provided and experimental results are compared for several solvents at different conditions.

Sand-Pack Experiments

The experimental set-up consisted of a sand-pack filled with sand (**Table 5-4**). To include the wormhole, a metal spring was loaded in the center of the sand-pack. The model was initially saturated with dead oil in a closed system at 40ºC, and cooled down to room temperature prior to establishing the test. Due to viscous nature of the heavy oil, the saturation phase took several days. Weight measurements were performed before

and after saturation and sand-pack was visually inspected. The saturated sand-pack was then inserted into the core holder (**Figure 5-3**).

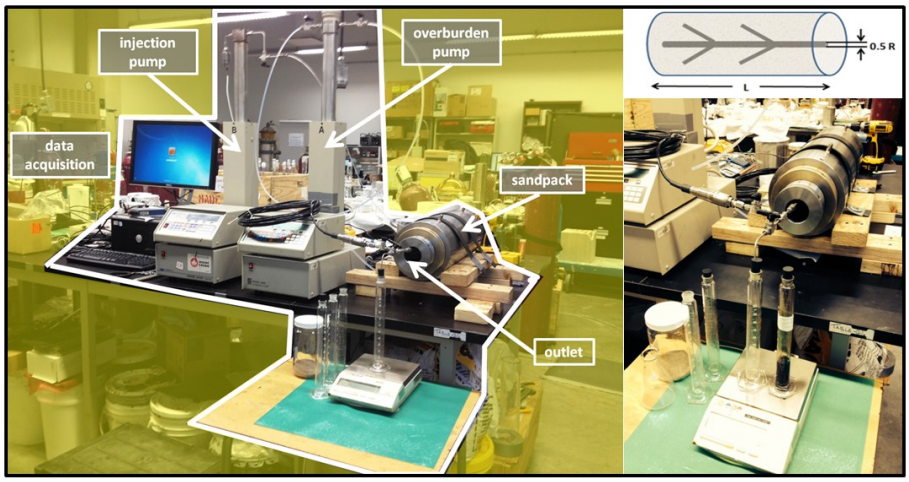

Figure 5- 3: Experimental set-up to study thermally aided cyclic solvent stimulation in the presence of wormholes.

Table 5- 5: Overall Sand-Pack Properties used in CSI Experiments.

	Low Pressure Tests	High Pressure Tests
Length (cm)	25	14
Cross-sectional area (cm^2)	102	
Sand size (μm)	250-500	
Porosity (fraction)	0.41	
Permeability (mD)	16100	
Wormhole coverage index (dimensionless)	0.0151	
Non-wormhole pore volume (cm3)	1030	577
Initial oil saturation (%)	100	100
Confining pressure (atm)	5.0	18.5
Wormhole configurations	Linear and branched	Only linear
Solvent type	C_7 and diluents	C_7 and CO_2

* Note that sand-pack is positioned horizontally during CSI experiment.

In the injection phase, the liquid solvent was first introduced into the wormhole, then the sand-pack was left isolated for a limited period of time (soaking phase). After the soaking period, the liquid solvent and oil were allowed to be produced (production phase). The experiment was aimed to mimic cyclic solvent stimulation, so that potentially several cycles can be repeated for each experiment. At each cycle, the amount of collected oil and solvent was determined with the help of refractometry. It was expected that some of the injected solvent would remain trapped inside the sand-pack after solvent phase. Therefore, in the final step, a solvent retrieval attempt was made by injecting low-temperature hot water. Because CHOPS wells are not thermally

completed, we had to limit the hot water phase to 50ºC. The aim was to see how much additional solvent could be retrieved from sand-pack considering experiment conditions. This part completed the experimental work and was then used to answer the concerns about economic efficiency of the process; i.e. how much of the injected solvent could be back-produced. It also gave an estimate of the ultimate recovery as well as practical insight to implement the process in field. Addition of the last phase (solvent retrieval) to cyclic solvent stimulation was the application of the steam-over-solvent technique in CHOPS reservoir, earlier proposed in fractured reservoir (SOS-FR) by Al-Bahlani and Babadagli (2009) and Naderi and Babadagli (2014). A schematic of the experiment is illustrated in **Figure 5-4**.

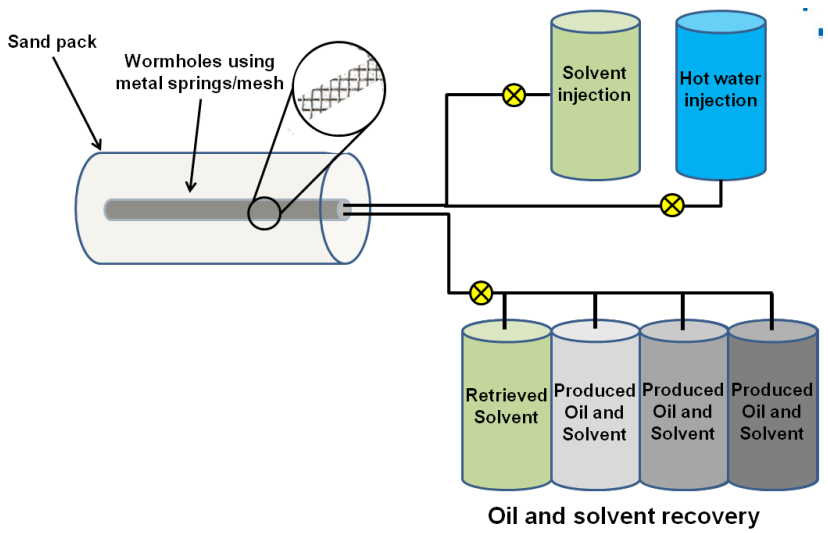

Figure 5- 4: Schematic of thermally aided cyclic solvent stimulation in the presence of wormholes.

To assure the injected fluid would first travel into the wormhole and then diffuse to non-wormhole domain, a chemical-heat resistant rubber was used to block the non-wormhole section of the sand-pack at the injection point. This is shown in **Figure 5-5**.

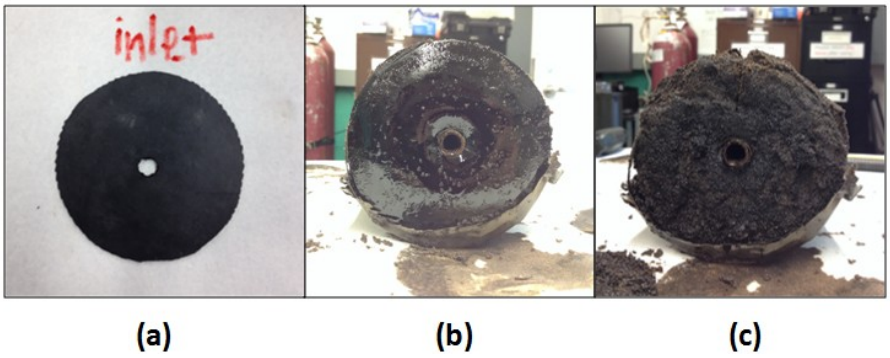

Figure 5- 5: Chemical and heat resistant rubber used at the inlet/outlet to ascertain that fluid injection/production is only through wormhole (a) rubber, (b) rubber inserted at the inlet/outlet, (c) rubber removed at the end of experiment.

Simulated Sand-Pack Characteristics

The sand-pack experiment was simulated by making its cylindrical shape out of a Cartesian grid (**Figure 5-6**). Be aware that a radial geometry could not be employed in a horizontal core since gravity was considered by default in Z-direction (or axis of cylinder) of so-called "r, θ, Z" space. Our model included 25 cells in X-, 18 cells in Y-, and 18 cells in Z-directions. For long sand-pack experiments (L=25 cm), the cell dimensions were 1.0cm, 0.678cm and 0.678cm, in X-, Y- and Z-directions, respectively. For sand-packs with 14 cm length, the cell dimensions were 0.560cm, 0.678cm and 0.678cm, in X-, Y- and Z-directions, respectively. To take a cylindrical shape out of a Cartesian grid, redundant cells were given zero pore volume. Associated porosity and permeability data for wormhole and non-wormhole domains are summarized in **Table 5-6**.

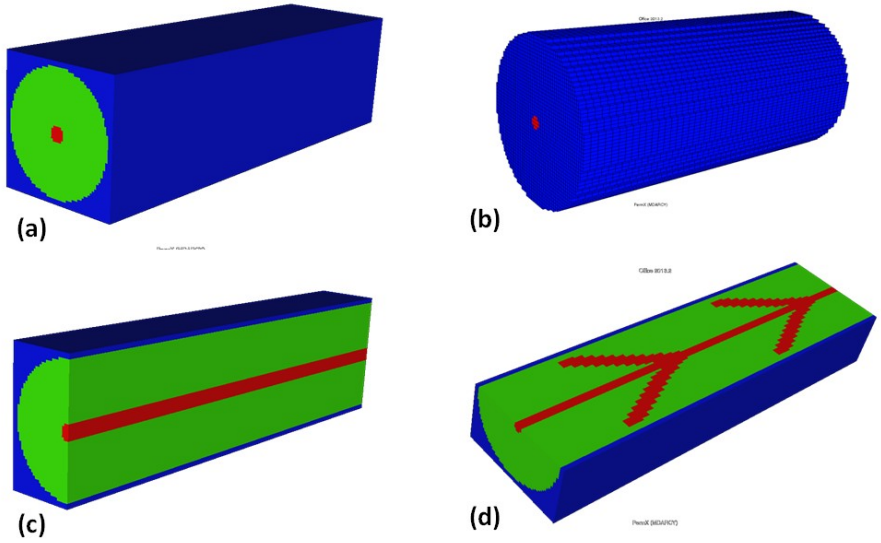

Figure 5- 6: (a) simulated sand-pack in Cartesian grid, (b) inactivating the redundant cells to get cylindrical shape, (c) linear wormhole shown in vertical cross-section of the sand-pack, (d) branched wormhole shown in horizontal cross-section of the sand-pack.

Table 5- 6: Grid Block Properties of Simulated Sand-pack Experiments.

	Porosity, %	Permeability, D	Saturation Number
Wormhole	0.99	8.1E+4	2 (Cross-shape K_r with S_{or} = 0)
Non-Wormhole	0.41	16.1	1 (See Figure 5-7 for K_r)

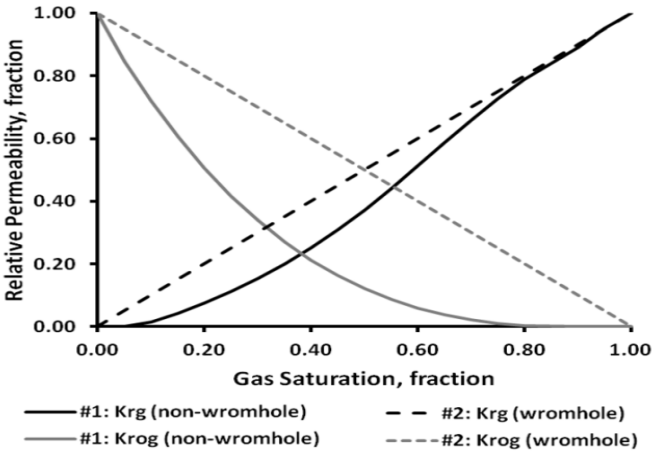

Figure 5- 7: Relative permeability curves used in non-wormhole (saturation region 1) and wormhole (saturation region 2) domains.

The fluid behavior was modeled using a tuned 6-component Peng-Robinson EOS with volume translation. The fluid modeling was detailed in Fluid Characterization and Modeling section of the paper. Note that the experiment may be modeled with fewer components. For instance, when C_1 and CO_2 were not injected into the sand-pack, the whole process could be modeled with only four components. To match the simulation results with sand-pack experiments, effective diffusion coefficients were treated as history matching parameters. It is worth mentioning that simulation models were only limited to solvent phase in which sand-pack temperature is assumed to remain unchanged. The solvent retrieval phase (hot water injection after solvent phase) was not modeled. Firstly, this is because handling convergence in Thermal-EOS-based models is practically onerous, and current commercial simulators cannot support such an option. Secondly, diffusion coefficient values would change with temperature. On top of that, when a thermal phase is going to be established, the role of molecular diffusion is negligible in comparison to viscosity reduction of heavy oil. An approach to overcome this difficulty is to set the initial conditions of thermal-K-value-based simulator with

"Enumeration" technique (ECLIPSE Manual 2014). Enumeration allows the initial solution to be specified directly. To do so, one can export liquid and gas compositions, pressures, and saturations of last report of compositional EOS-based model to initialize a thermal model explicitly. Care should be taken to use proper K-values in accordance with employed EOS in compositional simulations.

Fluid characterization and EOS modeling was performed with PVTi (Schlumberger). ECLIPSE Industry-Reference Compositional Simulator (Schlumberger) was used to model the solvent phase in CSI process. ECLIPSE Office Tool from Petrel package (Schlumberger) was used as post-processor software to launch simulation results.

Results and Discussions

Experiment 1: Low pressure injection of C7 in a linear wormhole. The first experiment was the low pressure (4.4 atm) injection of C_7 in a 25 cm long sand-pack with a linear wormhole. A constant volume of liquid C_7 (42 ml) was injected at a rate of 2 ml/min at each of five cycles of solvent injection. At the end of each C_7 injection cycle, the sand-pack was left isolated for 2 hr, and subsequently, was allowed to produce the resulted mixture to atmospheric pressure. After finishing the fifth cycle of solvent, 105 ml of hot water (50ºC) was injected into the sand-pack and left isolated for 30 min. Water and a mixture of oil and solvent were produced in a so-called "water phase," referring to water injection cycle. At each cycle, the amount of collected oil and solvent were determined and the resulted mixture was analyzed through gas chromatography and refractometry. **Figure 5-8** shows the liquid volume recovered during this experiment. Note that limited asphaltene precipitation is included in the oil phase volume.

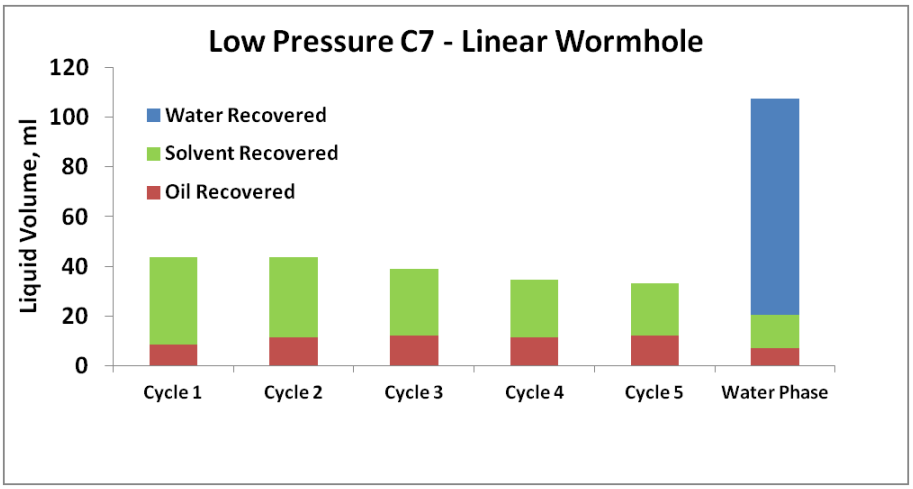

Figure 5- 8: Liquid volumes recovered during experiment 1 (low pressure injection of C7 in a linear wormhole).

After the whole experiment (solvent phase and hot water) was conducted, the sand-pack was visually inspected. This was not possible for all the experiments (the sand-pack was very fragile and could lose its consistency once brought out of the core holder sleeve [at the end of hot water phase]). For illustration purpose, residual oil and solvent after the whole experiment of low pressure C_7 injection (solvent phase and hot water injection phase) is given in **Figure 5-9**. Figure 5-9a is the picture of vertical cross-section of sand-pack taken at natural light. Figure 5-9b is an enhanced version with corrected white balance and exposure. As seen, a clear distinction of swept zone and unswept zone with respect to wormhole can be made. Unfortunately, this could only be done at the end of whole experiment including hot water phase, yet no firm conclusion can be made on the extent of solvent diffusion front (intuitively, it would be in the wormhole vicinity).

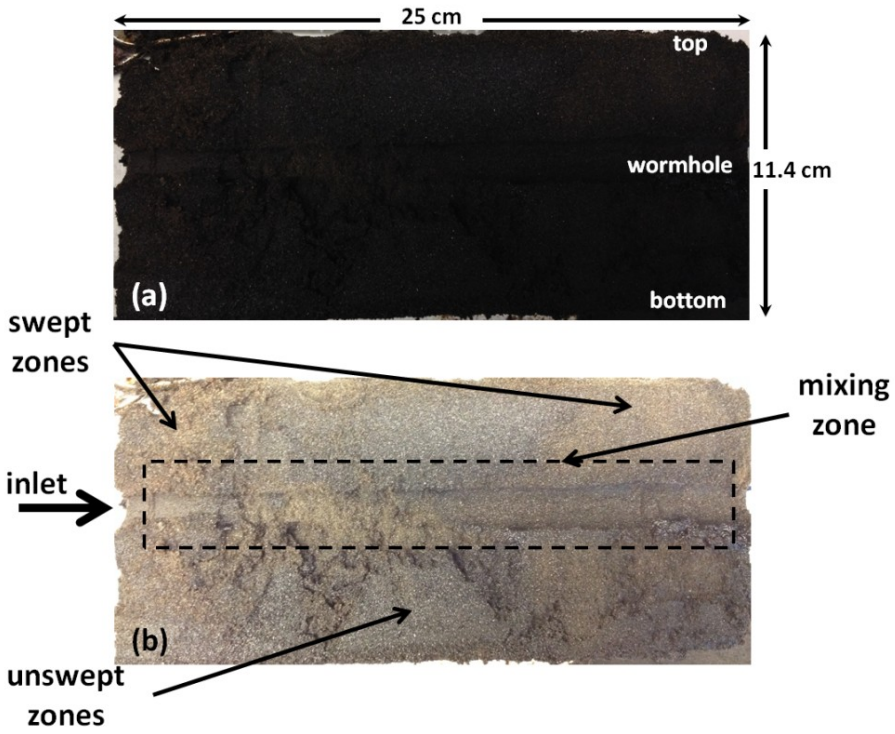

Figure 5- 9: Residual oil and solvent after the whole experiment of low pressure C7 injection (solvent phase and hot water injection phase) was conducted. (a) Cross-section of sand-pack at natural light, (b) enhanced version of (a) with corrected white balance and exposure.

An associated observation with C_7 cyclic injection was the precipitation and deposition of asphaltene in the collecting graduated cylinders (**Figure 5-10**). The flocculation of asphaltene in blocking some of the pores near the wormhole might be considered to affect oil production. It was difficult to detect asphaltene precipitation with the visual inspection of the sand-pack. However, the displacement process at the outlet was so fast that asphaltene precipitation at production phase of C_7 cyclic injection was either delayed until it reached the graduated cylinder, or occurred in the sand-pack but flowed easily along with oil and solvent mixture.

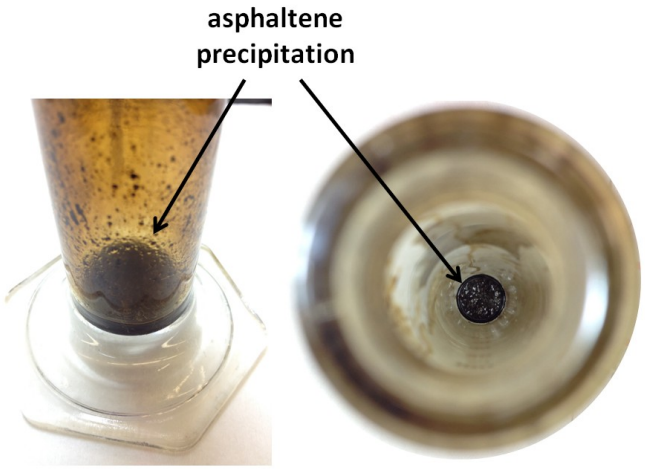

Figure 5- 10: Asphaltene precipitation observed after collecting oil and solvent (C7) mixture in graduated cylinder.

Experiment 2: Low pressure injection of diluents in a linear wormhole. In the second experiment, diluent oil (compositional description is shown in Table 5-3 and Figure 5-1) was used instead of C_7 as the liquid solvent. A similar procedure to experiment 1 was followed and the collected liquids were analyzed. The results are shown in **Figure 5-11**. Apart from solvent and oil recovery (which will be compared for all experiments in the next section), less asphaltene precipitation was observed for diluents. This is mainly due to its aromatic contents compared to C_7. Polarity, aromaticity, concentration of a given solvent, asphaltene type, and the mixing temperature are the key factors to determine the extent of asphaltene aggregation (Kariznovi et al. 2010).

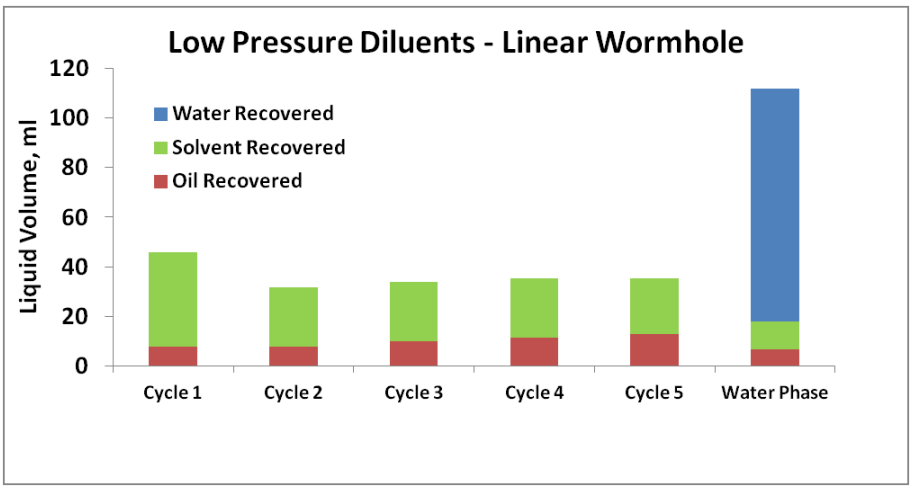

Figure 5- 11: Liquid volumes recovered during experiment (low pressure injection of diluents in a linear wormhole).

Experiment 3: Low pressure injection of C7 in a branched wormhole. In the third experiment, keeping the same Wormhole Coverage Index (WCI), the ratio of wormhole volume to whole sand pack, as in experiments 1 and 2, the configuration of wormhole was changed from linear to branched (see Figure 5-6c and 6d). Keeping a constant WCI, an increase in the number of branches or complexity of wormhole would increase the wormhole internal surface area and as a result the solvent could possibly interact with more surfaces areas of non-wormhole (matrix) domain. The results are shown in **Figure 5-12** and will be compared with other experiments in terms of solvent and oil recovery factor.

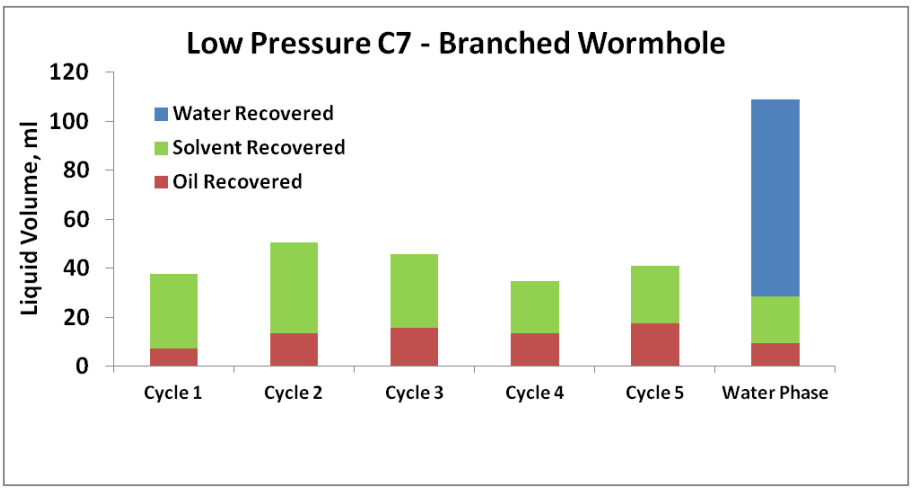

Figure 5- 12: Liquid volumes recovered during experiment 3 (low pressure injection of C7 in a branched wormhole).

Experiment 4: High pressure injection of C7 in a linear wormhole. Experiment 4 was conducted at a higher pressure (14.0 atm) in a 14 cm long sand-pack with a linear wormhole. As expected, more volumes of solvent were needed at each cycle to re-pressurize the sand-pack, but more liquid (solvent and oil mixture) was produced. **Figure 5-13** summarizes the liquid volume collected for this experiment.

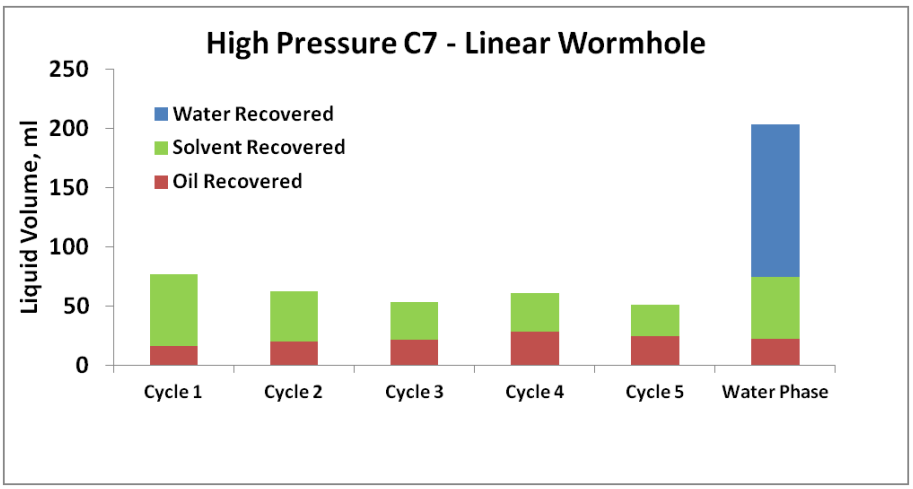

Figure 5- 13: Liquid volumes recovered during experiment 4 (high pressure injection of C7 in a linear wormhole).

Experiment 5: High pressure injection of CO2 in a linear wormhole. Experiment 5 was different from the other four experiments as it involved a gaseous solvent. CO_2 was injected at 14.0 atm and room temperature into the sand-pack saturated with dead oil at constant pressure. Sand-pack was in contact with CO_2 cylinder for about 30-45 min after the pressure inside sand-pack reached 14.0 atm and stabled. Next, the sand-pack was left isolated for 12 hr (soaking time) followed by liquid production to atmospheric pressure. The main observation was a very low liquid recovery rate in the form of foamy oil first (a mass of small bubbles of CO_2 formed in a dark viscous liquid at the outlet), and then a massive amount of free CO_2 (CO_2 breakthrough). This resulted in very low oil production with a high gas-oil ratio. Despite very low oil recovery factor (only 4%), we suggest that a great deal of attention should be given to CO_2 to discover how and under which circumstances CO_2 could activate and maintain foamy oil behavior. The foamy oil behaviour with different gases such as C_1, C_2, C_3 and CO_2 needs accurate and detailed experimentations, which is out of the scope of the current paper. The experimental and simulated results are compared in the last section. Note there is no hot water phase in case of CO_2 cyclic injection.

Ultimate Oil and Solvent Recoveries

Solvent retrieval is essential when a liquid solvent has been selected in the solvent phase. **Figure 5-14** compares the solvent recovery factor of different experiments at the end of solvent phase. In addition, the

efficiency of hot water phase is shown in terms of ultimate solvent recovery, or additional solvent that can be recovered during hot water phase. It is believed that a significant amount of solvent could be trapped during several cycles of solvent phase. Solvent recovery factor is defined as a volume ratio of cumulative recovered solvent to cumulative injected solvent.

Two observations can be made from Figure 5-14. First, the high pressure experiment yields lower solvent recovery factor at the end of solvent phase. At a higher pressure, the solvent can diffuse to further distances from wormhole domain, and this increases the chance that solvent would be trapped more. This is beneficial because one can operate the injection well at higher pressure, and deliver solvent to more of the non-wormhole domains in order to dilute more heavy oil. On the other hand, it is detrimental because solvent recovery gets lower and the process becomes uneconomic. Second, the hot water phase (even at low temperature of 50ºC) proves to be efficient in all of the experiments, and it performs best in the high pressure experiment. Therefore, solvent retrieval is possible and proved to give high values in experimental conditions. The main problem is then to find out an optimal operational condition at the field-scale to keep the whole process profitable.

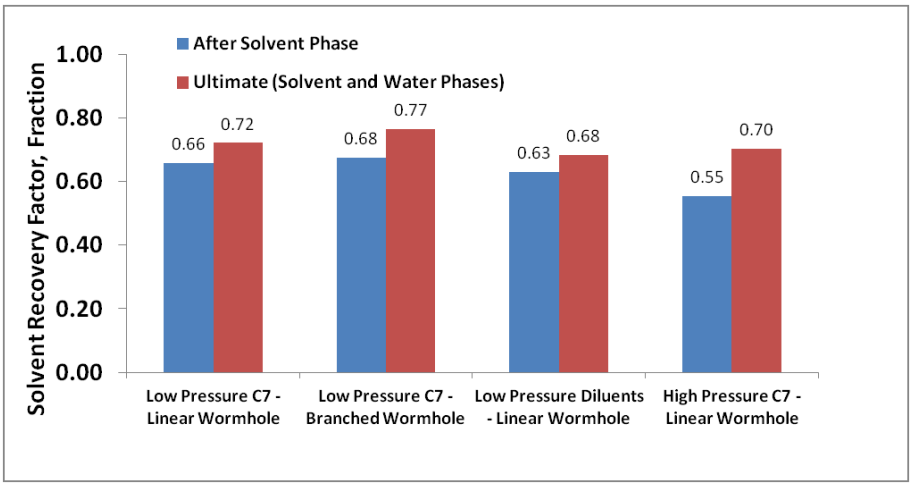

Figure 5- 14: Solvent recovery factor after solvent phase and whole experiment (solvent and hot-water phase).

Figure 5-15 compares the oil recovery factor for different experiments. Note that the solvent production was subtracted from liquid production to obtain Figure 5-15. It is evident that the performance of high pressure

experiment is far better than low pressure ones. In addition, some portion of oil recovery is associated to hot water phase. The main mechanisms of oil production during hot water phase are a combination of water imbibition and solvent-oil dilution which leads to oil viscosity reduction. This improves gravity drainage and thermal fluid convection/diffusion.

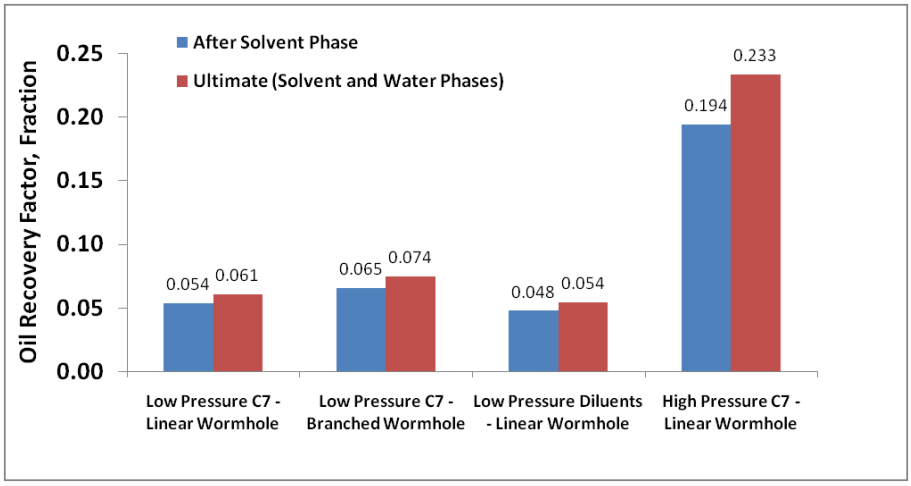

Figure 5- 15: Oil recovery factor after solvent phase and whole experiment (solvent and hot-water phase).

Simulation Results

In this section, the solvent cycles of each experiment are numerically modeled and the diffusion coefficients that yielded the best match will be selected. **Figure 5-16** demonstrates two different grid models.

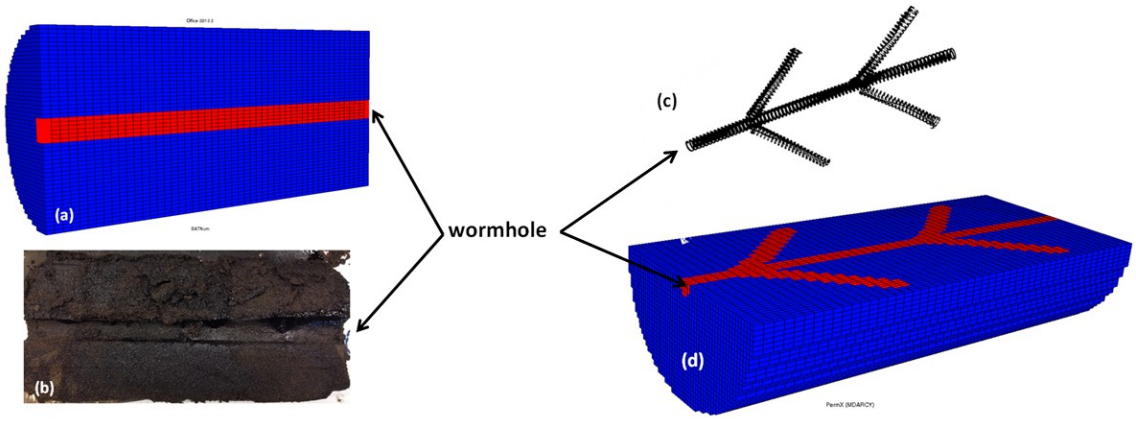

Figure 5- 16: (a) simulated and (b) linear wormhole shown in vertical cross-section of the sand-pack, (c) branched wormhole and (d) corresponding simulated model shown in horizontal cross-section of the sand-pack.

First, low pressure injection of C_7 experiments were considered. Liquid diffusion coefficients of C_7 were the only matching parameter. A value of 1.39E-2 cm^2/hr for effective liquid diffusion of C_7 provided an acceptable match. Simulated and experimental results are compared in **Figure 5-17**.

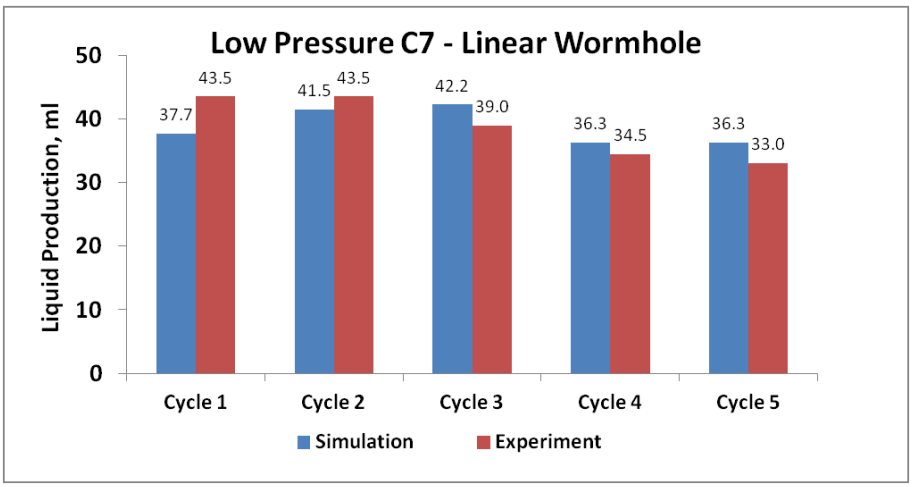

(a) Low pressure C7 injection in a linear wormhole.

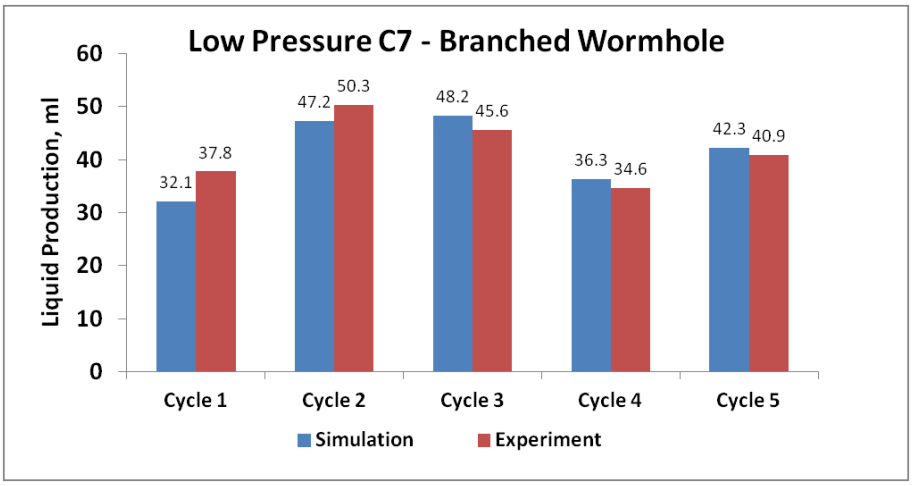

(b) Low pressure C7 injection in a linear wormhole.

Figure 5- 17: Simulated and experimental liquid volumes recovered during CSI experiments.

Figure 5-18a illustrates the top view of a horizontal cross section at the middle of sand-pack with a branched wormhole. The blue and red colors are reserved for non-wormhole and wormhole domains, respectively. **Figure 5-18b** shows the mixing zone of injected solvent with original oil after several cycles.

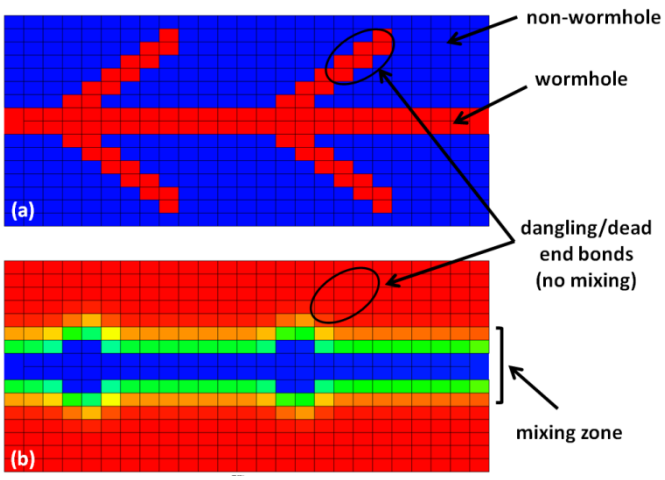

Figure 5- 18: (a) Top view of a horizontal cross section at the middle of sand-pack with branched wormhole. The blue and red colors are reserved for non-wormhole and wormhole domains, respectively. (b) Mixing zone of injected solvent with original oil after several cycles.

Note that the injected solvent could not initially invade all parts of the wormhole domain at the first cycle; rather the mixing front gradually develops and reaches so-called dangling or dead end bonds. If it is assumed that continuous sand production causes the wormholes to grow into a wormhole network, which connects the wells to each other, then the backbone of the network is defined as the set of bonds that are connected to the two (or multiple) wells having infinite conductance through paths that have no common bond. Removing a single bond from network backbone breaks the connection between two (or multiple) wells. A dangling bond is defined as the bond that disconnecting it from network backbone does not break the connection between two (or multiple) wells. Be aware that CSI could be potentially employed in multi-well CHOPS field, rather than a single CHOPS well suggested by Rangriz Shokri and Babadagli (2012) (**Figure 5-19**). All other parameters being equal, it appears that the backbone of wormhole network determines the efficiency of the cyclic solvent stimulation in branched (fractal) wormhole pattern, rather than local variation of dangling bonds.

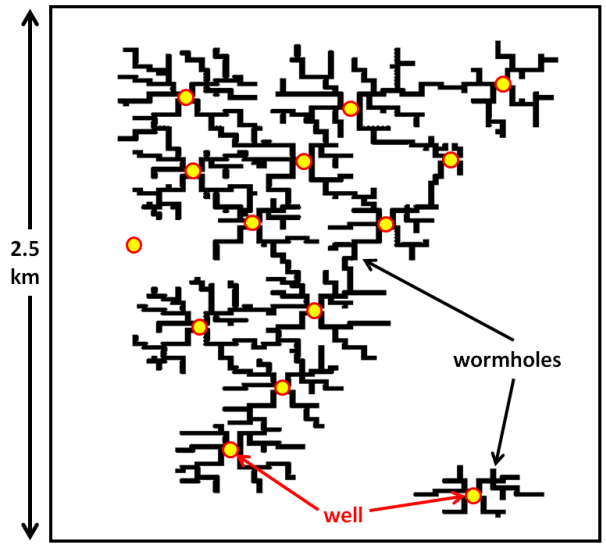

Figure 5- 19: Field-scale application of fractal-wormhole model to develop wormhole network based on sand production data (Rangriz Shokri and Babadagli 2012).

In the next step, the liquid diffusion coefficient of C_7 is a known input from last two experiments. This simplifies the matching process because C_7 is one of the components of diluents (see Figure 5-1). The cumulative liquid production of low pressure diluents experiment was matched to obtain the effective liquid diffusion coefficient for diluents equal to 1.33E-2 cm^2/hr. The results are shown in **Figure 5-20**.

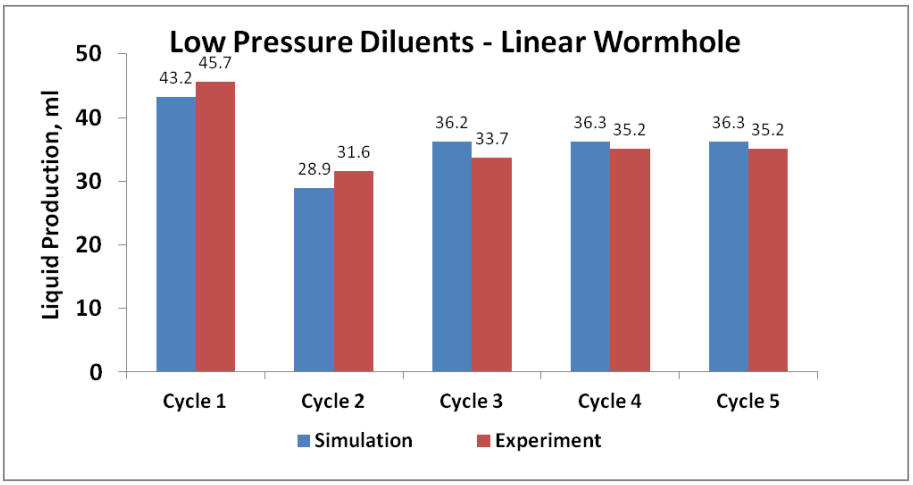

Figure 5- 20: Simulated and experimental liquid volumes recovered during low pressure injection of diluents in a linear wormhole.

C_7 injection at higher pressure leads to a larger increase of liquid production at each cycle. Be aware that to reach higher pressure, more amount of solvent should be injected. In this case, diffusion coefficients were the same as in the low pressure case.

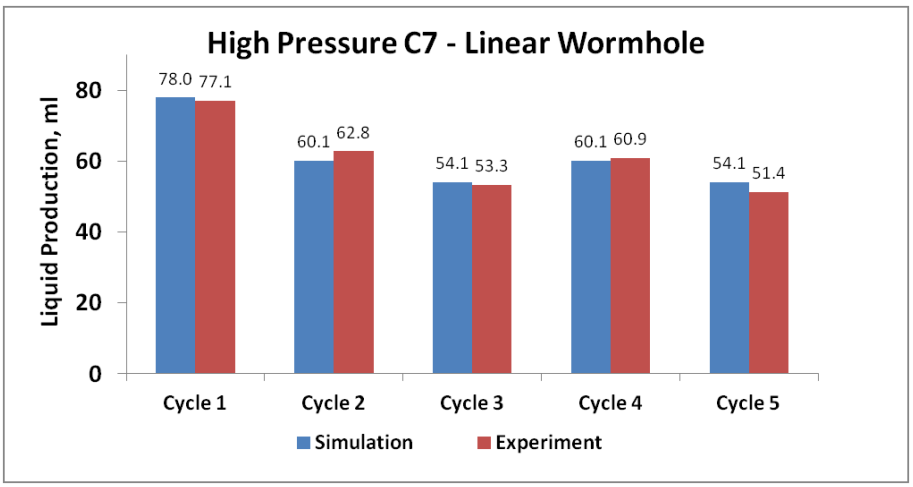

Figure 5- 21: Simulated and experimental liquid volumes recovered during high pressure injection of C7 in a linear wormhole.

CO_2 injection leads to a larger density difference compared to liquid solvent experiments. Because of high viscosity of heavy oil, CO_2 cannot mobilize the heavy oil towards the outlet as expected in conventional gas injection (inefficient gravity drainage). It should be mentioned that at experiment conditions (14 atm and room temperature), CO_2 contacts the oil as a gas phase. However, simulation model is insensitive to gas and liquid diffusion coefficients of CO_2. Gas and liquid diffusions are defined as diffusion of gas and oil components within the gas and oil phases, respectively. To match the experimental data, the introduction of cross-phase diffusion of gas into oil phase was required. This may be accounted as an approach to model delayed dissolution of a gas into heavy oil, a reverse concept compared to the release of gas from foamy oil. The effective cross-phase diffusion coefficient for CO_2 turned out to be 2.18 cm^2/hr. **Figure 5-22a** illustrates the extent of CO_2 invasion as a gas phase inside simulated sand-pack at the end of four cycles, which is a vertical cross-section of the model. **Figure 5-22b** shows the cross-diffusion of CO_2 into heavy oil as liquid phase and how it influences the intermediate pseudo-component of heavy oil (**Figure 5-22c**). Unfortunately, we were not equipped to visualize the sand-pack during the experiment.

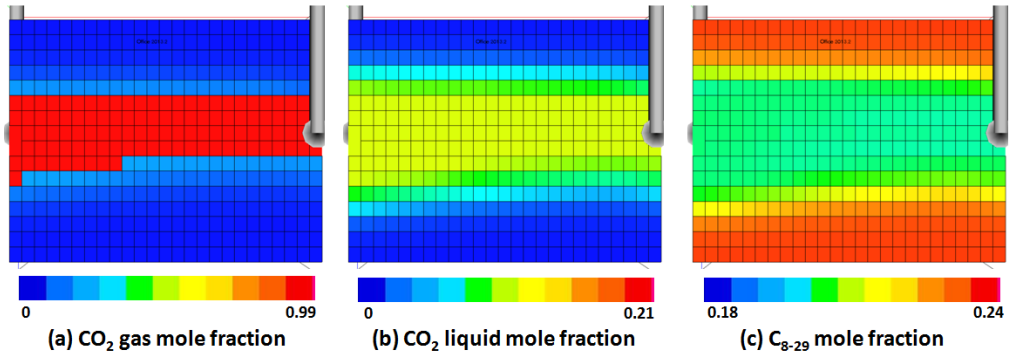

Figure 5- 22: Simulated CO_2 invasion during CSI process.

Figures 5-23 and 24 compare simulated results and experimental measurements of recovered oil and gas volumes at different cycles. The match quality of gas volumes may not be adequate. This might be related to foamy behavior that was observed in early oil production time (until CO_2 breakthrough). To obtain a relevant picture of the magnitude of foamy behavior of CO_2, more experimentation at different pressures is needed. To characterize the kinetics of the process, it is advised that non-equilibrium numerical models should be employed.

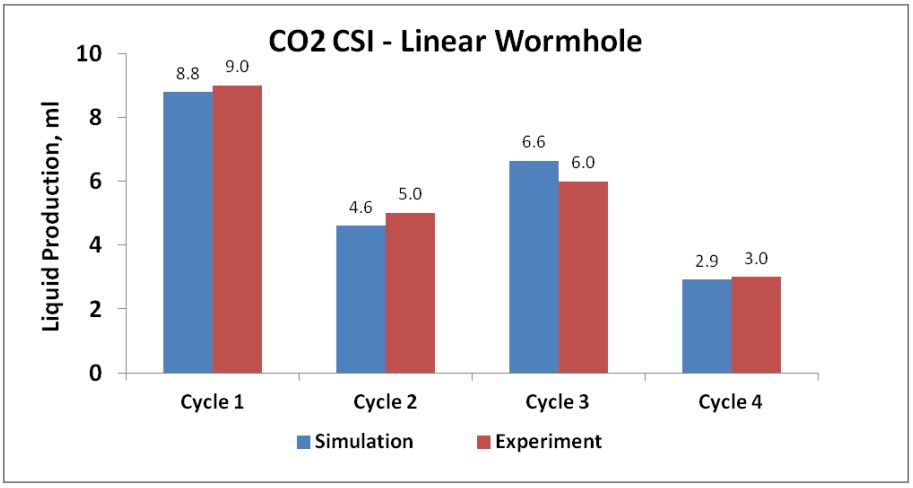

Figure 5- 23: Simulated and experimental liquid volumes recovered during CO_2 injection in a linear wormhole.

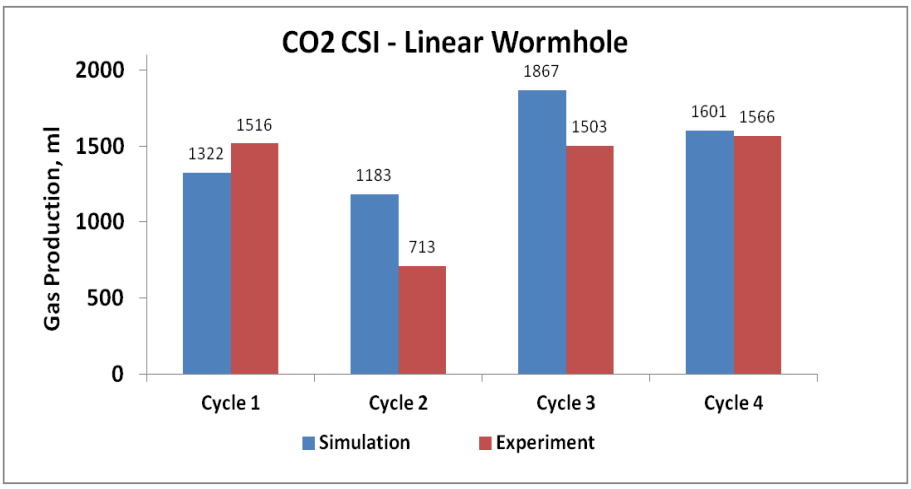

Figure 5- 24: Simulated and experimental gas volumes recovered during CO_2 injection in a linear wormhole.

Up-scaling Diffusion Process

To generate accurate predictions in field-scale simulation, there is a need to provide an up-scaling procedure from laboratory results of the CSI process. For this reason, the molecular diffusion coefficients must be adjusted to account for different tortuous paths of different rock types. This can be done through the definition of effective diffusion coefficient calculated as:

$$\frac{D_{eff}}{D_0} = \frac{1}{F\varphi} \tag{5-2}$$

where D_{eff} and D_0 are effective and pure diffusion coefficients, F is formation resistivity factor, and φ is porosity (Stalkup 1983). Formation resistivity factor, which is usually available in field-scale studies, can be related to pore geometry as:

$$F = \varphi^{-m} \tag{5-3}$$

in which the exponent m varies mainly with the degree of consolidation of the rock and is called the cementation exponent (Bassiouni 1994). Therefore, one obtains the following equation for effective diffusion:

$$D_{eff} = D_0 \, \varphi^{m-1} \tag{5-4}$$

Be aware that the obtained diffusion coefficients from history matching of experimental work are effective diffusion coefficients and must be adjusted first to obtain pure diffusion coefficients (in sand-pack experiments, porosity was 0.41 and m was estimated 1.3). Then, field-scale diffusion coefficients can be calculated based on different field properties. For instance, an effective diffusion of 1.39E-2 cm^2/hr was obtained for C_7. Assuming porosity of 0.41 and cementation exponent of 1.3 would yield D_0 equal to 1.88E-2 cm^2/hr. To obtain the effective diffusion in a case in which porosity is 0.32 (less porosity) and cementation factor is 2.0 (more consolidated sand), equation 5-4 results in a value of 6.0E-3 cm^2/hr. A smaller value of effective diffusion coefficient is because of the assumption of lower porosity and more consolidated sand compared to the experiment.

In addition to molecular diffusion, convective dispersion might be important in the CSI process. In our experiment, the solvent velocity from wormhole to non-wormhole domain is estimated to be in the order of 1 cm/hr. This results in a value of 0.008 to 0.02 for $v\sigma d_p/D_o$ if an average value of 0.36 cm is assumed for σd_p. Based on available literature (Perkins and Johnston 1963), molecular diffusion would dominate the process and dispersion might be neglected. However, it is recommended to perform a sensitivity analysis to get insight of each particular value used in field applications.

Conclusions and Remarks

With notion to the potential use of solvents in post-CHOPS, five experiments (liquid and gas solvents) were conducted to study the performance of thermally aided cyclic solvent stimulation. The interactions between wormhole and non-wormhole domains were inspected based on scaled wormhole/non-wormhole volume ratios (i.e. wormhole coverage index, WCI) and configurations.

It was observed that the high pressure experiment (liquid solvent) yielded higher oil recovery, but lower solvent recovery factor at the end of solvent phase. To make the process economically viable, a solvent retrieval attempt was made by injecting different -low- temperature hot water (due to thermal limitations of

CHOPS well completions). A post-flush hot-water was found to be efficient to increase both solvent and oil ultimate recovery factors in all of the experiments, and it performed best in the high pressure case.

A comprehensive EOS-based fluid modeling was presented and used to simulate the sand-pack experiments. Experimental and numerical results were analyzed and effective liquid diffusion coefficients for C_7 and diluents were obtained. It was also observed that diluents, compared to C_7, yielded less asphaltene precipitation due to aromatic contents of diluents. In addition, diffusion of CO_2 into heavy oil was analyzed through cross-phase diffusion concept. Hence, a framework for delayed dissolution of CO_2 was established.

It was observed that the use of light solvents (CO_2) could maintain the sand-pack pressure for a longer period (attributed to foamy oil phenomenon) compared to liquid solvent during production phase. But, the oil recovery from sole application of light solvent (RF=4%) was not as considerable as with the heavier solvents (RF=23%). These experiments suggest that an improved heavy oil recovery could be achieved using hybrid application of solvents and hot water in CHOPS reservoirs.

It was shown that injected solvent could not invade all parts of the branched wormhole domain at first cycle; rather, the mixing front gradually develops and reaches the so-called dangling or dead end bonds. It appears that the backbone of wormhole network determines the efficiency of the cyclic solvent stimulation in branched (fractal) wormhole patterns rather than local variation of dangling bonds.

Finally, to generate accurate predictions in field-scale simulation, an up-scaling procedure from laboratory results of the CSI process was suggested so that field-scale diffusion coefficients could be calculated based on different field properties. Also, it was shown that in theory, molecular diffusion would dominate the process and convective dispersion might be neglected. However, the best practice is to perform a sensitivity analysis on the uncertain field-scale variables.

References

Al Bahlani, A.M.M. and Babadagli, T. 2009. Laboratory and Field Scale Analysis of Steam Over Solvent Injection in Fractured Reservoirs (SOS FR) for Heavy Oil Recovery. Presented at the SPE Annual Technical Conference and Exhibition, New Orleans, Louisiana, 4-7 October. SPE 124047-MS. http://dx.doi.org/10.2118/124047-MS.

Alshmakhy, A. and Maini, B.B. 2012. A Follow-Up Recovery Method After Cold Heavy Oil Production. Presented at the SPE Heavy Oil Conference Canada, Calgary, Alberta, 12-14 June. SPE 157823-MS. http://dx.doi.org/10.2118/157823-MS.

Bassiouni, Z. 1994. Theory, Measurement and Interpretation of Well Logs, SPE Textbook Series Vol. 4, ISBN:978-1-55563-056-0.

Coskuner, G., Naderi, K., and Babadagli, T. 2013. An Enhanced Oil Recovery Technology as a Follow Up to Cold Heavy Oil Production with Sand. Presented at the SPE Heavy Oil Conference-Canada, Calgary, Alberta, Canada, 11-13 June. SPE-165385-MS. http://dx.doi.org/10.2118/165385-MS.

Du, Z., Chan, C., and Zeng, F. 2013. An Experimental Study of the Post - CHOPS Cyclic Solvent Injection Process. Presented at the SPE Heavy Oil Conference-Canada, Calgary, Alberta, Canada, 11-13 June. SPE-165524-MS. http://dx.doi.org/10.2118/165524-MS.

ECLIPSE TECHNICAL MANUAL, Schlumberger, 2014.

Ivory, J., Chang, J., Coates, R., and Forshner, K. 2010. Investigation of Cyclic Solvent Injection Process for Heavy Oil Recovery. *SPE J* **49** (09): 22–33. http://dx.doi.org/10.2118/140662-PA.

Kantzas, A. and Brook, G. 2004. Preliminary Laboratory Evaluation of Cold and Post-Cold Production Methods for Heavy Oil Reservoirs Part A: Ambient Conditions. *JCPT* **43** (10). http://dx.doi.org/10.2118/04-10-03.

Kantzas, A. and Brook, G. 2004. Preliminary Laboratory Evaluation of Cold and Post-Cold Production Methods for Heavy Oil Reservoirs Part B: Reservoir Conditions. *JCPT* **43** (10). http://dx.doi.org/10.2118/04-10-04.

Kariznovi, M., Nourozieh, H., and Abedi, J. 2009. Bitumen characterization and pseudo-components determination for equation of state modeling. *Energy and Fuels* **24** (1): 624-633.

Naderi, K. and Babadagli, T. 2014. Use of Carbon Dioxide and Hydrocarbon Solvents During the Method of Steam-Over-Solvent Injection in Fractured Reservoirs for Heavy-Oil Recovery From Sandstones and Carbonates. *SPE Res Eval and Eng* **17** (2): 286-301.

Perkins, T.K. and Johnston, O.C. 1963. A Review of Diffusion and Dispersion in Porous Media. Society of Petroleum Engineers. *SPE J* **3** (01): 70–84. http://dx.doi.org/10.2118/480-PA.

Rangriz Shokri, A. and Babadagli, T. 2012. An Approach to Model CHOPS (Cold Heavy Oil Production with Sand) and Post-CHOPS Applications. Presented at the SPE Annual Technical Conference and Exhibition, San Antonio, Texas, USA, 8-10 October. SPE-159437-MS. http://dx.doi.org/10.2118/159437-MS.

Rangriz Shokri, A. and Babadagli, T. 2014. Evaluation of Thermal/Solvent Applications with and without Cold Heavy Oil Production with Sand (CHOPS). *JCPT* **53** (2): 95-108.

Stalkup, F.I. 1983. Miscible Displacement, Vol. 8. Dallas, Texas: Monograph Series, SPE.

Tremblay, B. Sedgwick, G., and Forshner, K. 1997.Simulation of Cold Production in Heavy-Oil Reservoirs: Wormhole Dynamics. *SPE Res Eval. and Eng* **12** (2): 110-111.

Tremblay, B. Sedgwick, G., and Vu, D. 1999. CT Imaging of Wormhole Growth under Solution Gas Drive. *SPE Res Eval and Eng* **2** (1) 37-45.

Chapter 6: A Sensitivity and Uncertainty Analysis of Cyclic Solvent Stimulation for Post-CHOPS EOR: Application on an Actual Field Case

A version of this chapter was submitted to SPE Economics and Management.

Abstract

An uncertainty screening procedure was performed to assess the feasibility of cyclic solvent stimulation as a post-CHOPS (cold heavy oil production with sands) EOR (enhanced oil recovery) method. To achieve this, three cycles of cyclic solvent stimulation were modeled on a previously history matched Albertan CHOPS field with 15 wells. The results were compared with a base model at each cycle in terms of oil production, gas production and gas injection volumes. The emphasis was on both uncertain parameters (wormhole vertical location, strength of foamy oil, time-dependent gas dissolution/exsolution) and operational input (injection pattern, injection rate, injection/soaking time). It was shown that bottom-located wormholes and non-equilibrium gas dissolution/exsolution could highly affect incremental oil production and project NPVs, but unfortunately, they are unruly controlled. On the other hand, injection pattern, injection rate and injection/soaking time, as an operational input, can contribute to project profitability.

Next, an economic model was developed and after-tax NPV of the field was introduced as an economic indicator. This uncertainty analysis revealed that an increase in operational input such as injection rate may enhance oil recovery from a technical point of view, but does not necessarily increase project profitability (NPVs), yet an optimum value exists. It was shown such economic model had the priority to oil recovery factor or cumulative oil production as it could incorporate costs and sales simultaneously by performing continuous discounting, and allow the asset holder to maximize NPVs by selecting the best development strategy.

Introduction

A huge amount of oil (90% OIIP) is usually left behind in CHOPS (Cold Heavy Oil Production with Sands) reservoirs. Development of post-CHOPS (Cold Heavy Oil Production with Sands) EOR methods represents challenges and opportunities in terms of current technology and project profitability. CHOPS reservoirs offer low recovery factors (5-15%). Production of huge amount of sands during primary life of CHOPS reservoirs leaves a wormhole network signature behind, which impedes the follow-up EOR recovery processes.

Waterflooding experiences early breakthrough and steam-injection is not economically viable. The energy requirements and water consumptions in steam-based injections make solvent application an alternative. However, heterogeneity of wormhole structure also rejects continuous solvent injection, which is why cyclic solvent stimulation has recently gained attention (Rangriz Shokri and Babadagli, 2012, 2013, 2014).

In this method, the extended wormhole network (which connects different wells to each other within a field) can be used as a path to deliver solvents efficiently to non-recovered oil of non-wormhole domains. Pilot tests of similar process have been reported in literature and non-published works for CO_2, C_1, C_3, and C_4 as solvents (Kristoff et al., 2008). With notion to the substantial amount of solvent required in this process, examination of different uncertain parameters and operational input and obtain insights into improvement of project economics is needed.

Based on our previous publications (Rangriz Shokri and Babadagli, 2012, 2013, 2014), a history matched CHOPS field with 15 wells in Alberta was selected and uncertainty screening and quantifications on a follow-up cyclic solvent stimulation were performed. Wormholes were developed based on an integrated fractal-wormhole model honoring sand production history. Foamy oil and bubble nucleation, a characteristic of cold heavy oil production, were included through kinetic reactions. The effect of wormhole vertical location, strength of foamy oil and time-dependent gas dissolution/exsolution, injection pattern, injection rate and injection/soaking time were considered both on incremental oil production and project net present values. An economic model was developed based on different economic assumptions which yielded a single-valued economic indicator for comparison purposes.

Model Description

In this section, a summary of reservoir grid and fluid properties is provided. Major modeling basis and assumptions are explained and the implementation of field-scale cyclic solvent stimulation is discussed.

Reservoir Grid Properties

The full field reservoir model is located in Alberta at a depth of 425 mTVD and consists of 41, 41 and 5 grids in X, Y and Z-directions, respectively (**Figure 6-1**). Each single grid has dimensions of 60 m x 60 m x 1 m with notion to the fact that the wormhole layer could laterally develop in the top, middle or bottom layer. Initial reservoir pressure was 2583 kPa. A uniform random distribution function was used to assign the porosity and permeability data keeping an average value of 3,000 mD and 0.35 for absolute permeability and porosity of the non-wormhole domain, respectively. The assigned value of the wormhole network is a function of the assumed wormhole diameter, based on the laminar flow theory, such that absolute permeability can be calculated as $k = 12.67*10^6 r^2$ (equality of Darcy and Poiseuille's equations). Here k is permeability in Darcy and r is wormhole radius in cm, a value of 67,000 Darcy in this study. However, the absolute permeability of wormholes may be treated as a history matching parameter. **Table 6-1** summarizes the data used in simulation.

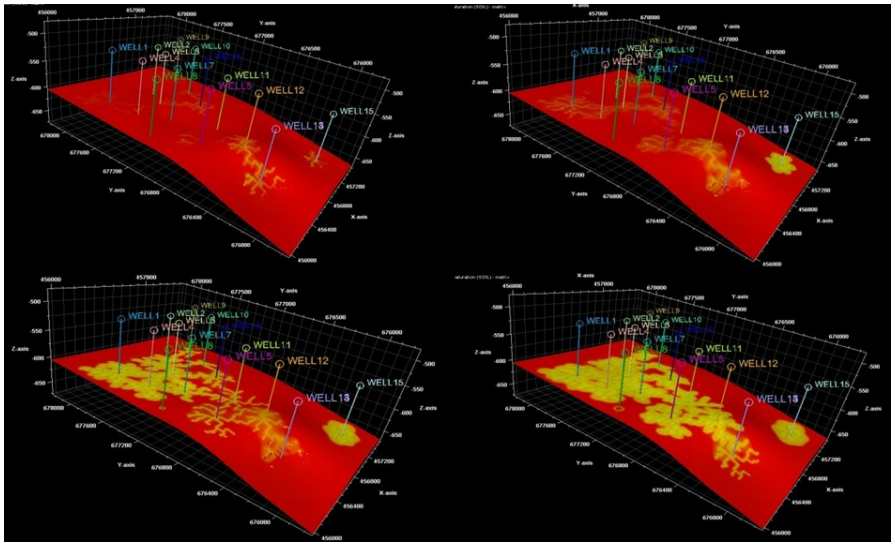

Figure 6- 1: Field scale wormhole-growth model at time t_1 to t_4 in a wormhole network plane.

Table 6- 1: Reservoir Properties used in Fluid Flow Simulation Models

Porosity	0.35
Horizontal permeability	3000 md
Vertical permeability	1500 md
Initial reservoir pressure	2583 kPa
Initial reservoir temperature	25 ºC
Reference depth at top of reservoir	425 mTVD
Initial oil saturation	0.75
Initial water saturation	0.25
Kro at connate water	1.0
Krw at irreducible oil	0.3
Krg at connate liquid	0.3
Krog at connate gas	1.0
Relative permeability correlations	Wyllie-Gardner
Three-phase relative permeability model	Stone's model II
Formation compressibility	1.8E-5 1/kPa
Reservoir rock heat capacity (Butler 1997)	2600 kJ/m^3 ºC
Reservoir rock thermal conductivity (Butler 1997)	660 kJ/m day ºC
Over/underburden rock heat capacity (Butler 1997)	2600 kJ/m^3 ºC
Over/underburden rock thermal conductivity (Butler 1997)	660 kJ/m day ºC
Bitumen thermal conductivity (Butler 1997)	11.5 kJ/m day ºC
Water thermal conductivity	1500 kJ/m day ºC
Gas thermal conductivity (Yazdani et al. 2011)	2.89 kJ/m day ºC

Wormhole growth is based on an integrated wormhole-fractal model that honors sand production history in a step-wise manner. At a selected time step, the wormhole growth is predicted and fluid flow simulator matches the production data. Then, the wormhole can grow more in accordance with sand production data and a fractal pattern in the next time step, followed by production history matching. This technique is referred to as "step-by-step" simulation. This procedure is repeated until it covers the whole production time or until it reaches a specified time by the user (Rangriz Shokri and Babadagli, 2012, 2014). For future reference, the heat loss to the overburden, underburden and sides of the reservoir was also considered in the post-CHOPS simulations. The rock type for heat loss can be identified based on initial temperature, rock conductivity, volumetric heat capacity and temperature dependence of heat capacity. A numerical method was adopted to calculate the heat loss rate per unit area based on rock conductivity and temperature gradient outside the reservoir (Table 6-1).

PVT and Fluid Modeling

The original dead oil was first characterized with the help of gas chromatography; then viscosity and density measurements were performed. The Peng-Robinson equation of state with volume translation was adopted to

match saturation pressure and GOR of dead oil mixture with C_1 and CO_2 separately (**Table 6-2**). Volume shifts were employed to match liquid density. The compositional fluid model was used to fit the Crookston coefficients. The main fluid properties are summarized in **Table 6-3**.

Table 6- 2: Fluid Properties of Original Dead Oil.

Parameter	Value
Dead oil viscosity (cP) @ 25 ºC	67400
Oil density (kg/m3) @ 25º C	1004
Saturation pressure with C1 (bars)	25.3
GOR at P_{sat} with C1	10-11
Saturation pressure with CO_2 (bars)	24.1
GOR at P_{sat} with CO_2	10-11
Saturated content (%)	25.57
Aromatic content (%)	31.17
Resin content (%)	26.77
Asphaltene content (%)	16.30

Table 6- 3: Fluid Properties for Foamy Oil Flow Models and Solvent Injection.

Component name	Heavy	Dissolved C1	Trapped C1	Free C1	Dissolved CO2	Trapped CO2	Free CO2
Component volatility type	Dead	Dead	Dead	Gas	Dead	Dead	Gas
Component compressibility type	Oil	Oil	Gas	Oil	Oil	Gas	Oil
Molecular weight (kg/kg-Mole)	450	16.04	16.04	16.04	44.01	44.01	44.01
Critical temperature (K)	783	190.6	190.6	190.6	304.7	304.7	304.7
Critical pressure (kPa)	970	4600	4600	4600	7390	7390	7390
K-value correlation:		$K(P, T) = (A + B/P + C.P) \exp[-D/(T-E)]$ P (pressure) in barsa and T (temperature) in K					
A, dimensionless	212	0	0	0	0	0	0
B (barsa)	10714.5	11650	11650	11650	11748.7	11748.7	11748.7
C (1/bars)	0	0	0	0	0	0	0
D (K)	2222	1058	1058	1058	1701	1701	1701
E (K)	266	0	0	0	0	0	0
		$Ln(Ln(\mu, cP)) = 22.2018 - 3.5098 Ln(T, ºC + 273)$					
Oil viscosity at 25 °C (cP)	67400	2.3	2.3	0.205	15	15	0.328

Note that both C_1 and CO_2 interact with heavy oil through the so-called "foamy behaviour". High viscosity oil traps small gas bubbles as they come out of solution, reducing the potential of bubble coalescence to form a continuous gas phase. This reduces the flow rate of the gas and provides drive energy for more oil

production (ECLIPSE Technical Manual 2013). The foamy oil behaviour was implemented with the help of kinetic models for both C_1 and CO_2. These models use the kinetic reactions from nucleation of gas bubbles until they are connected and form a single gas phase. In this approach, three gas components were used to represent gas in the oil phase (dissolved gas), foamy oil phase (dispersed gas), and gas phase (free gas). The trapped gas in foamy oil phase would then be modeled as an oil phase component to ensure that the trapped gas moves with the oil phase. The reactions can go in both ways - dissolved to free gas and free to dissolved gas with the transitional formation of dispersed gas in-between. This is referred to as delayed exsolution/dissolution. Finally, two first-order kinetic reactions were used to represent the liberation of gas from (1) dissolved gas to trapped gas and from (2) trapped gas to free gas and backwards.

Economic Assumptions

The objective of this study is to clarify the impact of uncertain parameters and operational input on oil recovery. However, the suitability of this work for industry should be economically justified. To this end, the last section of this paper is reserved to provide and discuss the preliminary results on the economic viability. An economic indicator was defined to encompass the after-tax net present value (NPV) of the field scale application of cyclic solvent stimulation process, previously suggested by Gossuin et al. (2010). The economic assumptions are summarized in **Table 6-4**. Note that discounting is performed continuously and the model allows for oil and gas price drift in time.

Table 6- 4: Economic Assumptions

Oil price ($/STB)	75
Gas price ($/MSCF)	10
Oil production/upgrade cost ($/STB)	7.13
Gas injection cost ($/MSCF)	5
Royalty rate (%)	5.6
Net income tax (%)	33
Inflation (%)	2
Discounting (%)	10

Results and Discussions

Base Model Description

To include the cyclic solvent stimulation as post-CHOPS, the history matched model was considered to experience a period of aggressive blow down until the reservoir pressure can no longer support more oil production (**Figure 6-2**). This status, referred to as full depletion, may not be the optimal operational conditions to start the cyclic solvent stimulation because emergence of solution gas would leave dead oil behind in reservoir. However, with such an option, one is able to show that the incremental oil is only caused due to implementation of proposed cyclic solvent stimulation. In the base model, it was assumed that the wormholes were developed in the middle of producing formation. The field development strategy was then to convert all of the production wells into injectors. Solvents (C_1 and CO_2) were injected through these injectors into the wormhole network for four months at a rate of 2,000 Sm3/day per well (CO_2 equilibrium dissolution was selected as the base case in solvent injection). This increases the reservoir pressure in addition to the possibility of oil dilution. All wells in the field were then shut in a soaking period for a certain time that could be optimized. In production phase, oil was produced from all wells with an economic minimum oil rate of 1 Sm3/day per well. This mimics a field scale huff'n'puff process rather than a single well. In other words, certain wells were used as injectors while the potential producers are shut-in. Then, all the wells were shut down were the soaking period. Finally, the producers were opened. The cycles potentially can be repeated.

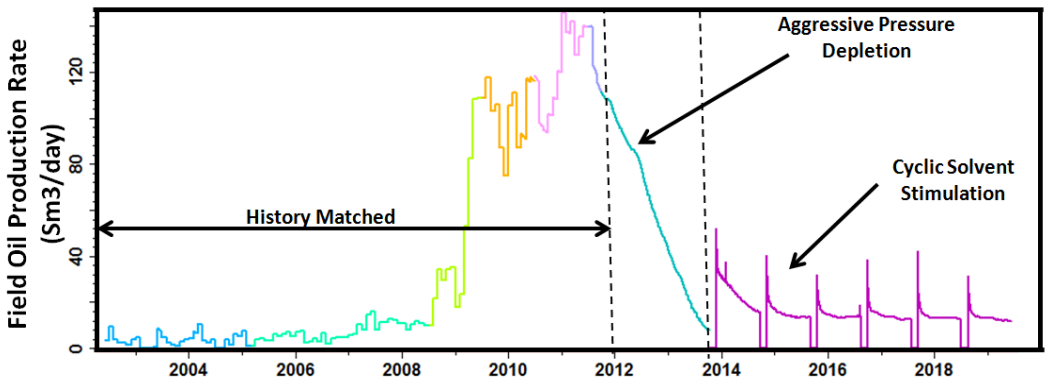

Figure 6- 2: Field oil production rate: history matched model followed by pressure depletion and cyclic solvent stimulation.

Selection of Injection Pattern

In the base case, all production wells were converted to injectors during cyclic solvent stimulation (truly huff'n'puff). Two other possible strategies are peripheral and central injections. In peripheral injection, only four production wells at the edge of CHOPS field are converted to injectors and the remaining wells act as producers. In this case, the injectors would push the oil towards central wells in a cyclic manner. In central injection, the injectors at the centre of the field would push the oil towards the reservoir edges (**Figure 6-3**).

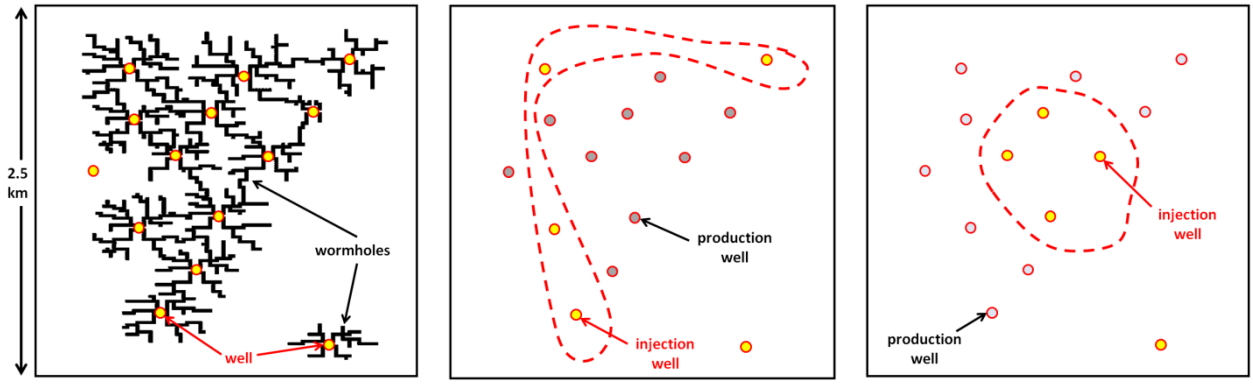

(a) Developed wormhole network (b) Peripheral wells injection (c) Central wells injection

Figure 6- 3: Possible cyclic solvent injection patterns in CHOPS reservoirs.

Figures 6-4-(a) through **-(c)** compare incremental oil production, gas production and gas injection volumes at each cycle. As seen, all-wells injection strategy yielded better performance, and central-wells ranked second. Due to high oil viscosity, CO_2 cannot reach all wormhole regions in the first cycle to saturate and hence mobilize all of its oil contents. Therefore, it is suggested that all wells be treated similarly to single huff'n'puff process.

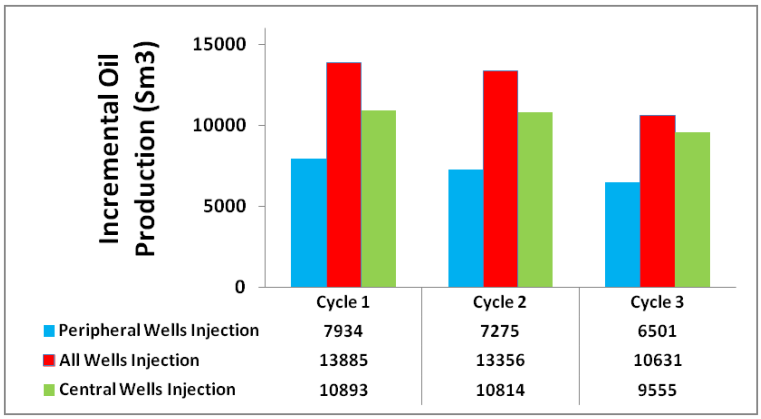

(a) Incremental oil production at each cycle for different injection patterns

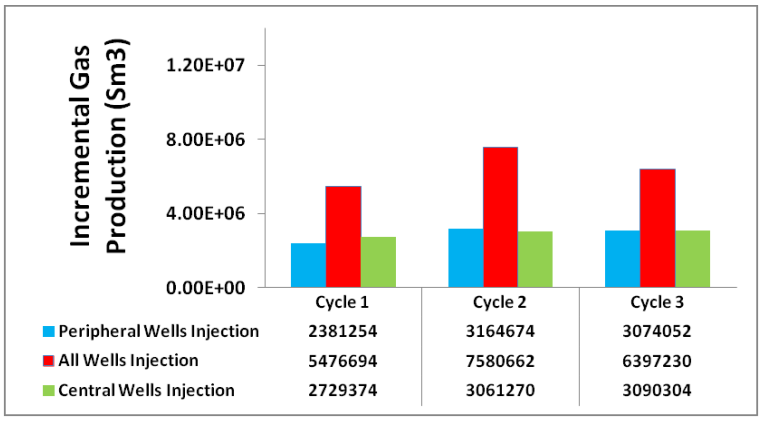

(b) Incremental gas production at each cycle for different injection patterns

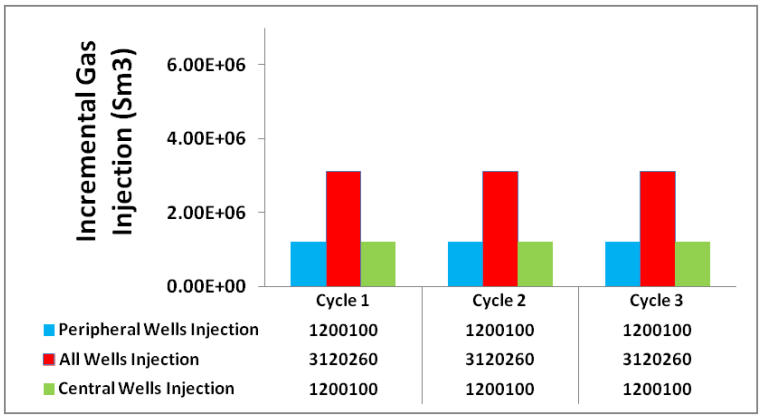

(c) Incremental gas injection at each cycle for different injection patterns

Figure 6- 4: Performance of cyclic solvent stimulation in different injection patterns.

Selection of Injection Rate

One of the common practices in the oil industry is to inject gas solvents at high rates in order to re-pressurize the reservoir more rapidly and cut down the project timelines. To study this, three different injection rates were considered for cyclic CO_2 stimulation. **Figures 6-5-(a)** through **-(c)** indicate that there is an optimum injection rate (with respect to injection time and strategy) to maximize ultimate oil recovery. Lower injection rate results in a less pressurized reservoir which cannot deliver sufficiently high oil production; on the other hand, higher injection rate provides too much gas in reservoir that cannot be instantaneously dissolved/diffused into heavy oil. This gas would be later produced as a free phase, reducing the productivity of CHOPS wells to deliver oil. Therefore, injection/soaking time and rate should be considered as two main optimization parameters along with kinetics of gas dissolution/exsolution to make the project economically viable.

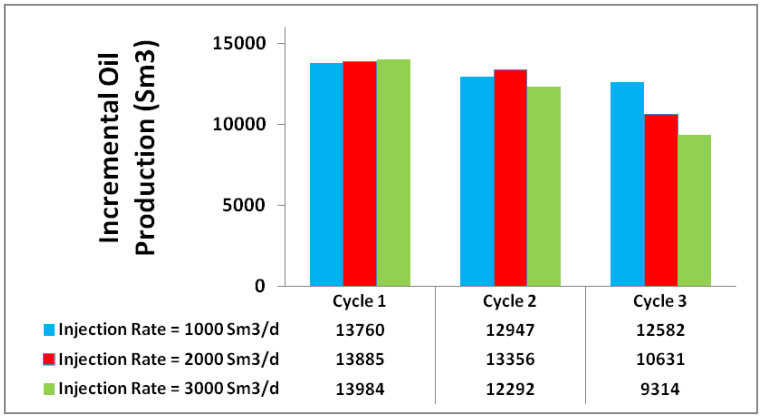

(a) Incremental oil production at each cycle for different injection rates

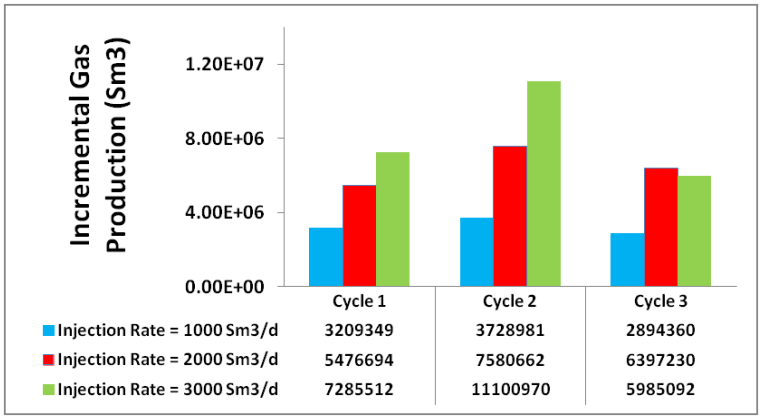

(b) Incremental gas production at each cycle for different injection rates

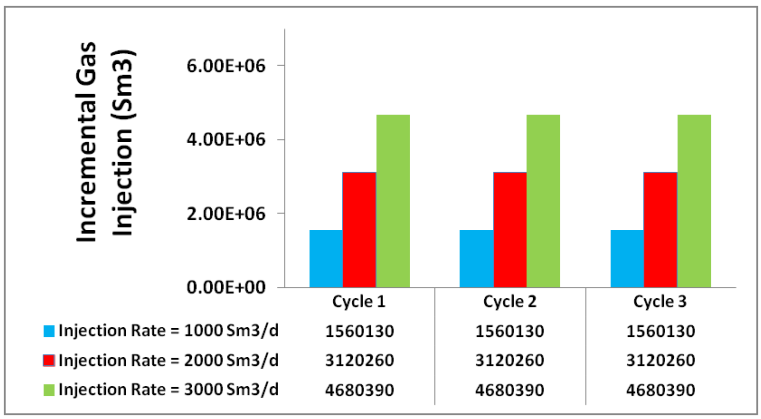

(c) Incremental gas injection at each cycle for different injection rates

Figure 6- 5: Performance of cyclic solvent stimulation with different injection rates.

Selection of Injection/Soaking Time

Figures 6-6-(a) through **-(c)** illustrate the results for oil production, gas production and gas injection of equal injection rate, but different injection/soaking times from 1 to 8 months, followed by 12 months oil production. Overall, the 4- and 8-month stimulations result in similar oil production, but with higher gas injection volumes for 8-month stimulation. Unfortunately, sensitivity analysis is unable to address the interaction of two or more parameters on the final outcome. This highlights the need to study such interactions among injection rate and time through optimization tools.

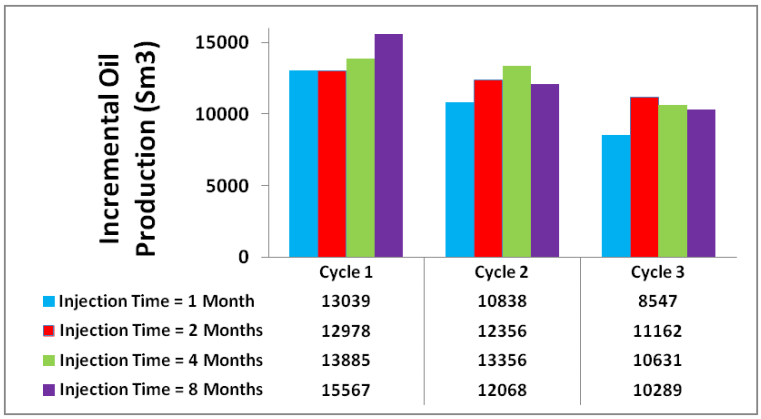

(a) Incremental oil production at each cycle for different injection times

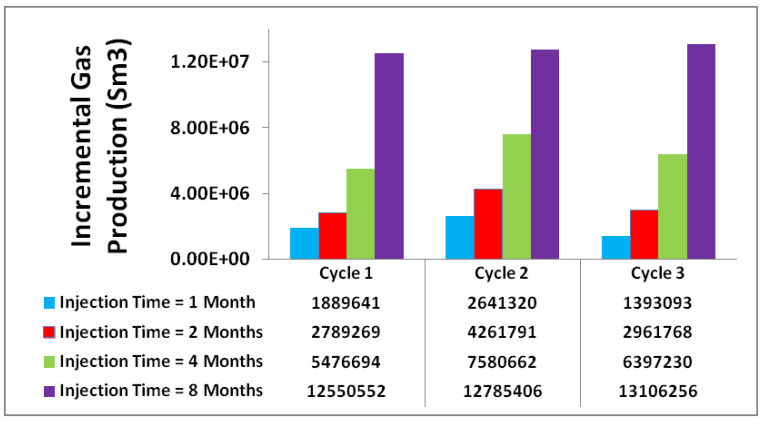

(b) Incremental gas production at each cycle for different injection times

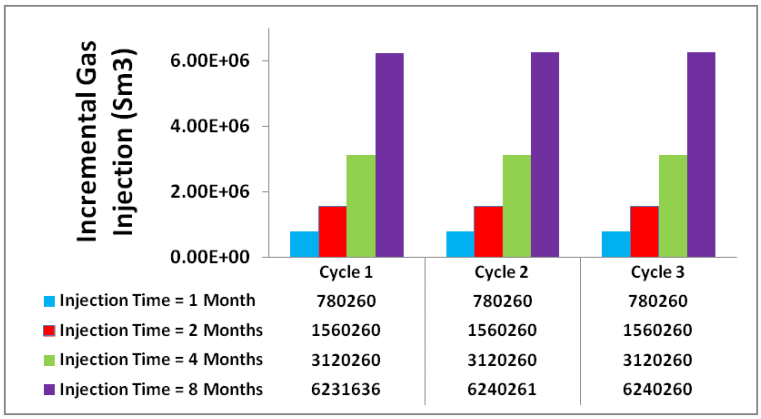

(c) Incremental gas injection at each cycle for different injection times

Figure 6- 6: Performance of cyclic solvent stimulation with different injection times.

Solvent Dissolution/Exsolution

During cyclic solvent stimulation, as there is such a phenomenon named foamy oil or delayed gas exsolution (it takes a while for solution gas to release and form a free-gas phase), the reverse process, the dissolution of gas into dead oil takes some time too. Non-equilibrium gas dissolution in oil can be modeled through kinetics reactions to represent this deviation from equilibrium. The parameters of such kinetic models can be obtained through history matching field data or laboratory experiments (ECLIPSE Technical Manual 2013). In this section, equilibrium and non-equilibrium gas dissolution of C_1 and CO_2 were compared (**Figures 6-7-(a)** through **-(c)**). CO_2 showed an overall better performance than C_1 as a gas solvent. Also, non-equilibrium

assumptions yielded much higher oil recovery disregarding the solvent type. Note that the solvent type is an operational decision, rather the time-dependent dissolution process is not a choice, but a governing mechanism and its strength should be studied prior to field development. There are techniques to hinder or accelerate the strength of foamy oil, but will not be addressed in this paper.

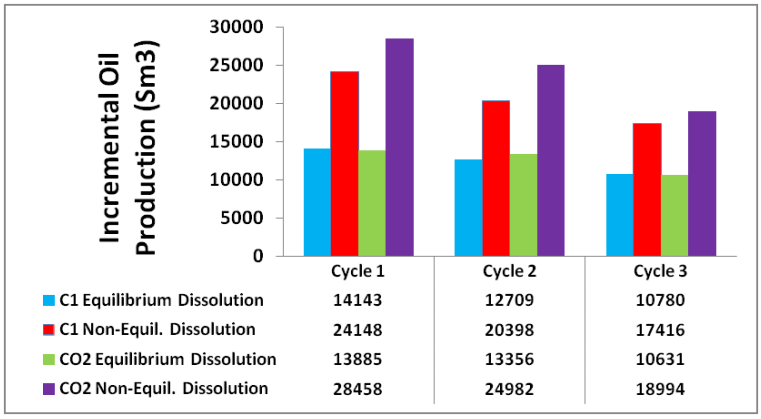

(a) Incremental oil production at each cycle for C1 and CO2 with delayed gas dissolution/exsolution

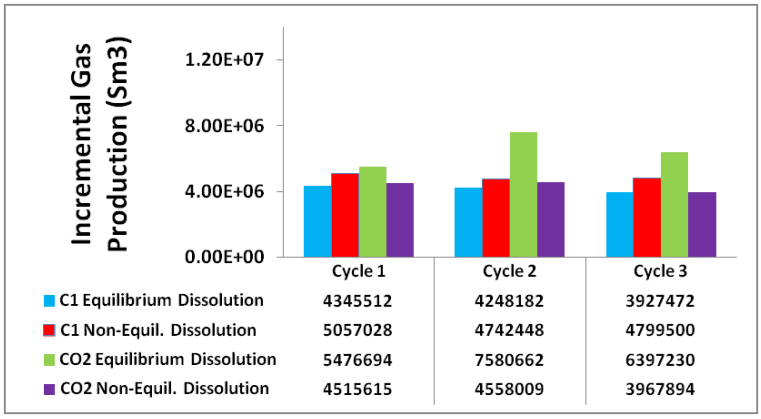

(b) Incremental gas production at each cycle for C1 and CO2 with delayed gas dissolution/exsolution

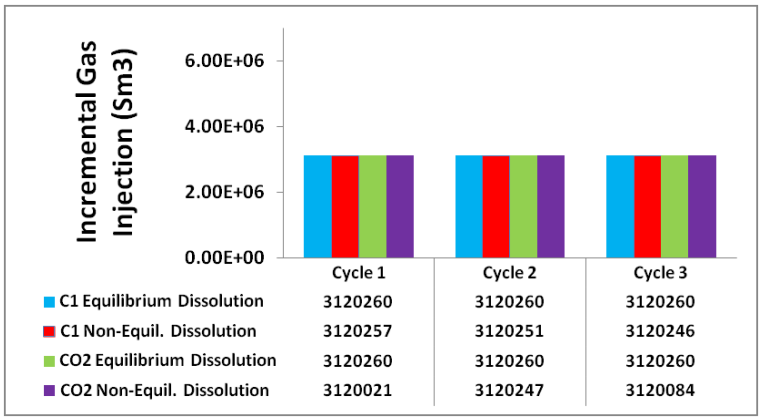

(c) Incremental gas injection at each cycle for C1 and CO2 with delayed gas dissolution/exsolution

Figure 6- 7: Performance of cyclic solvent stimulation for C1 and CO2 with delayed gas dissolution/exsolution.

Impact of Wormhole Vertical Location

Similar to time-dependent gas dissolution/exsolution, the vertical location of wormholes in producing formation is not an operational decision, but has a major influence on oil recovery. It should be emphasized that aggressive pressure drop during the primary CHOPS production is believed to be higher parallel to the reservoir bedding considering very thin reservoirs. Hence, the wormholes would possibly grow laterally in the direction of higher pressure drawdown. If no shale breaks are present, wormholes would preferentially develop in coarser sand grains than finer ones. Three possibilities for sand grain distribution are even block, upward coarsening and upward fining (**Figure 6-8**). Geologically speaking, it is more probable for wormhole network to develop at the formation top if upward coarsening (and even block) sequence is observed, which is the case for most of Albertan CHOPS reservoirs. Wormholes would develop in formation bottom if sand grains show upward fining trend (**Figures 6-9-(a)** and **-(b)** show the simulated wormholes developing at formation bottom and top, respectively).

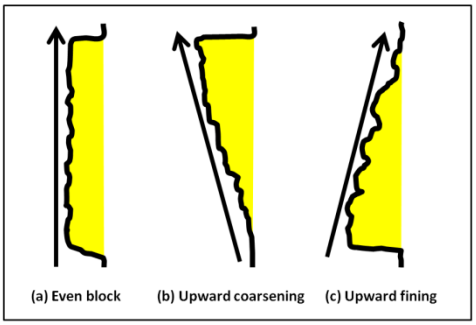

Figure 6- 8: Possible sand grain distribution in CHOPS reservoirs.

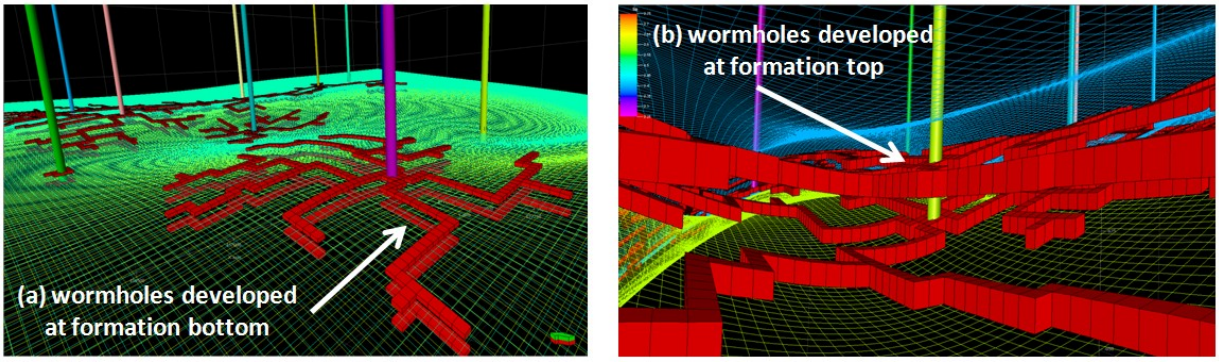

Figure 6- 9: Simulated wormhole network developed at (a) formation bottom and (b) formation top.

Figures 6-10-(a) through **-(c)** are incremental oil production, gas production and gas injection volumes resulted at the end of three cycles of solvent stimulation, assuming wormholes were developed at formation top, middle and bottom, separately. Wrong detection of wormhole vertical location could lead to over 200% error in estimating incremental oil recovery.

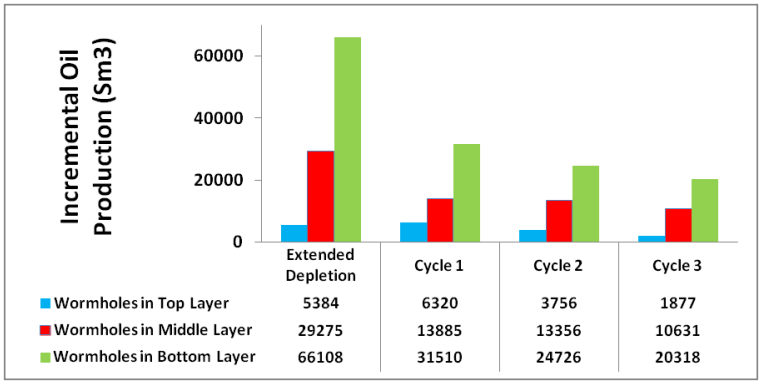

(a) Incremental oil production at each cycle for different wormhole locations

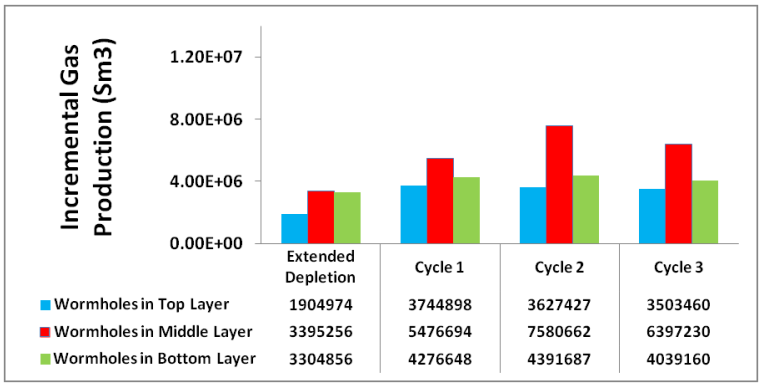

(b) Incremental gas production at each cycle for different wormhole locations

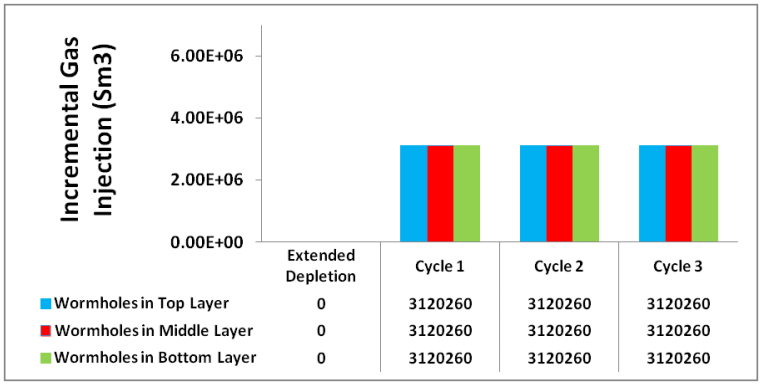

(c) Incremental gas injection at each cycle for different wormhole locations

Figure 6- 10: Performance of cyclic solvent stimulation for different wormhole locations.

Economic Analysis

As explained earlier, the objective of this study is to clarify the impact of uncertain parameters and operational input on oil recovery from a technical point of view, and not to add complexity of economic models. However, to justify the economics of the process, a single-valued economic indicator is introduced as the after-tax NPV of the field at the end of cyclic solvent stimulation process. Such a function has the priority to oil recovery factor or cumulative oil production as it incorporates costs and sales simultaneously by performing continuous discounting and allows the asset holder for oil and gas price drift in time. The net present value (*NPV*) is given by the sum of discounted cash flows of the development project with the discount rate given by the management as follows:

$$NPV = \sum_{t=0}^{N} \frac{NCF}{(1+i)^t} \qquad (6-1)$$

$$NCF = Sales - Cost/Expenses \qquad (6\text{-}2)$$

where *NCF* is the net cash flow, *i* is the discount rate and *t* is the time of the cash flow based on sales and expenses. Sales are calculated based on oil and gas production volumes and prices that might include the price inflation at each year. Royalty rate is directly applied to sales. Taxable income is calculated as the difference between sales and sum of royalty, operational and capital costs considering investment depreciation. Tax rate would be applied to taxable income. Thus, the cash flow can be calculated and discounted at each year. Such calculations would be beneficial to give insight into investment profitability of the project. Other decision-making indicators such as profitability index, internal rate of return, break-even price, and so on can then be quickly calculated.

Figures 6-11 and **12** show the results of the sensitivity analysis on the uncertain parameters and operational input covered in this paper. Note that sensitivity analysis enables the identification of key variables and discovery of maximum variations consistent with acceptability of the project. However, it ignores full dispersion of possible outcomes and probabilities attached to variations in primary variables. Inspecting Figures 6-11 and 12 confirms that wormhole vertical locations and solvent dissolution mechanisms are the major contributing parameters, but these factors are out of operator's control. On the other hand, choosing the right injection pattern as an operational input can help to implement cyclic solvent stimulation more efficiently, both from technical and economical points of view.

Injection time and rate indicate different impact on incremental oil production and NPVs (note that the middle vertical lines in Figure 6-11 and 12 demonstrate the base cases). For instance, a change in injection time from the base value (4 months) shows negative results, but it may increase the project profitability (higher NPV). Care should be taken to choose the right objective function in accordance with project objectives.

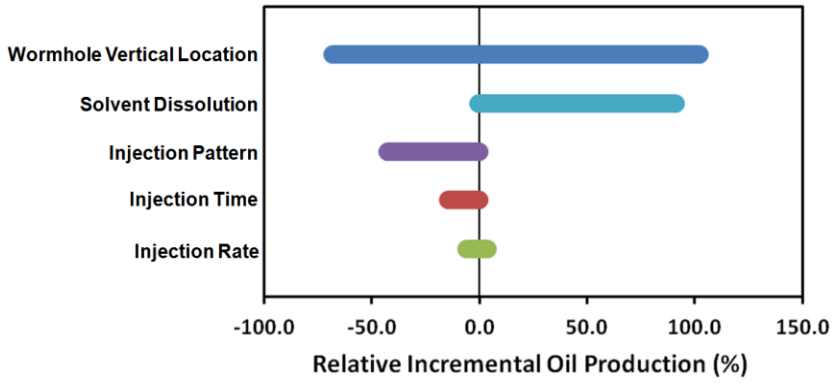

Figure 6- 11: Technical tornado plot shows relative incremental oil production.

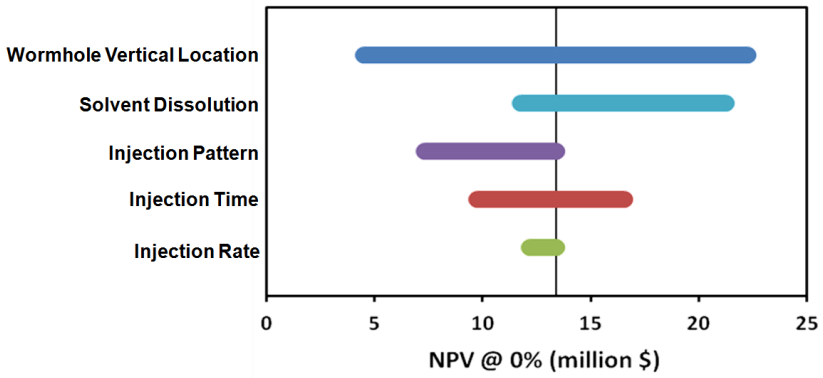

Figure 6- 12: Economical tornado plot shows project's net present value.

Conclusions and Remarks

With notion to potential use of gas solvents as a follow-up EOR technique for CHOPS reservoirs, an uncertainty screening framework was provided in a 15 wells Albertan CHOPS field. Field-scale cyclic solvent stimulation was performed and the main contributing factors - uncertain parameters and operational input - were recognized. It was shown that bottom-located wormholes and non-equilibrium gas dissolution/exsolution could highly affect incremental oil production and project NPVs, but unfortunately, they are unruly controlled. On the other hand, injection pattern, as an operational input, can contribute to project profitability. It was concluded that the best performance would be obtained if all wells were used as injector/producer in cyclic solvent stimulation, rather than a peripheral or central pattern.

The sensitivity analysis also revealed that an increase in injection rate and injection/soaking time do not necessarily enhance oil recovery, but an optimum value exists. To estimate the optimum values, an economics model was developed and after-tax NPV of the field was introduced as an economic indicator. The preliminary analysis showed that such a function had the priority to oil recovery factor or cumulative oil production because it incorporated costs and sales simultaneously by performing continuous discounting; hence, it would allow the asset holder to maximize NPVs and select the best development strategy.

References

ECLIPSE Technical Manual, Schlumberger. 2013.

Butler, R.M., 1997. Thermal Recovery of Oil and Bitumen. Prentice Hall.

Gossuin, J., Bailey, W.J., Couet, B., and Naccache, P. 2004. Steam-Assisted Gravity Drainage Optimization for Extra Heavy Oil, Proceeding of the 12th European Conference on the Mathematics of oil Recovery, Oxford, UK, September 6-8.

Kristoff, B.J, Knorr, K.D., Preston, C.K., Worth, K. and Sawatzky, R. 2008. Joint Implementation of Vapour Extraction – Heavy Oil Recovery Process" presented at the World Heavy Oil Congress, Edmonton, Alberta, 10-12 March.

Rangriz Shokri, A. and Babadagli, T. 2012. An Approach to Model CHOPS (Cold Heavy Oil Production with Sand) and Post-CHOPS Applications. Paper SPE 159437 presented at the SPE Annual Technical Conference and Exhibition, San Antonio, Texas, USA, 8-10 October.

Rangriz Shokri, A. and Babadagli, T. 2013. Modeling Thermal and Solvent Injection Techniques as Post-CHOPS Applications considering Geomechanical and Compositional Effects. Paper SPE 165534 presented at the SPE Heavy Oil Conf., Calgary, AB, Canada, 11-13 June.

Rangriz Shokri, A. and Babadagli, T. 2014. Evaluation of Thermal/Solvent Applications with and without Cold Heavy Oil Production with Sand (CHOPS). JCPT 53 (2): 95-108.

Yazdani, A., Alvestad, J., Kjonsvik, D., Gilje, E., Kowalewski, E., 2011. A Parametric Simulation Study for Solvent Co-injection Process in Bitumen Deposits. Paper SPE 148804 presented at the Canadian Unconventional Resources Conference, Calgary, Alberta, Canada, 15-17 November.

Chapter 7: Summary, Conclusions, Remarks and Contributions

Summary, Conclusions and Remarks

In this chapter, a general overview of the research is provided and the main conclusions and remarks are highlighted. Then, specific contributions to industry and literature are outlined.

1. A new workflow for quick CHOPS simulation at field scale was implemented based on a step-by-step simulation technique with a partial dual porosity approach. It is able to capture the growing nature of wormholes during CHOPS with an integrated fractal-wormhole model incorporating sand production history and wormhole network. Numerical simulation results indicated that a fractal pattern was more reliable to represent wormholes. In addition, it was shown that foamy oil flow can be easily modeled in practice using a modified version of gas relative permeability curve or, alternatively, with first-order kinetic reactions to replace the in-situ flash process.
2. After history matching of the CHOPS performance in the selected field, several post-CHOPS scenarios as modified versions of SOS-FR technique were studied at field scale. It was observed that in an iso-thermal process, additional oil can be produced from the wormhole network. The use of hot fluids as well as solvent-aided process would be effective in increasing oil recovery from non-wormhole domain.
3. A 3D Mechanical Earth Model was constructed to understand the contribution of production schedule on stress changes on a thin unconsolidated heavy oil reservoir in Alberta. The hydro-geomechanical model was used for assessment of near wellbore regions during cyclic injection and production. It was shown how stress arching re-distribute the cyclic injection-production induced stresses to flow around soft inclusions in the suspected wormhole layer. Because the wormholes were considered to be the main fluid path for reservoir to deliver the oil to wellbore region, it was argued that the coupling effect on fluid production might be considered negligible in restricted loading and unloading cycles with no significant sand production.

4. With notion to the potential use of solvents in post-CHOPS, several experiments (liquid and gas solvents) were conducted to study the performance of thermally aided cyclic solvent stimulation. The interactions between wormhole and non-wormhole domains were inspected based on scaled wormhole/non-wormhole volume ratios (i.e. wormhole coverage index, WCI) and configurations. It was observed that the high pressure experiment (liquid solvent) yielded higher oil recovery, but lower solvent recovery factor at the end of solvent phase. To make the process economically viable, a solvent retrieval attempt was made by injecting different -low- temperature hot water (due to thermal limitations of CHOPS well completions). A post-flush hot-water was found to be efficient to increase both solvent and oil ultimate recovery factors in all of the experiments, and it performed best in the high pressure case.
5. A comprehensive EOS-based fluid modeling was presented and used to simulate the sand-pack experiments. Experimental and numerical results were analyzed and effective liquid diffusion coefficients for C_7 and diluents were obtained. It was observed that diluents, compared to C_7, yielded less asphaltene precipitation due to aromatic contents of diluents. In addition, diffusion of CO_2 into heavy oil was analyzed through cross-phase diffusion concept. Hence, a framework for delayed dissolution of CO_2 was established. It was observed that the use of light solvents (CO_2) could maintain the sand-pack pressure for a longer period (attributed to foamy oil phenomenon) compared to liquid solvent during production phase. But, the oil recovery from sole application of light solvent (RF=4%) was not as considerable as with the heavier solvents (RF=23%). These experiments suggest that an improved heavy oil recovery could be achieved using hybrid application of solvents and hot water in CHOPS reservoirs.
6. It was shown that injected solvent could not invade all parts of the branched wormhole domain at first cycle rather the mixing front gradually developing and reaching the so-called dangling or dead end bonds. It appears that the backbone of wormhole network determines the efficiency of the cyclic solvent stimulation in branched (fractal) wormhole patterns, rather than local variation of dangling bonds.

7. To generate accurate predictions in field-scale simulation, an up-scaling procedure from laboratory results of the CSI process was suggested, so that field-scale diffusion coefficients can be calculated based on different field properties. Also, it was shown that, in theory, molecular diffusion would dominate the process and convective dispersion might be neglected. However, the best practice is to perform a sensitivity analysis on the uncertain field-scale variables.
8. An uncertainty screening framework was provided in a 15 wells Albertan CHOPS field. Field-scale cyclic solvent stimulation was performed and the main contributing factors - uncertain parameters and operational input - were recognized. It was shown that bottom-located wormholes and non-equilibrium gas dissolution/exsolution could highly affect incremental oil production and project NPVs, but unfortunately, they are unruly controlled. On the other hand, injection pattern, as an operational input, can contribute to project profitability. It was concluded that the best performance would be obtained if all wells were used as injector/producer in cyclic solvent stimulation, rather than a peripheral or central pattern. The sensitivity analysis revealed that an increase in injection rate and injection/soaking time do not necessarily enhance oil recovery, but an optimum value exists that should be determined from economics point of view.
9. An economics model was developed and after-tax NPV of the field was introduced as objective function for later optimization studies. The preliminary analysis showed such a function had the priority to oil recovery factor or cumulative oil production because it incorporated costs and sales simultaneously by performing continuous discounting; hence, it would allow the asset holder to maximize NPVs and select the best development strategy.

Specific Contributions

This research was aimed at finding a practical solution for enhanced oil recovery from CHOPS reservoirs. Considering the numerous failed attempts of viscosified water/polymer flooding and the inefficiency of thermal methods, wormholes were assumed for many researchers as drawbacks of CHOPS for further oil recovery. With a realistic approach, the initiative of this study was to take advantage of the wormhole network, which is quite reverse to the common negative beliefs. Although one may never be able to determine the actual trend of wormholes underground, our foremost contribution is to offer the industry a new technology to recover huge amount of remained heavy oil after CHOPS with the help of already-developed wormhole network. To show how and why this technology is efficient, we used both numerical and experimental approaches in accordance to our own engineering judgment. The following list is the specific -scientific and practical- contributions of this thesis to the literature:

Numerical Work.

- Providing a practical workflow for CHOPS modeling considering the growing nature of wormholes and foamy oil behaviour.
- Integrating the sand production data with fractal patterns (integrated wormhole-fractal model) for wormhole network growth to make every simulation job unique to each case study.
- Implementing kinetic reaction models for foamy oil flow to differentiate the formation of trapped and free gas from initial solution gas.
- Providing novel fractal-based upgridding and upscaling techniques in partial-dual porosity models.
- Validating the suggested workflow in single and field-scale studies with history matching on real production data provided by Canadian oil companies.
- Presenting simple workflows to assess the potential of Geomechanics during cyclic solvent stimulation, even with limited data.

- Analyzing field-wide deformation changes of coupled and uncoupled post-CHOPS models.
- Determination of effective diffusion coefficients for cyclic solvent stimulation based on experimental work.
- Providing uncertainty screening and quantification workflow as a building block for massive optimization of selected post-CHOPS strategies at the field-scale.

Experimental Work.

- Innovative experimental study of cyclic solvent stimulation in the presence of wormholes of different structures.
- Experimental and numerical evaluation of effective diffusion coefficient of liquid solvents during different experimental conditions.
- Investigating the impact of wormhole coverage index during cyclic solvent injection.
- Evaluating the economic feasibility of the process with the help of solvent retrieval phase.
- Gaining insight into the field application of the process with notion to reservoir condition.

Bibliography

Al Bahlani, A. M. M., and Babadagli, T. 2009. Laboratory and Field Scale Analysis of Steam Over Solvent Injection in Fractured Reservoirs (SOS FR) for Heavy Oil Recovery. Paper SPE 124047 presented at the SPE Annual Technical Conf. and Exh., New Orleans, Louisiana, 4-7 October.

Alshmakhy, A. and Maini, B. B. 2012. A Follow-Up Recovery Method After Cold Heavy Oil Production. SPE157823-MS presented at the SPE Heavy Oil Conference Canada, Calgary, Alberta, 12-14 June.

Bassiouni, Z. 1994. Theory, Measurement and Interpretation of Well Logs, SPE Textbook Series Vol. 4, ISBN:978-1-55563-056-0.

Bayon, Y. M., Cordelier, Ph. R., Coates, R. M., et al. 2002.Application and Comparison of Two Models of Foamy Oil Behavior of Long Core Depletion Experiments. SPE paper 78961 presented at the SPE International Thermal Operations and Heavy Oil Symposium and International Horizontal Well Technology Conference, Calgary, Alberta, Canada, 4–7 November.

Butler, R.M., 1997. Thermal Recovery of Oil and Bitumen. Prentice Hall.

Coombe, D., Tremblay, B., Tran, D., et al. 2001. Coupled Hydro-Geomechanical Modeling of the Cold Production Process. SPE paper 69719 presented at the SPE International Thermal Operations and Heavy Oil Symposium,Porlamar, Margarita Island, Venezuela, 12-14 March.

Coskuner, G., Naderi, K. and Babadagli, T. 2013. An Enhanced Oil Recovery Technology as a Follow Up to Cold Heavy Oil Production with Sand. Paper SPE 165385 presented at the SPE Heavy Oil Conf., Calgary, Alberta, Canada, 11-13 June.

Denbina, E.S., Baker, R.O., Gegunde, G.G., et al. 2001.Modeling Cold Production for Heavy Oil Reservoirs.*Journal of Canadian Petroleum Technology***40** (3).

Du, Z., Chan, C., and Zeng, F. 2013. An Experimental Study of the Post - CHOPS Cyclic Solvent Injection Process. Presented at the SPE Heavy Oil Conference-Canada, Calgary, Alberta, Canada, 11-13 June. SPE-165524-MS. http://dx.doi.org/10.2118/165524-MS.

Dusseault, M. 1993.Cold Production and Enhanced Oil Recovery. *Journal of Canadian Petroleum Technology* **32** (9): 16-18.

Dusseault, M. and El-Sayed, S. 1999. CHOP – Cold Heavy Oil Production. Paper presented at the 10th European Symposium on Imperial Oil Recovery, Brighton, UK, 18–20 August.

Dusseault, M., Bruno, M.S., and Barrera, J.A. 2001. Casing Shear: Causes, Cases, Cures. *SPE Drill. & Prod. Prac. J.* **16** (2): 98-107.

ECLIPSE Technical Manual, Schlumberger 2011.

Elkins, L.F., Morton, D., and Blackwell, W.A. 1972. Experimental Fireflood in a Very Viscous Oil-Unconsolidated Sand Reservoir, S. E. Pauls Valley Field, Oklahoma. Paper SPE 4086 presented at the 47th Annual Fall Meeting of the Society of Petroleum Engineers of AIME, San Antonia, Texas, 8–11 October.

Firoozabadi, A. 2001.Mechanisms of Solution Gas Drive in Heavy Oil Reservoirs.*Journal of Canadian Petroleum Technology*. **40** (3).

Gossuin, J., Bailey, W.J., Couet, B., and Naccache, P. 2004. Steam-Assisted Gravity Drainage Optimization for Extra Heavy Oil, Proceeding of the 12th European Conference on the Mathematics of oil Recovery, Oxford, UK, September 6-8.

Herwanger, J. and Koutsabeloulis, N. 2011. *Seismic Geomechanics: How To Build and Calibrate Geomechanical Models using 3D and 4D Seismic Data*. D.B. Houten, The Netherlands: EAGE Publications.

Huang, W., Marcum B., Chase, M.R., et al. 1998. Cold Production of Heavy Oil from Horizontal Wells in the Frog Lake Field.*SPE Reservoir Evaluation & Engineering*. **1** (6): 551-555.

Istchenko, C. M., and Gates, I. D. 2014. Well/Wormhole Model of Cold Heavy-Oil Production with Sand. *SPE J.* 19 (2), 260-269.

Istchenko, C.M. and Gates, I.D. 2011.The Well-Wormhole Model of Cold Production of Heavy Oil Reservoirs.SPE150633-MS presented at the SPE Heavy Oil Conference and Exhibition, Kuwait, 12-14 December.

Ivory, J., Chang, J., Coates, R., and Forshner, K. 2010. Investigation of Cyclic Solvent Injection Process for Heavy Oil Recovery. *SPE J* **49** (09): 22–33. http://dx.doi.org/10.2118/140662-PA.

Kantzas, A. and Brook, G. 2002.Preliminary Laboratory Evaluation of Cold and Post-Cold Production Methods for Heavy Oil Reservoirs Parts A and B. CIPC Paper 2002-079 presented at the Petroleum Society's Canadian International Petroleum Conference 2002, Calgary, Alberta, Canada, 11-13 June.

Kantzas, A. and Brook, G. 2004. Preliminary Laboratory Evaluation of Cold and Post-Cold Production Methods for Heavy Oil Reservoirs Part A: Ambient Conditions. *JCPT* **43** (10). http://dx.doi.org/10.2118/04-10-03.

Kantzas, A. and Brook, G. 2004. Preliminary Laboratory Evaluation of Cold and Post-Cold Production Methods for Heavy Oil Reservoirs Part B: Reservoir Conditions. *JCPT* **43** (10). http://dx.doi.org/10.2118/04-10-04.

Kariznovi, M., Nourozieh, H., and Abedi, J. 2009. Bitumen characterization and pseudo-components determination for equation of state modeling. *Energy and Fuels* **24** (1): 624-633.

Kobbe, W. 1997. AIME New York Meeting, American Institute of Mechanical Engineering Transactions, Vol. LVI, p. 814, February.

Kristoff, B.J, Knorr, K.D., Preston, C.K., Worth, K. and Sawatzky, R. 2008. Joint Implementation of Vapour Extraction – Heavy Oil Recovery Process" presented at the World Heavy Oil Congress, Edmonton, Alberta, 10-12 March.

Lebel, J.P. 1994. Performance Implications of Various Reservoir Access Geometries. Document presented at the 11th Annual Heavy Oil & Oil Sands Technical Symposium "Challenges and Innovations" March 2nd.

Liu, X. and Zhao, G. 2004. Effects of Wormholes on Cold Heavy Oil Production. Paper presented at the Petroleum Society's 5th Canadian International Petroleum Conference (55th Annual Technical Meeting), Calgary, Alberta, Canada, 8 – 10 June.

Liu, X. and Zhao, G. 2005a. A Fractal Wormhole Model for Cold Heavy Oil Production.*Journal of Canadian Petroleum Technology***44** (9): 31-36.

Liu, X. and Zhao, G. 2005b. Transient Pressure Behavior of Cold-Heavy Oil Production Wells. SPE paper 97791 presented at the SPE/PS-CIM/CHOA International Thermal Operations and Heavy Oil Symposium, Calgary, Alberta, Canada, 1-3 November.

Longuemare, P., Mainguy, M., Lemonnier, P., Onaisi, A., Gerard, C., Koutsabeloulis, N., 2002. Geomechanics in Reservoir Simulation – Overview of Coupling Methods and Field Case Study. Oil and Gas Science and Technology – Rev. IFP **57** (5): 471.

Loughead, D.J. and Saltuklaroglu, M. 1992. Lloydminster Heavy Oil Production: Why So Unusual. Paper presented at the 9th Annual Heavy Oil and Oil Sands Technology Symposium, Calgary, Alberta, Canada, 11 March.

Maini, B. B. and Sarma, H. K. 1993. Significant of Foamy-Oil Behavior in Primary Production of Heavy Oils.*Journal of Canadian Petroleum Technology***32** (9): 50-54.

Maini, B. B. 1999. Foamy Oil Flow in Primary Production of Heavy Oil under Solution Gas Drive. Paper SPE 56541 presented at the SPE International Conference, Houston, Texas, 3-6 October.

Mccaffrey, W. and Bowman, R. 1991. Recent Successes in Primary Bitumen Production. Paper presented at the 81st Annual Heavy Oil and Oil Sands Technical Symposium, 14 March.

Meza, B. 2001.Experimental Investigation of Sand Production into a Horizontal Well Slot.MSc Thesis, School of Mining and Petroleum Engineering, University of Alberta (Fall 2011).

Miller, K.A., Moore, R.G., Ursenbach, M.G., et al. 2002.Proposed Air Injection Recovery of Cold-Produced Heavy Oil Reservoirs.*JCPT***41** (3): 40-49.

Mohammed, M. and Babadagli, T. 2013. Efficiency of Solvent Retrieval during Steam-Over-Solvent Injection in Fractured Reservoirs (SOS-FR) Method: Core Scale Experimentation. Paper SPE 165528 presented at the SPE Heavy Oil Conf., Calgary, AB, Canada, 11-13 June.

Naderi, K. and Babadagli, T. 2014. Use of Carbon Dioxide and Hydrocarbon Solvents During the Method of Steam-Over-Solvent Injection in Fractured Reservoirs for Heavy-Oil Recovery From Sandstones and Carbonates. *SPE Res Eval and Eng* **17** (2): 286-301.

Perkins, T.K. and Johnston, O.C. 1963. A Review of Diffusion and Dispersion in Porous Media. Society of Petroleum Engineers. *SPE J* **3** (01): 70–84. http://dx.doi.org/10.2118/480-PA.

Rangriz Shokri, A. and Babadagli, T. 2014. Evaluation of Thermal/Solvent Applications with and without Cold Heavy Oil Production with Sand (CHOPS). *JCPT* 53 (2), 95-108.

Rangriz Shokri, A. and Babadagli, T. 2012a. Evaluation of Thermal/Solvent Applications withand Without Cold Heavy Oil Production with Sand (CHOPS). Paper SPE 158934 presented at the SPE Energy Conference, Developing Resources for Sustainability, Port-of-Spain, Trinidad, 11-13 June.

Rangriz Shokri, A. and Babadagli, T. 2012b. An Approach to Model CHOPS (Cold Heavy Oil Production with Sand) and Post-CHOPS Applications. Paper SPE 159437 presented at the SPE Annual Technical Conference and Exhibition, San Antonio, Texas, USA, 8-10 October.

Rangriz Shokri, A. and Babadagli, T. 2013. Modeling Thermal and Solvent Injection Techniques as Post-CHOPS Applications considering Geomechanical and Compositional Effects. Paper SPE 165534 presented at the 2013 SPE Heavy Oil Conf., Calgary, AB, Canada, 11-13 June.

Rivero, J. A., Coskuner, G., Asghari, K., et al. 2010. Modeling CHOPS Using a Coupled Flow-Geomechanics Simulator with Non-Equilibrium Foamy-Oil Reactions: A Multiwell History Matching Study. Paper SPE 135490 presented at the SPE Annual Technical Conference and Exhibition, Florence, Italy, 19-22 September.

Sanyal, T. and Al-Sammak, I. 2011.Analysis of the First CHOPS Pilot for Heavy Oil Production in Kuwait. Paper CSUG/SPE148966 presented at the Canadian Unconventional Resources Conference, Calgary, Alberta, Canada, 15-17 November.

Sawatzky, R. 2008-2009. Cold Production: Recovery Mechanisms and Field Performance. Presented as an SPE Distinguished Lecture in Calgary, Alberta, Canada.

Sawatzky, R.P., Lillico, D.A., London, M., et al. 2002.Tracking Cold Production Foot Prints. Paper 2002-086presented at the Petroleum Society's Canadian International Petroleum Conference 2002, Calgary, Alberta, Canada, 11–13 June.

Shandrygin, A., Dinariev, O., Mikhailov, D.,et al. 2010.Enhancing Efficiency of Steam-Thermal Treatment of Formations with High Viscosity Oil. Paper presented at the SPE Russian Oil and Gas Conference and Exhibition, Moscow, Russia, 26–28 October.

Sheng, J.J., Maini, B.B., Hayes, R.E., et al. 1997. Experimental Study of Foamy Oil Stability. *Journal of Canadian Petroleum Technology* **36** (4): 31–37.

Smith, G.E. 1986. Fluid Flow and Sand Production in Heavy Oil Reservoir under Solution Gas Drive. Paper SPE 15094 presented at the 56th California Regional Meeting of the Society of Petroleum Engineers, Oakland. CA, 2–4 April.

Squires, A. 1993. Inter-Well Tracer Results and Gel Blocking Program. Technical paper presented at the 10th Annual Heavy Oil and Oil Sands Technical Symposium, 9 March.

Stalkup, F.I. 1983. Miscible Displacement, Vol. 8. Dallas, Texas: Monograph Series, SPE.

Tan, T., Slevinsky, R., and Jonasson, H. 2003.A New Methodology for Modeling of Sand Wormholes in Field Scale Thermal Simulations.Paper presented at the Canadian International Petroleum Conference, Calgary, Alberta, 10–12 June.

Tang, G.Q., Firoozabadi, A. 2003. Gas- and Liquid-Phase Relative Permeabilities for Cold Production from Heavy Oil Reservoirs.*SPE Reservoir Evaluation and Engineering***6** (2): 70-80.

Tremblay, B. Sedgwick, G. and Forshner, K. 1996. Imaging of Sand Production in a Horizontal Sand Pack by X-Ray Computed Tomography.*SPE Formation Evaluation***11** (2): 94-98.

Tremblay, B. Sedgwick, G., Forshner, K. 1997.Simulation of Cold Production in Heavy-Oil Reservoirs: Wormhole Dynamics.*SPE Reservoir Evaluation & Engineering* **12** (2): 110–111.

Tremblay, B. Sedgwick, G., and Vu, D. 1998a. CT Imaging of Sand Production in a Horizontal Sand Pack Using Live Oil. Paper 98-78 presented at the 49th Annual Technical Meeting of the Petroleum Society, Calgary, Alberta, Canada, 8–10 June.

Tremblay, B. Sedgwick, G., and Forshner, K. 1998b. Modeling of Sand Production from Wells on Primary Recovery.JCPT **37** (3): 41–50.

Tremblay, B. Sedgwick, G., and Vu, D. 1999a. CT Imaging of Wormhole Growth under Solution Gas Drive. *SPE ResEval&Eng***2** (1) 37-45.

Tremblay, B., Sedgwick, G., and Vu, D. 1999b.A Review of Cold Production in Heavy Oil Reservoirs. Paper 2008 presented at the 10th European Symposium on Improved Oil Recovery, Brighton, UK, 18-20 August.

L'Université de Franche-Comté. 2014. Fractalyse - Fractal Analysis Software 2.4. **http://www.fractalyse.org/fr-home.html**

Urgelli, D., Durandeau, M., Foucault, H., et al. 1999. Investigation of Foamy Oil Effect from Laboratory Experiments. Paper SPE 54083 presented at the SPE International Conference, Bakersfield, California, USA, 17-19 March.

VISAGE Technical Manual, Schlumberger. 2013.

Wang, Y. Chen, C., and Dusseault, M.B. 2001. An Integrated Reservoir Model for Sand Production and Foamy Oil Flow during Cold Heavy Oil Production.Paper SPE 69714 presented at the SPE International Thermal Operations and Heavy Oil Symposium, Palomar, Margarita Island, Venezuela, 12–14 March.

Wang, Y. and Chen, C. Z. 2002. Simulating Cold Heavy-Oil Production with Sand by Reservoir-Wormhole Model. Paper presented at the Canadian International Petroleum Conference, Calgary, Alberta, Canada, 11-13 June.

Wong, R.C.K. 2003.Sand Production in Oil Sand under Heavy Oil Foamy Flow.*JCPT***42** (3).

Wyllie, M.R.J., and Gardner, G.H.F. 1958. The Generalized Kozeny-Carmen Equation - Its Application to Problems of Multi-Phase Flow in Porous Media. World Oil, 146, 121.

Yale, D. P., Hoda, N., and Wang, J. 2012. Enhancing the CHOPS Process through Reservoir Conditioning, World Heavy Oil Congress, Aberdeen, UK, 10-13 September.

Yazdani, A., Alvestad, J., Kjonsvik, D., Gilje, E., Kowalewski, E., 2011. A Parametric Simulation Study for Solvent Co-injection Process in Bitumen Deposits. Paper SPE 148804 presented at the Canadian Unconventional Resources Conference, Calgary, Alberta, Canada, November 15-17.

Yeung, K. 1995.Cold Flow Production of Crude Bitumen at the Burnt Lake Project, Northeastern Alberta. Paper presented at the 1995 UNITAR International Conference on Heavy and Tar Sands, Houston, Texas, 12-17 February.

Yuan, J.Y, Tremblay, B., and Babchin, A. 1999. A Wormhole Network Model of Cold Production in Heavy Oil. Paper SPE 54097 presented at the SPE International Thermal Operations and Heavy Oil Symposium, Bakersfield, California, 17–19 February.

Yuan, J.Y., Babchin, A., and Tremblay, B. 2002. A Model for Sand Transport through a Partially-Filled Wormhole in Cold Production. *JCPT* **41** (4): 25-32.